DOT-VNTSC-FAA-11-11
DOT-FAA-AEE-2012-02

FLOATPLANE SOURCE NOISE MEASUREMENTS

Summary of Measurements, Data and Analyses for the

Cessna 182S Skylane and
De Havilland Canada DHC-2 Beaver

Final Report
January 2012

Prepared for:

U.S. Department of Transportation
Federal Aviation Administration
Western-Pacific Region
Special Programs Staff, AWP-1SP
Lawndale, CA 90261

U.S. Department of Transportation
Federal Aviation Administration
Office of Environment and Energy,
AEE-100
Washington, DC 20591

Prepared by:
U.S. Department of Transportation
Research and Innovative Technology Administration
John A. Volpe National Transportation Systems Center
Environmental Measurement and Modeling Division, RTV-41
Cambridge, MA 02142

REPORT DOCUMENTATION PAGE

Form Approved OMB No. 0704-0188

1. AGENCY USE ONLY (Leave blank)	2. REPORT DATE	3. REPORT TYPE AND DATES COVERED
	January 2011	Final Report

4. TITLE AND SUBTITLE
Floatplane Source Noise Measurements
Summary of Measurements, Data and Analyses for the Cessna 182S Skylane and De Havilland Canada DHC-2 Beaver

5. FUNDING NUMBERS
FP01 – JD7RD

6. AUTHOR(S)
Michael Lau, David Senzig, Paul Bevillard, Eric R. Boeker, Christopher J. Roof, Robert Samiljan, Charles Tyndall, Christopher Scarpone, Michael Kim, Cynthia Lee

7. PERFORMING ORGANIZATION NAME(S) AND ADDRESS(ES)
U.S. Department of Transportation
Research and Innovative Technology Administration
John A. Volpe National Transportation Systems Center
Environmental Measurement and Modeling Division, RVT-41
Cambridge, MA 02142-1093

8. PERFORMING ORGANIZATION REPORT NUMBER
DOT-VNTSC-FAA-11-11

9. SPONSORING/MONITORING AGENCY NAME(S) AND ADDRESS(ES)
1) U.S. Department of Transportation
Federal Aviation Administration
Western-Pacific Region
Special Programs Staff, AWP-1SP
Lawndale, CA 90261

(2) U.S. Department of Transportation
Federal Aviation Administration
Office of Environment and Energy, AEE-100
Washington, DC 20591

10. SPONSORING/MONITORING AGENCY REPORT NUMBER
DOT-FAA-AEE-2012-02

11. SUPPLEMENTARY NOTES
FAA Program Managers: Barry Brayer and Keith Lusk (AWP, Western-Pacific Regional Office, Special Programs Staff); Jim Skalecky, Rebecca Cointin, Bill He (AEE, Office of Environment and Energy, Noise Division)

12a. DISTRIBUTION/AVAILABILITY STATEMENT	12b. DISTRIBUTION CODE

13. ABSTRACT (Maximum 200 words)
The U.S. Department of Transportation, John A. Volpe National Transportation Systems Center (Volpe Center), Environmental Measurement and Modeling Division, provides technical support to the Federal Aviation Administration (FAA), with the cooperation of the National Park Service (NPS), in the development of Air Tour Management Plans (ATMPs) for National Parks with commercial air tours. In September 2010, the Volpe Center measured source noise for two floatplane aircraft that have been identified as participating in commercial air tour operations over National Parks: Cessna 182S and De Havilland Canada DHC-2. This document describes the planning and execution of the noise study, overviews the data reduction procedures, and presents final data adjusted to standard conditions.

14. SUBJECT TERMS
Aircraft noise, air tours, floatplane, noise measurements, noise, propeller aircraft, Integrated Noise Model, INM, Air Tour Management Plan, Aviation Environmental Design Tool, AEDT

15. NUMBER OF PAGES
100

16. PRICE CODE

17. SECURITY CLASSIFICATION OF REPORT	18. SECURITY CLASSIFICATION OF THIS PAGE	19. SECURITY CLASSIFICATION OF ABSTRACT	20. LIMITATION OF ABSTRACT
Unclassified	Unclassified	Unclassified	

NSN 7540-01-280-5500

Standard Form 298 (Rev. 2-89)
Prescribed by ANSI Std. 239-18
298-102

METRIC/ENGLISH CONVERSION FACTORS

ENGLISH TO METRIC		METRIC TO ENGLISH	
LENGTH (APPROXIMATE)		**LENGTH (APPROXIMATE)**	
1 inch (in)	= 2.5 centimeters (cm)	1 millimeter (mm)	= 0.04 inch (in)
1 foot (ft)	= 30 centimeters (cm)	1 centimeter (cm)	= 0.4 inch (in)
1 yard (yd)	= 0.9 meter (m)	1 meter (m)	= 3.3 feet (ft)
1 mile (mi)	= 1.6 kilometers (km)	1 meter (m)	= 1.1 yards (yd)
		1 kilometer (km)	= 0.6 mile (mi)
AREA (APPROXIMATE)		**AREA (APPROXIMATE)**	
1 square inch (sq in, in^2)	= 6.5 square centimeters (cm^2)	1 square centimeter (cm^2)	= 0.16 square inch (sq in, in^2)
1 square foot (sq ft, ft^2)	= 0.09 square meter (m^2)	1 square meter (m^2)	= 1.2 square yards (sq yd, yd^2)
1 square yard (sq yd, yd^2)	= 0.8 square meter (m^2)	1 square kilometer (km^2)	= 0.4 square mile (sq mi, mi^2)
1 square mile (sq mi, mi^2)	= 2.6 square kilometers (km^2)	10,000 square meters (m^2)	= 1 hectare (ha) = 2.5 acres
1 acre = 0.4 hectare (he)	= 4,000 square meters (m^2)		
MASS – WEIGHT (APPROXIMATE)		**MASS – WEIGHT (APPROXIMATE)**	
1 ounce (oz)	= 28 grams (gm)	1 gram (gm)	= 0.036 ounce (oz)
1 pound (lb)	= 0.45 kilogram (kg)	1 kilogram (kg)	= 2.2 pounds (lb)
1 short ton = 2,000 pounds (lb)	= 0.9 tonne (t)	1 tonne (t)	= 1,000 kilograms (kg) = 1.1 short tons
VOLUME (APPROXIMATE)		**VOLUME (APPROXIMATE)**	
1 teaspoon (tsp)	= 5 milliliters (ml)	1 milliliter (ml)	= 0.03 fluid ounce (fl oz)
1 tablespoon (tbsp)	= 15 milliliters (ml)	1 liter (l)	= 2.1 pints (pt)
1 fluid ounce (fl oz)	= 30 milliliters (ml)	1 liter (l)	= 1.06 quarts (qt)
1 cup ©	= 0.24 liter (l)	1 liter (l)	= 0.26 gallon (gal)
1 pint (pt)	= 0.47 liter (l)		
1 quart (qt)	= 0.96 liter (l)		
1 gallon (gal)	= 3.8 liters (l)		
1 cubic foot (cu ft, ft^3)	= 0.03 cubic meter (m^3)	1 cubic meter (m^3)	= 36 cubic feet (cu ft, ft^3)
1 cubic yard (cu yd, yd^3)	= 0.76 cubic meter (m^3)	1 cubic meter (m^3)	= 1.3 cubic yards (cu yd, yd^3)
TEMPERATURE (EXACT)		**TEMPERATURE (EXACT)**	
[(x-32)(5/9)] °F	= y °C	[(9/5) y + 32] °C	= x °F

QUICK INCH - CENTIMETER LENGTH CONVERSION

Inches	0			1			2		3			4		5
Centimeters	0	1	2	3	4	5	6	7	8	9	10	11	12	13

QUICK FAHRENHEIT - CELSIUS TEMPERATURE CONVERSIO

°F	-40°	-22°	-4°	14°	32°	50°	68°	86°	104°	122°	140°	158°	176°	194°	212°
°C	-40°	-30°	-20°	-10°	0°	10°	20°	30°	40°	50°	60°	70°	80°	90°	100°

For more exact and or other conversion factors, see NIST Miscellaneous Publication 286, Units of Weights and Measures. SD Catalog No. C13 10286

Acknowledgements

The authors of this report wish to express their sincere gratitude to all who helped make this a successful study, including contracted test pilots Bill Sprague and Chuck Perry, whose professional flying enabled the collection of sufficient test data with a minimum number of passbys. The staff at Fairchild International Airport was also instrumental in the successful completion of this study. In particular, the efforts of Doug Sandau, Port Angeles Airport and Marina Manager, and Jeff Williams, Fairchild International Airport Maintenance, were invaluable.

Table of Contents

Section Page

1 INTRODUCTION 10
1.1 Background and Objectives 10
1.2 Report Organization 11

2 TEST AIRCRAFT DESCRIPTIONS 12
2.1 Cessna 182S Skylane 12
2.2 De Havilland Canada DHC-2 Beaver 12

3 MEASUREMENT DATES AND TEST SITES 14
3.1 Measurement Schedule 14
3.2 Source Noise Measurement Site 14
3.3 Water Landing Measurement Site 15

4 INSTRUMENTATION 17
4.1 Acoustic System 17
4.2 Aircraft Tracking System 18
4.3 Onboard Aviation Instrumentation 21
4.4 Meteorological System 21
4.5 Digital Photo Scaling 22

5 MEASUREMENT SETUP 24
5.1 Source Noise Measurements 24
5.2 Water Landing Noise Measurements 26

6 MEASUREMENT PROCEDURES 28
6.1 Acoustic Technicians 28
6.1.1 Deployment 28
6.1.2 During an Event 28
6.1.3 End of Measurement Day 29
6.2 Test Director 29
6.2.1 Deployment 29
6.2.2 During an Event 29
6.2.3 End of Measurement Day 30
6.3 TSPI System Operator 30
6.3.1 Deployment 30
6.3.2 During an Event 30
6.3.3 End of Measurement Day 30

7 TEST SERIES DESCRIPTIONS 31
7.1 Series Definitions for Source Noise Measurements 31
7.2 Water Landing Noise Measurement Series 32

7.3 DHC-2 Lateral Directivity Noise Measurement Series 33
7.4 Summary of Events Collected 34

8 DATA PROCESSING AND NOISE MODEL DATA DEVELOPMENT 37
8.1 Noise Metrics 37
8.2 Data Development Methodology 37
8.3 Volpe Center Data Processing Software 37
8.3.1 MiniFAR Version 2.05 38
8.3.2 LCorrect 40
8.4 Noise-Power-Distance Curves 41
8.5 Spectral Classes 41

9 QUALITY ASSURANCE 43
9.1 Calibration 43
9.2 Time of Day 43
9.3 External Contamination 43
9.4 Test Aircraft TSPI 44

10 RESULTS 45
10.1 Source Noise Results 45
10.2 Appendix F Certification Noise Results 45
10.3 Water Landing Noise Results 47
10.4 DHC-2 Lateral Directivity Noise Results 48

APPENDIX A: AIRCRAFT PERFORMANCE DATA 53
A.1 Cessna 182S 53
A.1.1 Aircraft Descriptions and Performance Data 53
A.1.2 Aerodynamic Coefficients (B, C, D) 55
A.1.3 Aerodynamic Coefficients (R) 59
A.1.4 INM Data 62
A.2 De Havilland DHC-2 62
A.2.1 Aircraft Description and Performance Data 62
A.2.2 Aerodynamic Coefficients (B, C, D) 63
A.2.3 Aerodynamic Coefficients (R) 66
A.2.4 INM Data 69

APPENDIX B: METEOROLOGICAL DATA 70

APPENDIX C: TIME SPACE POSITION INFORMATION (TSPI) 72

APPENDIX D: AIRCRAFT NOISE POWER DISTANCE DATA 75
D.1 Cessna 182S Noise Power Distance Tables 76
D.2 De Havilland Canada DHC-2 Noise Power Distance Tables 79
D.3 Cessna 182S LAE NPD Plots 82
D.4 De Havilland Canada DHC-2 LAE NPD Plots 86

APPENDIX E: SPECTRAL CLASS 89
E.1 Cessna 182S Spectral Class Comparison 90
E.2 DHC-2 Spectral Class Comparison 93

APPENDIX F: ACRONYMS AND ABBREVIATIONS 95

REFERENCES 97

List of Figures

Figure Page

Figure 1. Cessna 182S Skylane Test Aircraft ... 12
Figure 2. DHC-2 Beaver Test Aircraft ... 13
Figure 3. Aerial Photo of Fairchild International Airport ... 15
Figure 4. Location of Water Landing Noise Measurements ... 16
Figure 5. Acoustic Instrumentation Setup ... 17
Figure 6. TSPI DGPS Base Station Setup ... 19
Figure 7. TSPI DGPS Rover Unit Setup ... 19
Figure 8. Meteorological Instrumentation Setup ... 22
Figure 9. Microphone and Test Director Locations ... 24
Figure 10. Overhead View of an Acoustic Station Setup ... 25
Figure 11. Side View of Microphone Orientation ... 26
Figure 12. Water Landing Noise Measurements Microphone and Test Area Locations ... 26
Figure 13. Microphone Placed on Ediz Hook for Water Landing Noise Measurements ... 27
Figure 14. Overhead View of Event Series 900: Water Landing Noise ... 33
Figure 15. Overhead View of a Pair of Example Lateral Directivity Events ... 34
Figure 16. Overview of the MiniFAR Process ... 39
Figure 17. MiniFAR Graphical User Interface ... 39
Figure 18. LCorrect Process ... 40
Figure 19. Comparison of 182S Spectra of Water Landing and Approach Events ... 47
Figure 20. Comparison of DHC-2 Spectra of Water Landing and Approach Events ... 48
Figure 21. Exhaust System of the DHC-2 Installed on Right Side of the Aircraft ... 51
Figure 22. Spectral Comparison of Left and Right Side of the DHC-2 ... 52
Figure 23. TSPI Plot of an 182S Simulated Departure from Land ... 57
Figure 24. TSPI Plot of Departure from Water ... 57
Figure 25. TSPI Plot of a Series 400 Departure Cruise Climb ... 60
Figure 26. Regression Line Used to Define Angle of Departure for the 182S ... 60
Figure 27. TSPI Plot of a DHC-2 Departure ... 65
Figure 28. TSPI Plot of a Series 300 Standard Departure ... 67
Figure 29. Regression Line Used to Derive Angle of Departure for the DHC-2 ... 68
Figure 30. 182S 100 Series LAE Data (Ref. Spd. = 160 kts.) ... 82
Figure 31. 182S 200 Series LAE Data (Ref. Spd. = 160 kts.) ... 82
Figure 32. 182S 300 Series LAE Data (Ref. Spd. = 160 kts.) ... 83
Figure 33. 182S 400 Series LAE Data (Ref. Spd. = 160 kts.) ... 83
Figure 34. 182S 500 Series LAE Data (Ref. Spd. = 160 kts.) ... 84
Figure 35. 182S 600 Series LAE Data (Ref. Spd. = 160 kts.) ... 84
Figure 36. 182S Event 910 (Water Landing) LAE Data (Ref. Spd. = 160 kts.) ... 85
Figure 37. DHC-2 100 Series LAE Data (Ref. Spd. = 160 kts.) ... 86
Figure 38. DHC-2 300 Series LAE Data (Ref. Spd. = 160 kts.) ... 86
Figure 39. DHC-2 400 Series LAE Data (Ref. Spd. = 160 kts.) ... 87
Figure 40. DHC-2 500 Series LAE Data (Ref. Spd. = 160 kts.) ... 87
Figure 41. DHC-2 600 Series LAE Data (Ref. Spd. = 160 kts.) ... 88

Figure 42. DHC-2 Event 940 (Water Landing) LAE Data (Ref. Spd. = 160 kts.) 88
Figure 43. 182S Average 1000-ft 100 Series LFO Spectrum (normalized) 90
Figure 44. 182S Average 1000-ft 200 Series LFO Spectrum (normalized) 90
Figure 45. 182S Average 1000-ft 300 Series DEP Spectrum (normalized) 91
Figure 46. 182S Average 1000-ft 400 Series DEP Spectrum (normalized) 91
Figure 47. 182S Average 1000-ft 500 Series APP Spectrum (normalized) 92
Figure 48. 182S Average 1000-ft 600 Series APP Spectrum (normalized) 92
Figure 49. DHC-2 Average 1000-ft 100 Series LFO Spectrum (normalized)............................. 93
Figure 50. DHC-2 Average 1000-ft 300 Series DEP Spectrum (normalized)............................. 93
Figure 51. DHC-2 Average 1000-ft 400 Series DEP Spectrum (normalized)............................. 94
Figure 52. DHC-2 Average 1000-ft 500 Series APP Spectrum (normalized)............................. 94
Figure 53. DHC-2 Average 1000-ft 600 Series APP Spectrum (normalized)............................. 94

List of Tables

Table | Page

Table 1. Characteristics of the Cessna 182S Skylane 12
Table 2. Airplane Characteristics of the DHC-2 Beaver Test Aircraft 13
Table 3. Measurement Schedule 14
Table 4. LD824 Settings 18
Table 5. TAMS System Specifications and Measurement Tolerances 22
Table 6. Microphone Locations and Orientation 25
Table 7. 182S Test Series Descriptions 32
Table 8. DHC-2 Test Series Descriptions 32
Table 9. Measured Aircraft Noise Data and Specifications for Appendix F Certification Events 46
Table 10. L_{ASmx} Comparison of Left and Right Side Noise Levels of the DHC-2 49
Table 11. L_{AE} Comparison of Left and Right Side Noise Levels of the DHC-2 49
Table 12. L_{PNTSmx} Comparison of Left and Right Side Noise Levels of the DHC-2 50
Table 13. L_{EPN} Comparison of Left and Right Side Noise Levels of the DHC-2 50
Table 14. Summary of Performance Parameters During 182S Flight Tests 53
Table 15. Summary of 182S INM Coefficients 62
Table 16: Summary of Performance Parameters During DHC-2 Flight Tests 63
Table 17. Summary of DHC-2 INM Parameters 69
Table 18. Cessna 182S Event Meteorological Data 70
Table 19. De Havilland DHC-2 Event Meteorological Data 71
Table 20. Cessna 182S Event TSPI Data 73
Table 21. De Havilland DHC-2 Event TSPI Data 74
Table 22. Cessna 182S L_{AE} NPDs 76
Table 23. Cessna 182S L_{ASmx} NPDs 76
Table 24. Cessna 182S LEPN NPDs 77
Table 25. Cessna 182S L_{PNTSmx} NPDs 77
Table 26. Cessna 182S Water Landing NPDs 78
Table 27. De Havilland Canada DHC-2 L_{AE} NPDs 79
Table 28. De Havilland Canada DHC-2 L_{ASmx} NPDs 79
Table 29. De Havilland Canada DHC-2 L_{EPN} NPDs 80
Table 30. De Havilland Canada DHC-2 L_{PNTSmx} NPDs 80
Table 31. De Havilland Canada DHC-2 Water Landing NPDs 81
Table 32. INM Spectral Class Assignments 89

1 INTRODUCTION

1.1 Background and Objectives

The National Parks Air Tour Management Act of 2000 (NPATMA)[1] calls for the regulation of commercial air tour operations over units of the National Park system, and directs the Federal Aviation Administration (FAA), with the cooperation of the National Park Service (NPS), to develop Air Tour Management Plans (ATMPs) for all National Parks with commercial air tours[*]. Currently, approximately 85 parks will need ATMPs. The Volpe National Transportation Systems Center (Volpe Center) is providing technical support to the ATMP program. An important element of this support is the computer modeling of air tour aircraft, which is used in the assessment potential noise impacts to the National Park resources. In accordance with the results of the Federal Interagency Committee on Aircraft Noise (FICAN) review,[2,3] the FAA's Integrated Noise Model (INM) Version 6.2[4,] is the best-practice modeling methodology currently available for evaluating aircraft noise in the National Parks[†,5,6]. INM Version 6.2 was the latest version at the time of this determination. Since then, INM Versions 6.2a, 7.0, 7.0a, 7.0b, 7.0c which have further algorithmic and database updates, have been released. Further, the FAA has begun developing the Aviation Environmental Design Tool (AEDT), a new tool that will allow for the evaluation of noise, emissions and fuel burn interdependencies. AEDT will incorporate and expand upon the capabilities of existing FAA environmental tools, including INM.

INM has a comprehensive aircraft database and is regularly updated with new aircraft source data. The FAA seeks to enhance the INM aircraft database for ATMP-related analyses by collecting noise source data suitable for modeling the many flight configurations flown by air tour aircraft in National Parks. Based on the Volpe Center's review of INM's aircraft source noise database and the aircraft known to be used to conduct air tours in National Parks[‡], the FAA sponsored noise and performance data collection and development for the following two floatplane aircraft: Cessna 182S Skylane and de Havilland Canada DHC-2 Beaver.

In September of 2010, the Volpe Center conducted controlled noise measurements of the 182S and DHC-2. The objective of the measurements was to collect source noise and performance data suitable for modeling various flight configurations flown by air tour aircraft, and fulfill the data input requirements for both INM and AEDT. At the request of the FAA, Volpe also conducted two additional sets of measurements; a) Federal Aviation Regulations Part 36[7] (FAR 36) Appendix F noise certification type measurements, when applicable, to update FAA's

---

[*] With the exceptions of parks in Alaska and the Grand Canyon

[†] Since 1978, the standard tool for conducting aircraft noise assessments has been the FAA's INM. INM is a computer program used by over 700 organizations in more than 50 countries to assess changes in noise impact due to aircraft operations. Requirements for the use of INM use are defined in FAA Order 1050.1E, Environmental Impacts: Policies and Procedures and Federal Aviation Regulations (FAR) Part 150, Airport Noise Compatibility Planning.

[‡] The FAA is in the process of developing an Air Tour Operating Authority (ATOA) data repository (database) to record, track and manage Interim Operating Authority (IOA) and Operating Authority (OA) information on commercial air tour operators and the National Park units over which they operate.

Advisory Circular AC-93-2 on quiet technology designation and b) noise measurements of amphibious aircraft during water landings.

1.2 Report Organization

This report is organized into nine sections and eight appendices:

- Section 1 presents the background and objective of the noise measurements, as well as an outline of this document
- Section 2 describes the two test aircraft used during noise measurements
- Section 3 discusses the measurement schedule, site selection process, and an overview of the selected measurement site
- Section 4 describes the instrumentation used for the measurements
- Section 5 is an overview of instrumentation and personnel locations during measurements
- Section 6 discusses the measurement protocol executed during measurements
- Section 7 provides descriptions of the measurement series as well as a summary of events collected
- Section 8 discusses the data processing procedures and the transformation of the collected data into a form suitable for noise models
- Section 9 provides a summary of the measurement results
- Appendix A presents the aircraft performance data necessary for INM / AEDT database tables
- Appendix B provides the test day meteorological data
- Appendix C provides the time-space-position-information data for the test aircraft
- Appendix D highlights the computed noise-power-distance tables for each test aircraft
- Appendix E presents the spectral class assignments and a comparison of the spectral data collected
- Appendix F provides a list of acronyms and abbreviations used in this report

2 TEST AIRCRAFT DESCRIPTIONS

2.1 Cessna 182S Skylane

The Cessna 182S is a single-engine, propeller-driven aircraft designed and manufactured by Cessna Aircraft Company. The 182S, first flown in July 1996, is an updated version of the 182, sporting a newer engine (see Table 1 below), interior, and avionics panel. The aircraft is designed to carry 1 crew member and up to 3 passengers. The amphibious, floatplane version of the 182S was the test aircraft for this study.

Figure 1. Cessna 182S Skylane Test Aircraft

Table 1. Characteristics of the Cessna 182S Skylane

Aircraft Manufacturer	Cessna Aircraft Company
Aircraft Model	182S Skylane
Aircraft Type	Single Propeller
Maximum Gross Take-off Weight (lb)	3,100
Number and Type of Engine(s)	1 Textron Lycoming IO-540-AB1A5
Engine Horse Power (HP)	230
Blade Manufacturer / Model Number	Hartzell / HC-F3YR-1RF (3 bladed)
Number of Passengers	3

2.2 De Havilland Canada DHC-2 Beaver

The DHC-2 is a single-engine, propeller-driven engine aircraft designed and manufactured by de Havilland Canada. The aircraft can be equipped with either a Pratt & Whitney (P&W) R985 radial piston engine or a P&W PT6A6 turboprop engine, which offers higher horsepower and higher take-off weight. The test aircraft for this study was equipped with the R985 piston engine. The aircraft is designed to carry 2 crew members and up to 6 passengers. The aircraft used during measurements was the *non*-amphibious version of the DHC-2.

Figure 2. DHC-2 Beaver Test Aircraft

Table 2. Airplane Characteristics of the DHC-2 Beaver Test Aircraft

Aircraft Manufacturer	De Havilland Canada
Aircraft Model	DHC-2 Beaver Mk I
Aircraft Type	Single Propeller
Maximum Gross Take-off Weight (lb)	5,090
Number and Type of Engine(s)	(1) Pratt & Whitney R985 AN14B
Engine Horse Power	450
Blade Manufacturer / Model Number	Hartzell HC-B3R30 (3 bladed)
Number of Passengers	6

3 MEASUREMENT DATES AND TEST SITES

3.1 Measurement Schedule

The measurement dates and test aircraft flown are summarized in Table 3 below.

Table 3. Measurement Schedule

Date	Aircraft	Measurement Type
Tuesday 9/21/10	182S	Source Data
Wednesday 9/22/10	DHC-2	Source Data
Thursday 9/23/10	AM: 182S PM: DHC-2	Water Landing

3.2 Source Noise Measurement Site

Acoustical considerations in selecting the measurement site location included the following:

- To minimize the effect of altitude on aircraft performance, the elevation of the measurement site should be below 2,000 feet above mean sea level (AMSL);
- To lessen the risk of external acoustic contamination, a measurement site should have a relatively quiet ambient environment with minimal aircraft operations; and
- To eliminate the need of acoustic corrections due to terrain undulations, the measurement site should have a long stretch of flat terrain near the test runway, where a microphone array is expected to be placed.

Final selection of a measurement site was made through a screening process of potential sites considering the above factors, as well as the proximity of potential test aircraft. This minimized both the fuel and time costs of chartered aircraft. Because the available DHC-2 Beaver test aircraft was a non-amphibious floatplane i.e., could only land on water, a measurement site near a water dock was required. Volpe personnel typically board the aircraft on the day of the test to install and operate the aircraft tracking system, as well as assist the pilot's navigation during test runs.

After review of the above considerations, William Fairchild International Airport (FAA identifier: CLM, elevation: 291 ft) located in Port Angeles, WA, was selected. It was determined in a previous, unrelated noise study, that CLM was well-suited for noise measurements, meeting the above considerations for a measurement site. CLM is also in close proximity to both the chartered aircraft and an accessible water dock.

Figure 3 provides an aerial view of CLM with the test runway, microphone locations, and nominal flight path identified. CLM has two asphalt paved runways (08-26 and 13-31). During the previous noise measurement program at CLM it was determined that the northwest end of runway 08-26 was the best test runway because of its isolation from other noise sources and also the available space to place a microphone array. As such, the test aircraft flew alongside Runway 08-26, from southeast to northwest, during the noise measurements. The centerline microphone was set up at the northwest end of Runway 08-26. The sideline microphone was located 500 feet from the centerline microphone.

Figure 3. Aerial Photo of Fairchild International Airport

3.3 Water Landing Measurement Site

In addition to the source noise measurements, the Volpe Center conducted noise measurements of the test floatplanes landing on water. This test was conducted at the Port Angeles Harbor, approximately three miles away from CLM. Figure 4 below is an aerial photo of the testing area, identifying the location of the microphone system during measurements. Also highlighted in the photo is the dock where Volpe technicians boarded the aircraft to install the aircraft tracking system (later discussed in Section 4.2) on the non-amphibious DHC-2 test aircraft.

Figure 4. Location of Water Landing Noise Measurements

4 INSTRUMENTATION

This section presents a description of the instrumentation used during the Floatplane source noise measurements.

4.1 Acoustic System

Each acoustic system consisted of a Brüel and Kjær (B&K) Model 4189 ½-inch electret microphone powered by a B&K Model 2671 preamplifier. A B&K Model UA0207 3.5-inch windscreen was used to reduce wind-generated noise on the microphone diaphragm. The microphone, preamplifier, and windscreen were installed on top of a tripod with the microphone diaphragm set at 4 feet above ground level (AGL). The primary recording device was a Larson Davis Model 824 (LD824) sound level meter/real-time spectral analyzer. Data were also recorded simultaneously with a backup Sound Devices Model 744T (SD744T) digital audio recorder. A GPS time-code generator, Masterclock model GPS200A, was used to provide the backup recording device with an accurate time base. The primary recording device time was also synched manually to the GPS time-code generator. The acoustic instrumentation setup is presented in Figure 5. Table 4 shows the settings used for the LD824 during data collection.

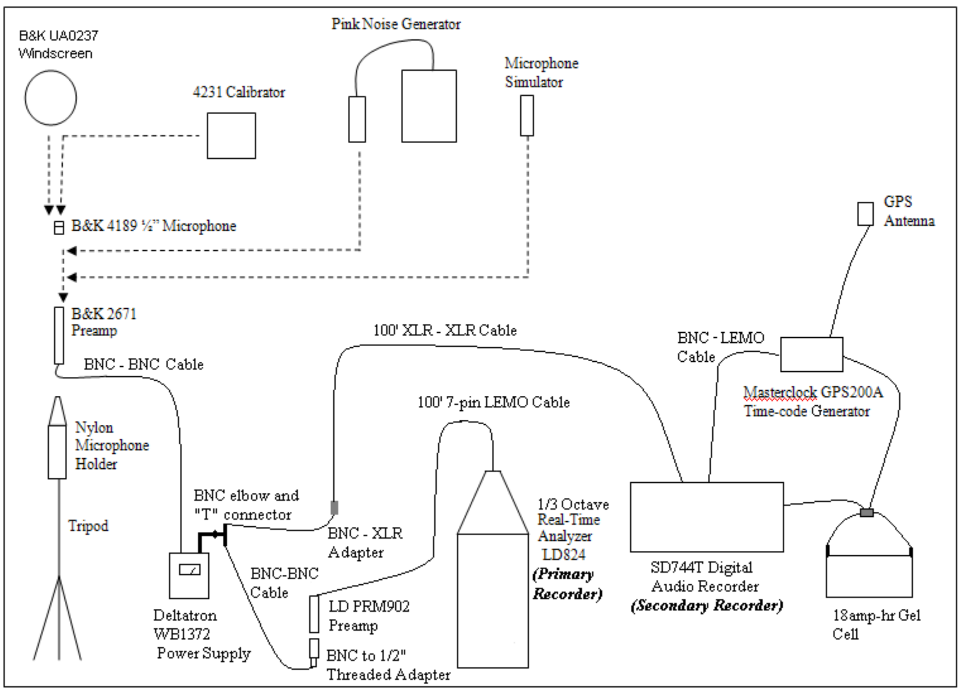

Figure 5. Acoustic Instrumentation Setup

Table 4. LD824 Settings

Parameter	Setting
Detector	Slow
Broadband Frequency Weighting	A
Spectra Bandwidth	$^1/_3$ Octave Band
Spectra Frequency Weighting	Flat
Time History Interval	½ Second

4.2 Aircraft Tracking System

A differential Global Positioning System (DGPS) was used as the primary aircraft guidance and tracking system during measurements. The specific system was the Time-Space-Position-Information (TSPI) System Version 6.591, a DGPS designed by the Volpe Center for use in transportation environmental measurements (refer to Volpe Center Time-Space-Position-Information System User's Guide[8] for more information). The Volpe Center TSPI system is configured to track vehicles in motion and survey stationary points to within ± 20 centimeter accuracy, while recording time-stamped X-Y-Z-coordinate position data at a rate of twice per second and velocity data once every two seconds. In addition to obtaining TSPI for test aircraft during measurements, the Volpe Center TSPI system serves additional purposes:

1. Conduct a site survey of the measurement site to establish a local coordinate system and determine instrumentation locations; and
2. Provide real-time guidance and position information of the aircraft to the pilot and Test Director.

The Volpe Center TSPI system consists of a base station and a rover unit, each of which receives GPS satellite signals via a receiver and transmits or receives differential corrections via a transceiver.

- **Base Station** – Consists of a NovAtel PROPAK-V3-RT2 receiver, GLB Model SNTR150 transceiver tuned to a frequency of 136.325 MHz, GPS antenna, radio antenna, and supporting cabling. See Figure 6 for a diagram of this portion of the system.

- **Rover Unit** - Usually installed onboard the test aircraft, consists of a NovAtel PROPAK-V3-RT2 receiver, GLB Model SNTR150 transceiver, a laptop installed with Volpe Center's TSPI software, and supporting cabling. Figure 7 depicts a typical Rover Unit setup onboard a test aircraft.

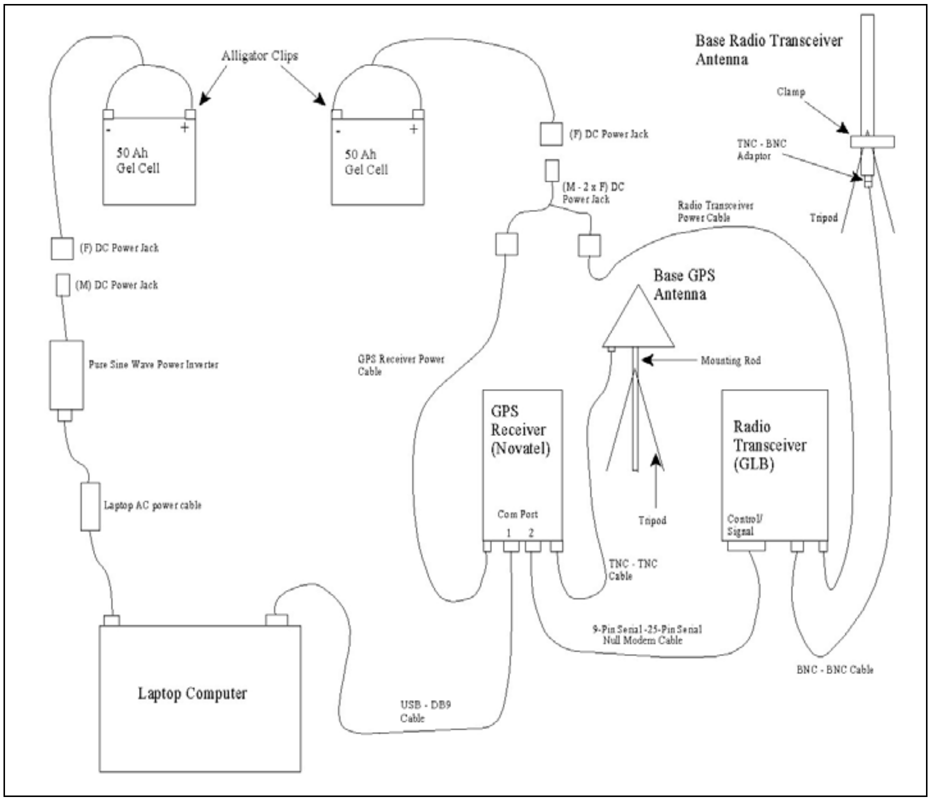

Figure 6. TSPI DGPS Base Station Setup

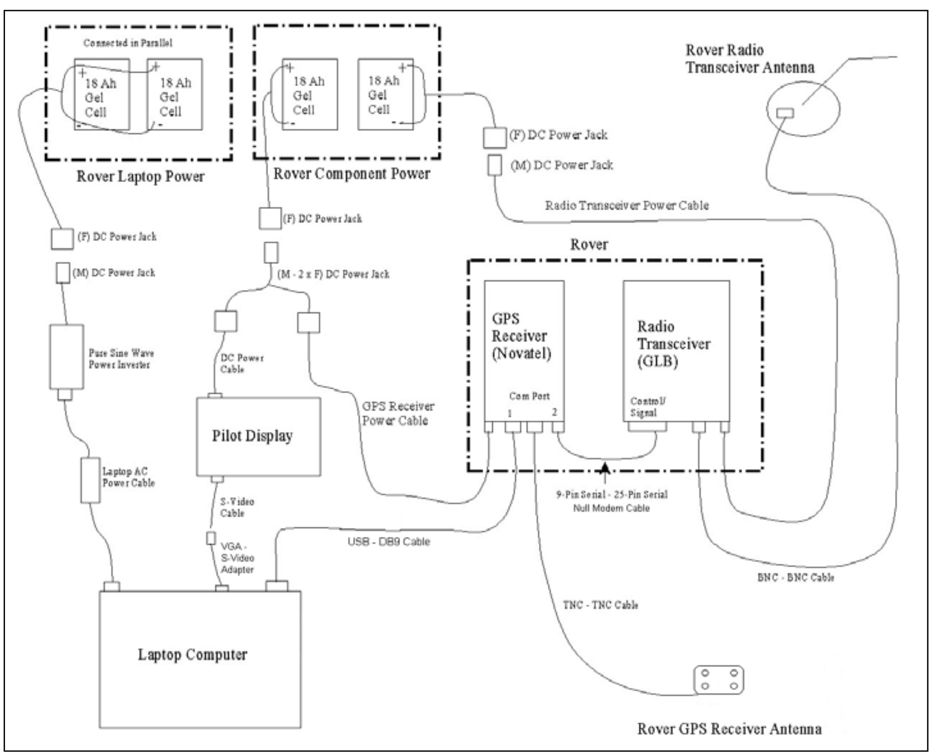

Figure 7. TSPI DGPS Rover Unit Setup

4.3 Onboard Aviation Instrumentation

The test aircraft were outfitted with standard instruments that tracked altitude, flight path, and speed of the aircraft. The onboard TSPI Rover operator was also equipped with a ContourHD helmet video camera in order to record video of the aircraft's instrument gauges. In the event the TSPI system was unavailable, a digital photo scaling method was planned to be used in conjunction with these recordings to determine aircraft position and state. This backup method was not used during data processing since the TSPI system was available throughout the recorded passbys.

4.4 Meteorological System

Two Qualimetrics Transportable Automated Meteorological Stations (TAMS) were used to measure surface wind speed and direction, relative humidity, air temperature, and barometric pressure at one-second intervals throughout the tests. Each of the TAMS units was positioned with sensors at 4 feet AGL to match the height of the microphones.

One TAMS unit was set up near the centerline microphone station as the primary data collection unit. The other unit was set up near the Test Director to provide a real-time display of the meteorological data; this allowed the Test Director to determine if meteorological conditions were within acceptable tolerances during each measurement run. The meteorological instrumentation setup is illustrated in Figure 8. Table 5 provides manufacturer-provided TAMS system specifications and measurement tolerances. Meteorological tolerances were based on Appendix F and G of FAR 36 and Chapter 8 of ICAO Annex 16[9] (Annex 16).

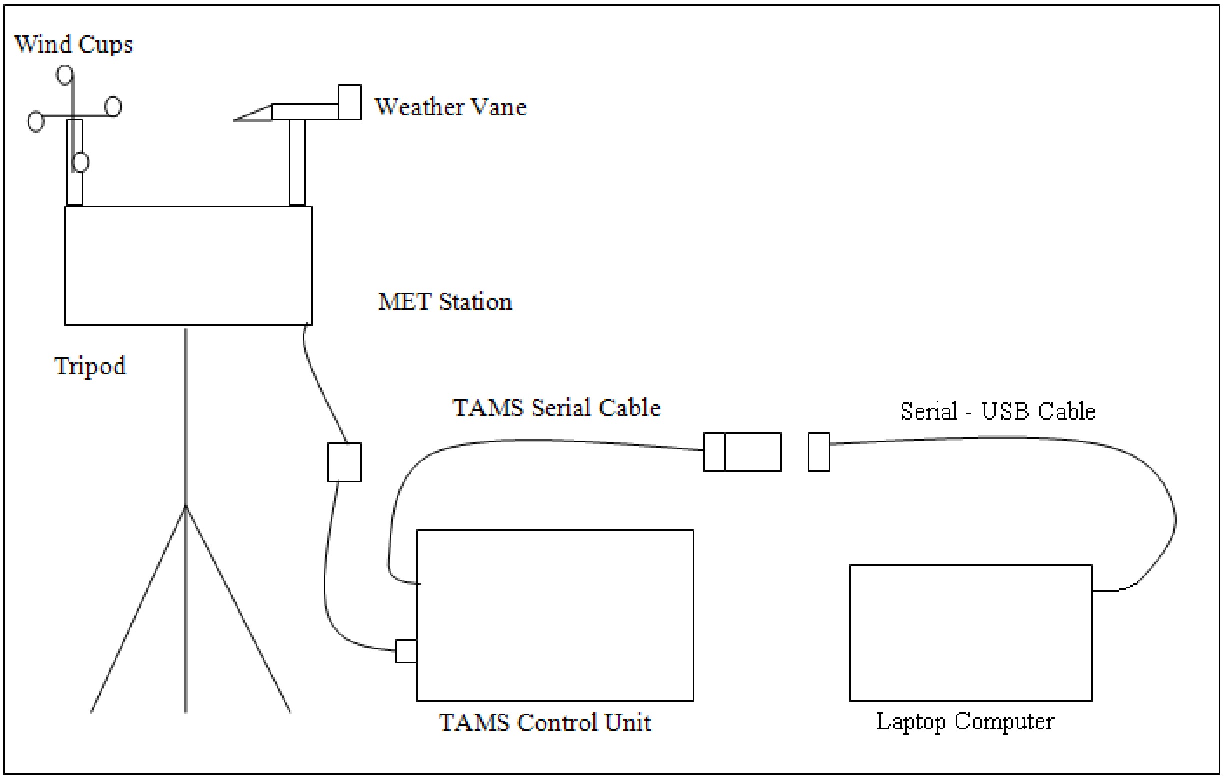

Figure 8. Meteorological Instrumentation Setup

Table 5. TAMS System Specifications and Measurement Tolerances

Data	Range	Resolution	Accuracy	FAR 36 / Annex 16 Measurement Limit
Temperature (^{0}F)	-40 to +130	1^{0}F	±1^{0}F	36 to 95^{0}F
Relative Humidity (%)	0 to 100%	1%	±3%	20 to 95%
Wind Speed (kts)	2 to 48	1	±1 or ±5%, whichever is greater	10 average*, 5 average crosswind*
Wind Direction (degrees)	0 to 360	10	±5 RMSE	N/A
Precipitation (in)	N/A	N/A	N/A	0

* The average velocity is determined using a 30-second averaging period spanning the 10 dB sound level rise and fall time interval.

4.5 Digital Photo Scaling

In the event the TSPI system was unavailable, tracking of the test aircraft would have been achieved by using a digital photo-scaling system. The system consisted of a Canon EOS D60 digital camera with a fixed focal length 200mm lens. It would have been used to photograph the test aircraft when it was directly overhead the centerline microphone location. Photo scaling allows for calculation of the altitude of the aircraft when it is flying over the centerline microphone, where it is assumed to be the loudest point in a flight path. The digital photo scaling system was located near the centerline microphone observers table.

It was not necessary to deploy the photo-scaling system during the tests.

5 MEASUREMENT SETUP

5.1 Source Noise Measurements

Two acoustic stations were set up during source noise measurements: a centerline and sideline microphone. The centerline microphone station was set up at the northwest end of Runway 08-26. The sideline microphone was located 500 feet from the centerline microphone. A Test Director was stationed in a centralized location with a full view of the flight path, but far enough away from the acoustic systems to avoid contamination of the acoustic data. The Test Director was also located in close proximity to a staging area for meeting with pilots and installing the TSPI system onboard the aircraft. Figure 9 provides an aerial view of CLM with the microphone and Test Director locations identified.

Figure 9. Microphone and Test Director Locations

At each microphone station, Volpe field technicians monitored and operated the acoustic recording instrumentation. The field technician and acoustic recording instrumentation were located at acoustic observer tables, approximately 100 ft from their respective microphones. This distance ensured field personnel did not contaminate the sound-level data. The placement of a field technician at each acoustic location also eliminated the need for long cables, which minimized the potential radio signal interference inherent to their use. Figure 10 shows an overhead schematic view of the acoustic observer tables relative to the microphones.

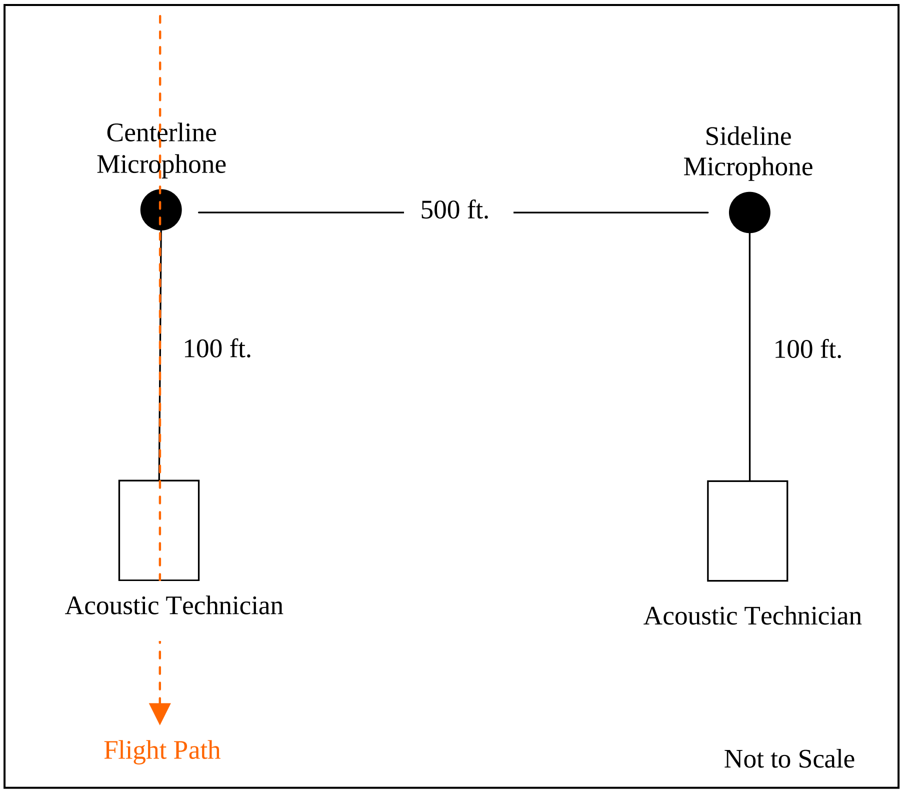

Figure 10. Overhead View of an Acoustic Station Setup

All the microphones were placed at 4 feet AGL and oriented nominally for grazing incidence i.e., diaphragm at 90 degrees relative to the anticipated direction of the noise source (centerline microphone) and at approximately 45 degrees for the sideline microphone. Table 6 summarizes this setup while Figure 11 illustrates a side view of a microphone configuration.

Table 6. Microphone Locations and Orientation

Microphone	X-Coordinate (ft)	Y-Coordinate (ft)	Height (ft)	Angle (°)
Centerline	0	0	4	90
Sideline	0	500	4	45

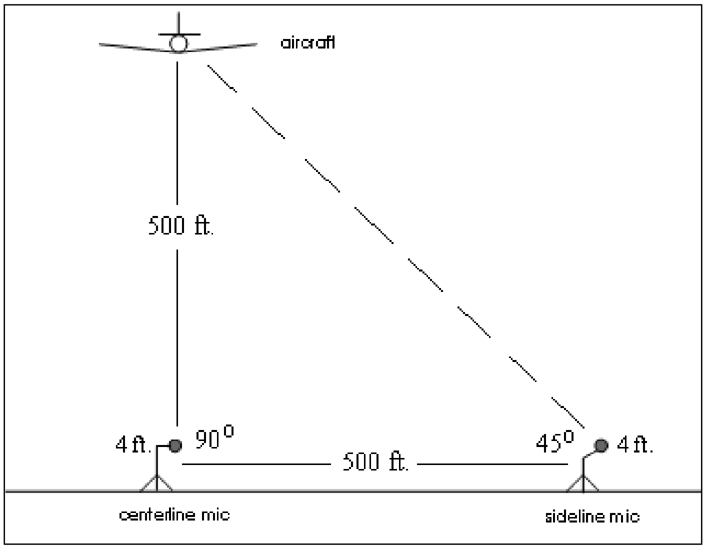

Figure 11. Side View of Microphone Orientation

5.2 Water Landing Noise Measurements

A single microphone system was set up on Ediz Hook, a strip of land partially encompassing Port Angeles Harbor. The landing area used for the noise measurements was in a body of water south of the microphone location, where floatplanes typically land in the harbor. Figure 12 shows the microphone location, test area, and nominal flight path of the test floatplanes during measurements.

Figure 12. Water Landing Noise Measurements Microphone and Test Area Locations

Similar to the source data noise measurements, a Volpe field technician monitored and operated the acoustic recording instrumentation approximately 100 ft from the microphone. The microphones were placed 4 feet AGL and oriented at an incident angle of 0°. The photo in Figure 13 shows the microphone set-up.

Figure 13. Microphone Placed on Ediz Hook for Water Landing Noise Measurements

6 MEASUREMENT PROCEDURES

This section describes the measurement procedures performed by Volpe technicians during the floatplane noise measurements.

6.1 Acoustic Technicians

6.1.1 Deployment

The acoustic systems were deployed at the locations as described in Section 5. The microphone tripods were anchored to the ground to avoid the risk of the tripod tipping over. A space blanket was secured to the operators table for rain contingency. All microphones were calibrated using the following standard procedure:

1. A B&K 4231 calibrator was mounted on the microphone and a sine wave signal of 114 decibels (dB) at 1 kHz was applied to the system. The LD824 was calibrated to this reference signal. One minute of calibration tone was recorded and levels indicated on the LD824 and 744T backup recorder were noted on log sheets.
2. The microphone was removed and a pink noise generator was applied to check the frequency response of the system. One minute of pink noise was recorded and levels indicated on the LD824 and 744T were noted on log sheets.
3. A microphone simulator was then applied to the system to measure the system noise floor and ensure no outside interference was present. At this point +20 dB gain was added to the LD824 to raise the lower range of the system to help identify any anomalous signals. One minute of the noise floor was recorded and levels indicated on the LD824 and 744T were noted on log sheets. The +20 dB gain was then removed from the LD824.
4. The microphone was replaced, and then the calibrator was reapplied to verify that the LD824 reads the same initial calibration reading performed in Step 1. Another minute of calibration tone was recorded and levels indicated on the LD824 and 744T were noted on log sheets.

6.1.2 During an Event

During an event, each acoustic technician performed the following:

- Recorded the maximum A-weighted slow-scale sound level (L_{ASmx}) observed on the LD824 on the log sheet. The observer also checked the L_{ASmx} for consistency and repeatability, i.e., the L_{ASmx} values for events in the same series should generally be similar in sound level.
- Confirmed and noted that the recording instrumentation indicated a minimum 20-dBA rise and fall during an event.
- Noted any audible external contamination.
- If possible, confirmed that the aircraft route was straight, at a constant speed with no anomalous flight characteristics, and over the centerline, as appropriate.
- Collected ambient measurements periodically throughout the measurement day.

- Performed a time synchronization using the Masterclock GPS200A throughout the measurement day.

At the end of each pass-by event, technicians at the sideline microphones signaled to the technician at the center position whether 20-dBA rise and fall was observed on their respective LD824. The technician at the center position then radioed to the Test Director if a 20-dBA rise and fall was attained at all microphone locations.

6.1.3 End of Measurement Day

At the end of the day a calibrator was reapplied to check for any drift that may have occurred during the day. Similar to during deployment, a minute of calibration tone was recorded and levels indicated on the LD824 and SD744T recorder were noted on log sheets. The systems were then broken down and removed from the site.

6.2 Test Director

6.2.1 Deployment

The TSPI tracking system base station and the primary meteorological system were deployed at the Test Director's location. While the field team deployed the acoustic, TAMS, and TSPI systems the Test Director, TSPI System Operator (see Section 6.3), and pilots conducted a Pilot Brief, including discussions regarding the test flight series to be flown, as well as communication protocols, local terrain features, and aircraft operations.

6.2.2 During an Event

During an event, the Test Director performed the following:

- Announced, via 2-way radio, the start of an event, including event number.
- Monitored the tracking data to verify the aircraft was within tolerances.
- Listened for potential external contamination.
- Monitored wind speed in real time via the TAMS meteorological system.
- Recorded the following in the log sheet:
    - Wind speed and direction;
    - Tracking information; and
    - Any external contamination.
- Announced, via 2-way radio, the end of event.

After the end of an event, the Test Director received an update from the acoustic technicians as to the event quality at their microphone locations. Based on their input, monitored wind speed and aircraft tracking data, and input from the pilot, a determination was made on the overall quality of the event; this was done to ensure that an adequate number of events were collected for each series. The Test Director then identified the next event series and number and announced it to the pilot and acoustic technicians.

6.2.3 End of Measurement Day

At the end of the day the Test Director, TSPI System Operator, and pilots conducted a Pilot Debrief. During this briefing the quality of individual events was discussed, and potential improvements for future implementation were identified.

6.3 TSPI System Operator

6.3.1 Deployment

The TSPI system rover unit was installed onboard the test aircraft prior to measurements at the staging area. The Test Director, TSPI System Operator, and pilots conducted the Pilot Brief, while the field team deployed the acoustic, TAMS, and TSPI systems.

6.3.2 During an Event

During an event, the TSPI System operator performed the following:

- Selected tolerances for the pilot guidance display.
- Verified the Test Director was receiving data from the rover station.
- Monitored the TSPI system to verify that the pilot flew within the assigned tolerances.
- Recorded actual flight parameters (Power, flaps, speed, and inlet turbine temperature) during the event.

The TSPI System Operator was also responsible for continued communication with the pilot throughout the events. This is important in general because pilots who do not regularly participate in noise measurement flight tests are not always aware of the ramifications of some decisions during flight. For this reason, the Volpe Center often deploys an acoustic technician who is also a certified pilot as the TSPI System Operator.

6.3.3 End of Measurement Day

At the end of the day the TSPI System Operator participated in the Pilot Debrief.

7 TEST SERIES DESCRIPTIONS

7.1 Series Definitions for Source Noise Measurements

The modeling methodology in INM relies strongly on the source noise and performance characteristics defined in its aircraft noise and performance database. Procedures for using and developing these databases are described in SAE-AIR-1845[10], the INM Technical Manual, and ECAC Document 29[11] / ICAO Document 9911[12]. The aircraft noise and performance database defines the noise source for an aircraft state and is structured in a way that allows the model to reflect how aircraft noise sources change with aircraft state.

The test series described in this section were designed to capture the test aircraft noise signature as a function of aircraft state. Typically the state of the aircraft includes the aircraft operational mode (e.g. departure) and its power state, although flap state and speed are also important factors. Changes in source noise due to aircraft speed are accounted for with modeling adjustments, which are discussed in later sections. Test series included level fly-over (LFO), approach (APP), and departure (DEP) flight configurations. The different test series were varied by:

- Flight configuration
    - Operational mode
    - Descent angle
    - Flap setting
- Reference altitude
- Reference speed
- Power settings

In addition, a series of 1,000 feet AGL LFO events with the test aircraft at maximum continuous power settings were flown to simulate the settings described in FAR 36 Appendix F, Section F36.111, “Flight Procedures”. These series are flown for research and comparison purposes.

Individual events for each test series were flown to have reasonable confidence in the collected data. This typically meant three passes that were free from observable external contamination, track deviations outside of acceptable limits, and acceptable meteorological conditions, for each series. Descriptions of the test series for each test aircraft are provided in Table 7 and 8.

Table 7. 182S Test Series Descriptions

Test Series	Description
100	LFO: Tour Cruise @ 500 ft
200	LFO: Normal Cruise* @ 500 ft
300	DEP: Standard
400	DEP: Cruise Climb
500	APP: Flaps Initial
600	APP: Flaps 20
800	LFO: Appendix F Certification Type
900	Water Landing

Table 8. DHC-2 Test Series Descriptions

Test Series	Description
100	LFO: Tour Cruise @ 500 ft
200	LFO: Appendix F Certification Type
300	DEP: Standard
400	DEP: Cruise Climb
500	APP: Flaps Initial
600	APP: Flaps Final
900	Water Landing

7.2 Water Landing Noise Measurement Series

Series 900 events were designated for water landing noise measurements and consisted of the test aircraft landing at targeted distances of 300, 600, 900, and 1,200 feet from the microphone. To best capture the noise created by the impact of the aircraft onto the water, the test aircraft attempted to land in an area directly in front of the microphone. As illustrated in Figure 14 below, this was done by several passbys at various distances from the microphone.

* The difference between tour and normal cruises are the reference speeds. Reference speeds were chosen to be representative of fast, normal cruise and slow, tour cruise speeds.

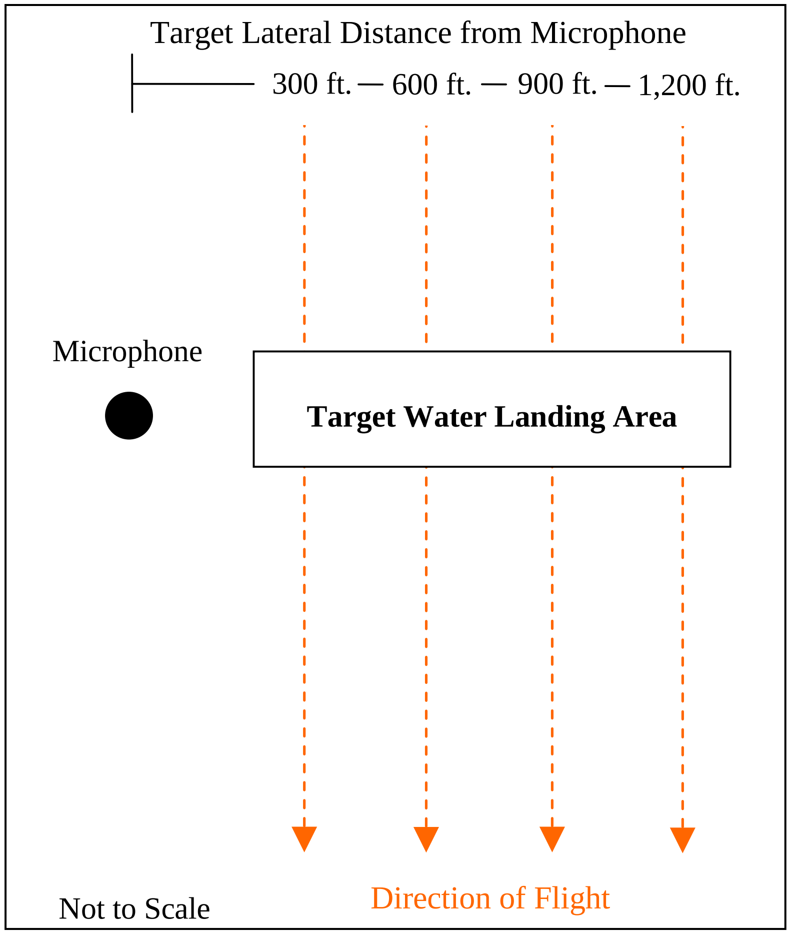

Figure 14. Overhead View of Event Series 900: Water Landing Noise

7.3 DHC-2 Lateral Directivity Noise Measurement Series

It was observed by field personnel during measurements that the DHC-2 exhibited louder noise levels at the sideline microphones than the centerline microphone. This was later confirmed during review of the processed NPD data, which can be found in Appendix D of this report. Accordingly, an additional series of LFOs was flown in the opposite direction in order collect data to check for lateral directivity of the DHC-2 (e.g., data for the other side of the aircraft). This supplemental series consisted of the DHC-2 test aircraft performing tour cruises at 500 feet, similar to the Series 100 events, with a sideline microphone 500 feet to the left and then right of the aircraft (relative to direction of travel). Figure 15 below illustrates an example of a pair of DHC-2 lateral directivity measurements.

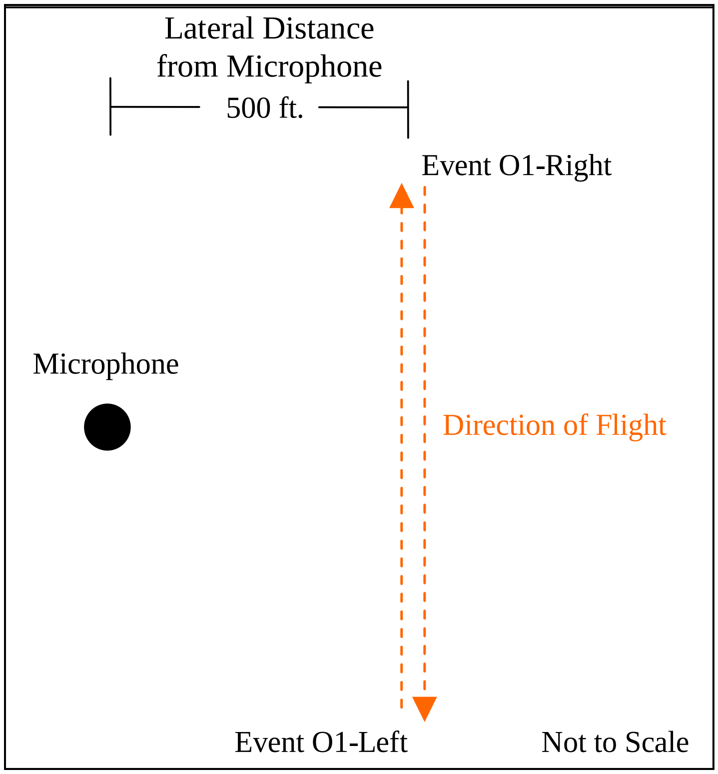

Figure 15. Overhead View of a Pair of Example Lateral Directivity Events

7.4 Summary of Events Collected

A total of 53 passby events were recorded during the 182S and DHC-2 source noise measurements. The events varied in flight configuration, reference altitude, power and speed as described in the previous section. Of the 53 total measured events, 41 passed quality assurance (QA, see Section 9). Only data from events that passed QA are included in the results and appendices of this report. Events were omitted on the following basis:

- *Contamination*, including an audible noise source from anything other than the test aircraft was detected during data recording by field personnel and/or identified later in the laboratory data analysis process (See Section 9.3); or
- *Incorrect aircraft settings*, including wrong power or flap setting, aircraft speed, or altitude and/or out-of-tolerance position.

For the water landing noise measurements, a total of 10 events were recorded. Of the 10 recorded events, 8 events were of poor acoustic quality, i.e., they were not loud enough to exceed the ambient noise by 10 decibels. Because the noise produced from the water landing did not exceed the 10 decibel rise and fall required in the FAR 36 / Annex 16 data processing methodology (described in the next Section), those events could not be evaluated. The only 2 events that were able to be processed and analyzed were the water landing events where the aircraft landed at approximately 200 feet from the microphone and barely exceeded the ambient noise by 10 decibels.

A total of 6 pairs of events were collected for the lateral directivity measurements of the DHC-2. Each pair of events consisted of the aircraft flying opposite directions of flight to capture noise levels from both sides of the aircraft. Three out of the six pairs of these events passed quality assurance and were evaluated.

8 DATA PROCESSING AND NOISE MODEL DATA DEVELOPMENT

This section describes the data reduction and analysis methodology undertaken to process the as-measured data and the procedures used to transform these data into a form suitable for the INM/AEDT*. Noise model data development included the production of Noise Power Distance (NPD) curves, which are series of noise metrics as a function of power and distance, and spectral class assignments. The process of developing the NPD and spectral class data are described in this section and the resultant data are presented in Appendix D and E, respectively.

8.1 Noise Metrics

NPD data for measured events were generated for four different noise metrics: sound exposure level (SEL), denoted by the ANSI[13] symbol L_{AE}; maximum, slow time- and A-weighted sound level (MXSA), denoted by the ANSI symbol L_{ASmx}; effective perceived noise level (EPNL), denoted by the ANSI symbol L_{EPN}; and tone-adjusted, maximum, slow time-weighted, perceived noise level (MXSPNT), denoted by the ANSI symbol L_{PNTSmx}. Appendix D provides these data in tabular format. Graphical representations of the NPD data are also presented in Appendix D for L_{AE} only.

8.2 Data Development Methodology

The as-measured sound pressure level (SPL), meteorological, and tracking data were processed in accordance with the FAR 36 / Annex 16 methodology to generate a set of sound level metrics. Specifically, the sound level metrics were derived using the FAR 36 / Annex 16 simplified procedure. In the simplified process L_{AE}, L_{ASmx}, L_{EPN}, and L_{PNTSmx} metrics are generated using as-measured spectral and tracking data taken at the time of L_{ASmx}. NPD curves generated in the simplified method are considered Type 2 NPDs within the FAR 36 framework. These metrics were derived for both microphones for each aircraft event, representing the center and sideline noise characteristics of the test aircraft.

8.3 Volpe Center Data Processing Software

To expedite the processing of large amounts of data using a modified version of the FAR 36 / Annex 16 simplified method, the Volpe Center utilized two internally developed, data processing software programs. The first, MiniFAR version 2.05, combines all field data and outputs a text file with calculated test day noise metrics. MiniFAR also contains an easy method for visually screening events for obvious contamination and missing data

* As noted earlier, the FAA has begun developing a new tool called the Aviation Environmental Design Tool (AEDT) that will allow for the evaluation of noise and emissions interdependencies. AEDT will incorporate and expand upon the capabilities of existing FAA tools, including INM.

parameters. LCorrect version 3.02 was then used to take the test day noise metrics from MiniFAR and adjust them to the SAE-AIR-1845 reference day conditions, which is commonly used for modeling purposes. LCorrect also generates the distance-based data needed to create NPD curves.

8.3.1 MiniFAR Version 2.05

MiniFAR requires the following as-measured data input parameters:

- Sound level time history;
- Aircraft TSPI data time history;
- Microphone locations (X, Y and Z, in local coordinates);
- Meteorological data time history;
- Corrections to be applied to the as-measured data, including microphone frequency response, windscreen insertion loss, and calibration drifts; and
- Observer logs that include event start and stop times, as well as notes on contamination (converted into comma delimited (.csv) files).

MiniFAR uses the above data and creates a single file containing event-based $L_{AE,}$ L_{ASmx}, L_{EPN}, L_{PNTSmx} data, along with the un-weighted, one-third octave spectra at the time of L_{ASmx}. MiniFAR also appends to this file supplemental data that may be easily referenced at a later time; these include slant dance, wind speed and direction, aircraft speed at time of max, etc. Figure 16 presents an overview of the MiniFAR process.

MiniFAR also allows the user to visually examine events as an initial screening for external contamination. The technician may use this capability to detect any missing input parameters that would affect the computation of the noise metrics. Figure 17 shows a screenshot of MiniFAR's user interface.

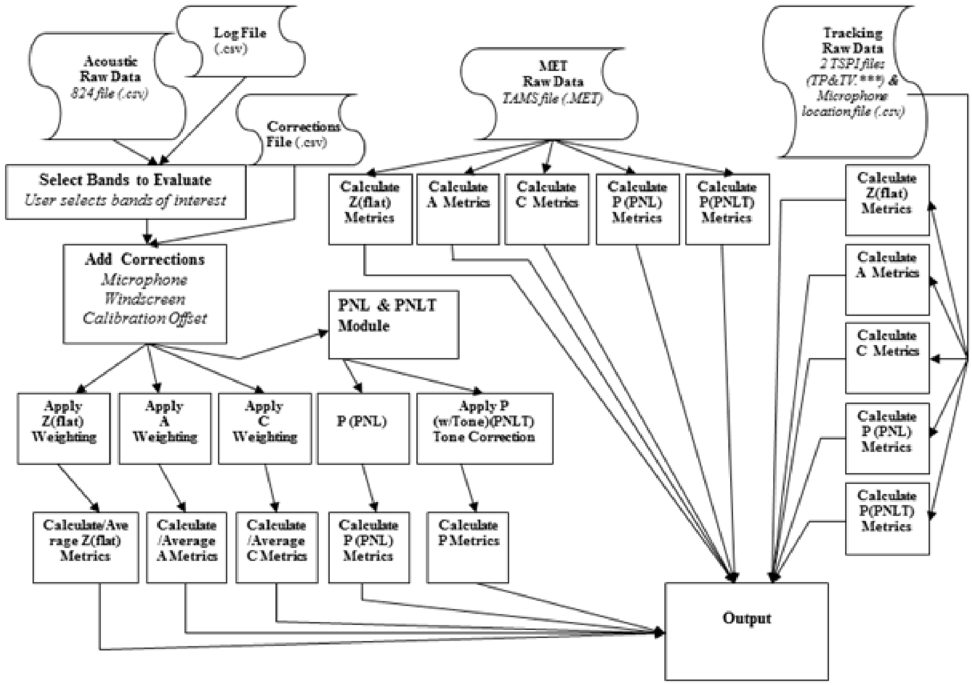

Figure 16. Overview of the MiniFAR Process

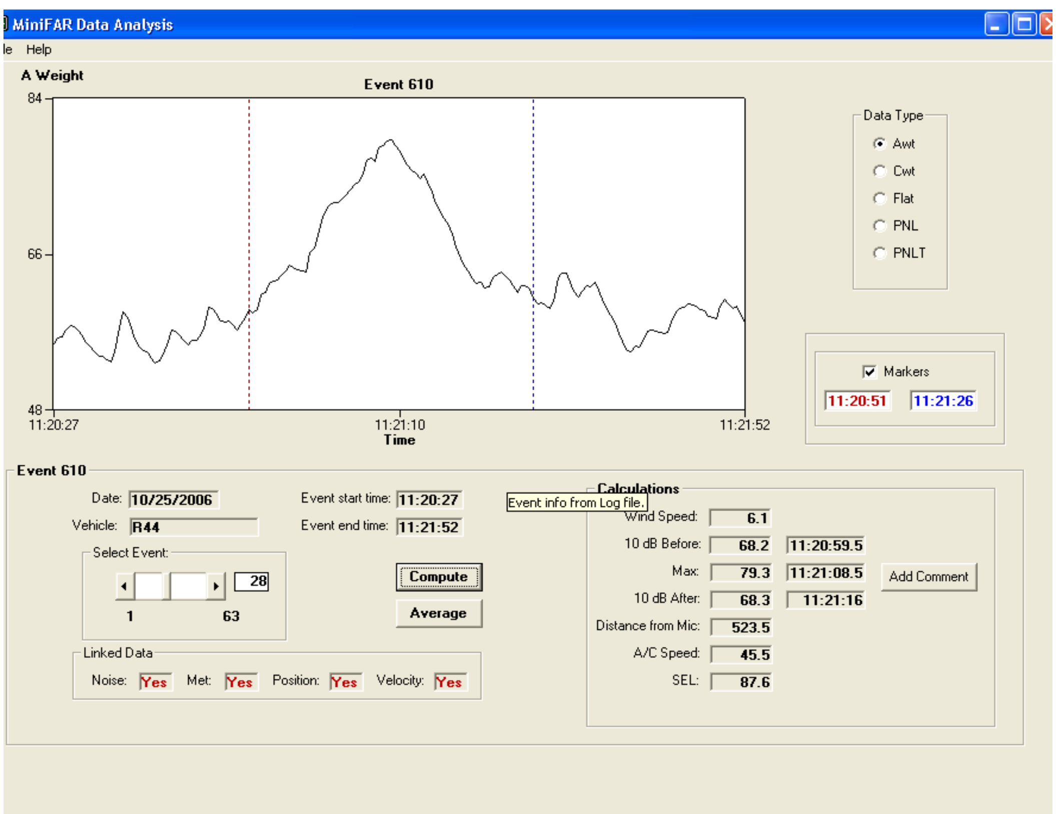

Figure 17. MiniFAR Graphical User Interface

MiniFAR averages the absolute- and cross-wind speeds for an event during data processing. These wind speeds were reviewed during processing and any events where the wind speeds exceeded the FAR 36 / Annex 16 absolute limit of 10 knots and/or the cross wind speed limit of 5 knots would have been discarded. A review of the wind speed data during processing resulted in 0 events discarded due to excessive wind speeds.

8.3.2 LCorrect

LCorrect uses the test day noise metrics, meteorological, aircraft speed, and slant distance results generated by MiniFAR to calculate noise metrics at 10 standard INM NPD distances, ranging from 200 to 25,000 feet, with SAE-AIR-1845 reference day atmospheric conditions. LCorrect also takes the un-weighted spectrum at time of maximum sound level produced by MiniFAR and adjusts it to the 10 aforementioned distances. For the purpose of INM database development, the spectrum adjusted to 1,000 feet was used. Figure 18 shows an overview of the LCorrect process.

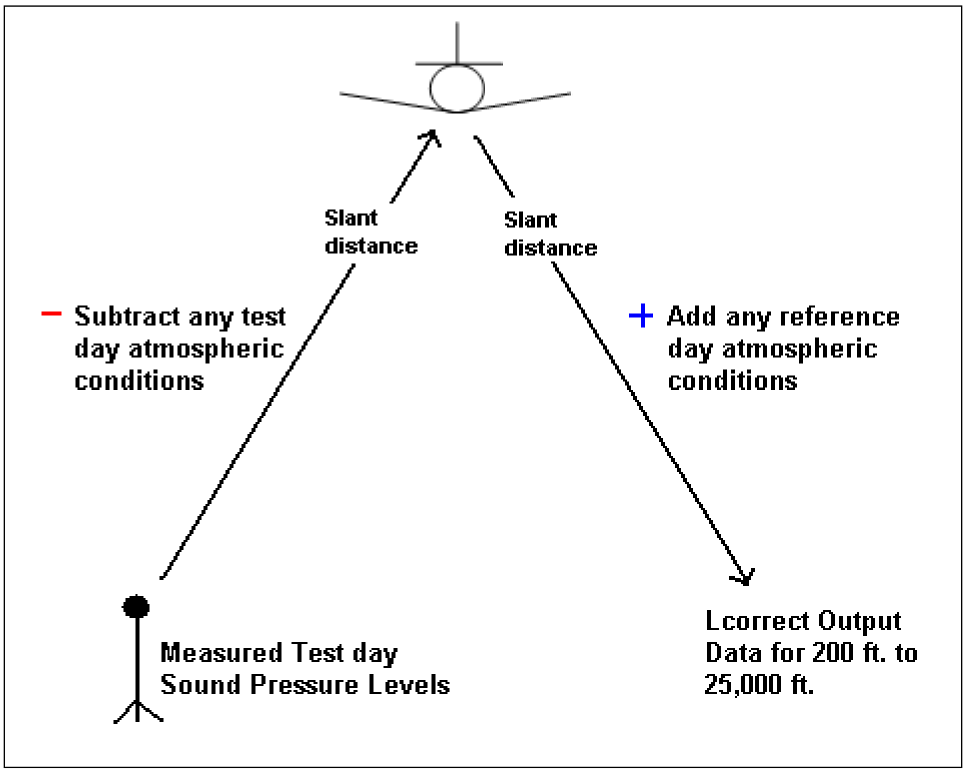

Figure 18. LCorrect Process

Consistent with SAE-AIR-1845 which, along with FAR 36 / Annex 16, is the foundation for processing data for inclusion in the INM / AEDT, NPD curves for exposure-based, fixed-wing aircraft noise metrics were adjusted in LCorrect to a reference speed of 160 knots. LCorrect computes the reference speed adjustment by applying a duration adjustment to the aircraft NPD curves in order to account for the effect of time-varying aircraft speed. This duration adjustment is made using the following equation from Section 3.7 of the INM Technical Manual:

$$DUR_{ADJ} = 10 \log_{10}[160/AS_{seg}] \qquad \text{[Eq. 1]}$$

where:

AS_{seg} is the aircraft reference speed at the closest point of approach between the aircraft and the microphone.

The L_{AE} and L_{EPN} values in Appendix D of this report are adjusted to the reference speed using the above methodology. Since the L_{ASmx} and L_{PNTSmx} metrics are assumed to be independent of speed, no duration adjustment is applied to these metrics. Test day and reference speeds are found in the TSPI data tables in Appendix C.

8.4 Noise-Power-Distance Curves

NPD curves for the center and sideline of the test aircraft for each event were generated with the software and method described in the previous section. The data for each event were then grouped by configuration and power setting (series), and arithmetically averaged together. The resulting NPD curves are presented in Appendix D for the $L_{AE,}$ L_{ASmx}, L_{EPN}, and L_{PNTSmx} metrics.

8.5 Spectral Classes

Spectral classes are the INM/AEDT database of operation-mode-specific spectral data that represent groups of aircraft. Spectral class assignments, which are determined by the FAA Office of Environment and Energy's (AEE) INM/AEDT development team, are computed in accordance to Appendix D of the INM Technical Manual.

The processed spectral data consist of two sets of un-weighted, one-third octave-band sound levels measured at the time of maximum sound level, L_{ASmx} or $L_{PNLTSmx}$, and corrected to a reference distance of 1,000 feet. From these sets of data, a spectral class is assigned for each condition. Since the processed data are representative of a range of thrust parameter values, spectral class assignments are based on the maximum departure and minimum approach thrust values[*].

There are three propagation phenomena in INM/AEDT which are spectrally dependant: atmospheric absorption and shielding caused by barriers or terrain. As a result, spectral class assignments are based on both, the "shape" of the spectral data and the behavior of these three effects. The assignment process consisted of 5 steps:

1. Normalization and computation of free-field effect.

---

[*] Spectral data representative of other submitted thrust values are examined to verify that no large errors result from this assumption.

2. Comparison of aircraft spectral shape to spectral class shapes.
3. Comparison of atmospheric absorption effects calculated using aircraft spectra and those of the spectral classes.
4. Comparison of ground effects calculated using aircraft spectra and those of the spectral classes.
5. Comparison of barrier effects calculated using aircraft spectra and those of the spectral classes.

Ideally, the spectral class assignments resulting from steps 2 through 5 were identical and a final assignment was made without further analysis. If they were not consistent, the data were examined and either 1) a spectral class assignment was made based on a "majority rule", or, if no clear majority existed, 2) the possibility of the creation of a new spectral class was considered. The resulting spectral class assignments are provided in Appendix E of this report.

9

QUALITY ASSURANCE

The quality of the measured and processed data is crucial since they will be used to develop noise model input data for the AEDT/INM database and ultimately used in modeling exercises, including environmental analyses in support of ATMPs. Special care was given to inspecting the data in the field during data collection and in the lab during data processing.

9.1 Calibration

At the beginning of each measurement day, the acoustic systems were calibrated and integrity of the noise floor checked. A calibration was also done at the end of each measurement day to determine if a calibration drift existed during the measurement period. During the source data measurements documented herein no calibration drifts occurred. If a calibration drift of up to 0.5 dB had occurred, then it would have been corrected for during data processing. The MiniFAR software (Section 0) is capable of correcting for calibration drifts during its calculation of noise metrics. If a calibration drift exceeded 0.5 dB, then the data would have been deemed invalid and not included in the data processing.

9.2 Time of Day

To ensure a uniform time source across all data acquisition systems, the Masterclock GPS200A time code generators were used as the “gold standard” time base during data collection. LD824 SLMs, which were the primary recording devices, were set to the time displayed on the time code generator. The GPS200A was used to provide the backup recording device with the precise GPS time. Field personnel also used the time code generator when transcribing notes onto field logs. Meteorological stations had their system time synched with the same GPS time code. The time displayed on the TSPI system was crosschecked with the GPS200A and fuel burn data acquisition system to ensure they were in uniform, therefore synchronizing the aircraft tracking acoustic, and fuel burn data. During processing, MiniFAR links the acoustic, field log, TSPI, and meteorological data together using this uniform time base.

9.3 External Contamination

During field measurements two acoustic observers, stationed approximately 100 feet from each microphone, noted in field logs the effects of any potentially contaminating noise sources. These field notes were displayed in the MiniFAR software. Accordingly, the user was able to view these notes in conjunction with a visual display of the event’s sound level time history to determine if the external noise contaminated the event. Events where contamination was seen in the time history by this initial screening process were discarded. During post-process inspection of the generated NPD curves and one-third octave spectral data, the field logs were referred to once again to help identify any external contamination to the data.

9.4 Test Aircraft TSPI

The TSPI System operator on board the test aircraft monitored the TSPI in real time to ensure the position of the aircraft remained within tolerance during the event. Any events where the aircraft was out of tolerance were discarded and repeated. In addition, the Test Director on the ground monitored the test aircraft position with a real-time feed from the TSPI System.

10 RESULTS

10.1 Source Noise Results

Results from the source noise measurements are presented in the appendices. Specifically:

- Appendix A consists of the aircraft performance data necessary to build the INM / AEDT database tables
- Appendix B lists the test day meteorological data used in the processing of the acoustic data
- Appendix C presents a summary of the TSPI data used in the processing of the acoustic data
- Appendix D contains the NPD data, developed as described in Sections 8.2 and 8.3, in tabular and graphical format
- Appendix E provides the spectral class assignments, developed as described in Section 8.5, and un-weighted spectral data at time of L_{ASmx} for each aircraft and test series

10.2 Appendix F Certification Noise Results

The auxiliary test series, Series 800 for the 182S and Series 200 for the DHC-2, were events where the test aircraft flew in accordance with the requirements outlined in FAR 36 Appendix F. These series were performed as part of an effort to update FAA's Advisory Circular AC-93-2 on quiet technology designation*. The measured noise results and aircraft specifications typically reported in AC-93-2 are presented in Table 9 below.

* FAA AC-93-2 contains certification levels for aircraft certified under FAR 36 Appendix F. As such Appendix F type measurements on the DHC-2 and 182S were performed. However, comparisons between measured levels vs. certification levels could not be done, because the DHC-2 does not have certification levels as it is an old aircraft that pre-dates FAR 36 and the 182S is certified under Appendix G.

Table 9. Measured Aircraft Noise Data and Specifications for Appendix F Certification Events

MANUFACTURER	MODEL	MTOW	ENGINE DATA				PROPELLER						MEASURED NOISE LEVEL (dBA)
		1000#	MFR	MODEL	NO.	SHP	MFR	MODEL	DIAMETER (in)	BLADES	PITCH	RPM	
CESSNA	182S SKYLANE	3.10	TEXTRON LYCOMING	IO-540-AB1A5	1	230	HARTZELL	HC-F3YR-1RF	84	3	V	2400	76.2
DEHAVILLAND	DHC-2 BEAVER MK I	5.09	PRATT & WHITNEY	R985 AN14B	1	450	HARTZELL	HC-B3R30	95.5	3	V	2200	85.3

10.3 Water Landing Noise Results

As mentioned in Section 7.4, the splash noise produced by the test aircraft landing on water was relatively quiet and resulted in only 2 out of 10 water landing events meeting the minimum required 10 decibel rise and fall. The Cessna 182S water landing event number 910, where the aircraft landed 197 feet from the microphone, had a L_{ASmx} of 69.2 dB. The De Havilland Canada DHC-2 water landing event number 940, in which the aircraft landed 236 feet from the microphone, had a L_{ASmx} of 65.5 dB. It was observed by onsite Volpe personnel that the predominant noise during the water landing events was the engine and propeller noise of the floatplane rather than the noise from the impact of the water landing. To verify, a comparison was made of the spectral data from the water landing and source noise approach events. Figure 19 and Figure 20 below are plots of the un-weighted spectral data taken at time of L_{ASmx} for approach events (Series 600) compared to water landing events. The spectrum for the water landing events were significantly lower than the approach events for most of the 1/3 octave bands, indicating that the aircraft can land with very low noise. A comparison of the overall L_{ASmx} levels between these two types of events was also conducted. For the 182S, the L_{ASmx} level for the water landing event was 19 dB lower than the approach event. For the DHC-2, the water landing L_{ASmx} level was 12.5 dB lower than the approach event.

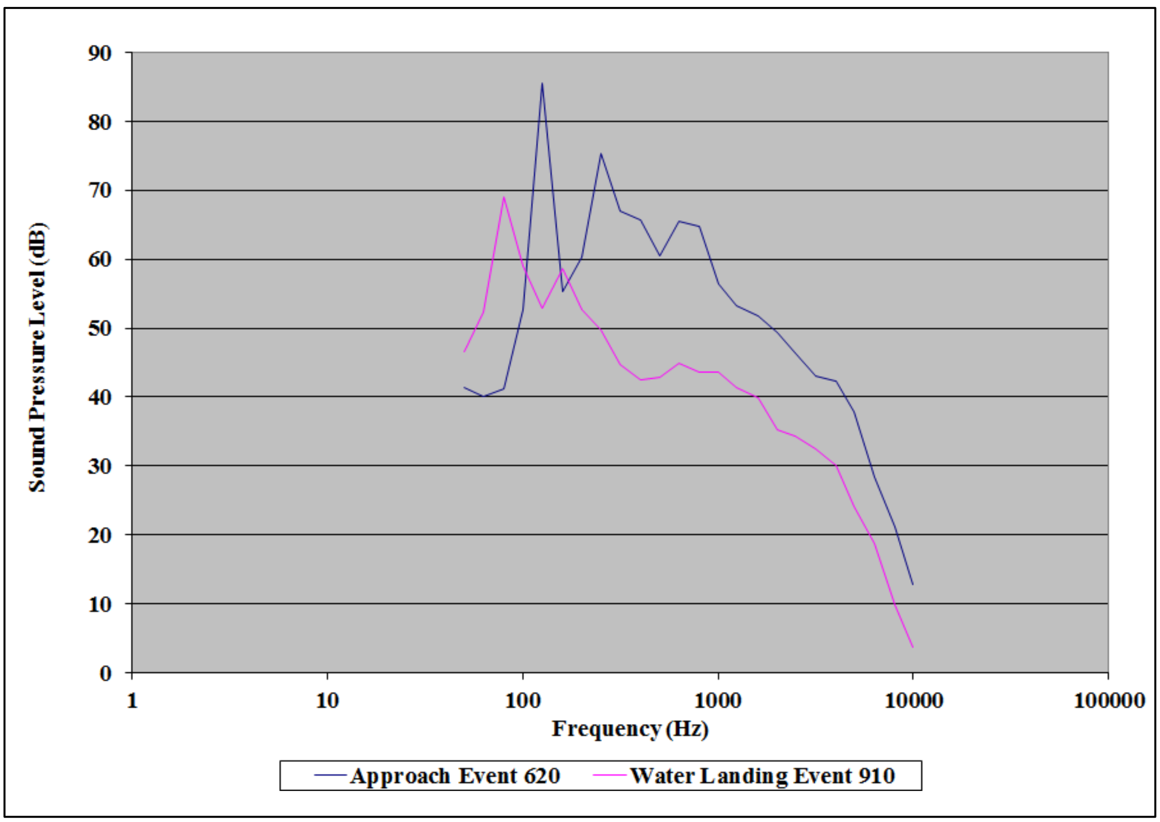

Figure 19. Comparison of 182S Spectra of Water Landing and Approach Events

Figure 20. Comparison of DHC-2 Spectra of Water Landing and Approach Events

10.4 DHC-2 Lateral Directivity Noise Results

During source noise measurements of the DHC-2, onsite Volpe personnel noticed that noise from one side of the aircraft was louder than the other. This same phenomenon was not present for the Cessna 182S. A comparison of the DHC-2 left and right side (relative to direction of travel) data are presented in Tables 10 through 13 below. The lateral data, corrected to the SAE-AIR-1845 reference day atmospheric conditions and reference speed of 160 knots, are presented for the four noise metrics L_{AE}, L_{ASmx}, L_{EPN} and L_{PNTSmx}. It can be seen in the data that the right side of the DHC-2 exhibited louder noise levels for all four noise metrics.

Table 10. L_{ASmx} Comparison of Left and Right Side Noise Levels of the DHC-2

L_{ASmx} @ 160 kts					
	Aircraft Left		Aircraft Right		Delta (Left - Right)
Dist. (ft)	Average	Std. Dev.	Average	Std. Dev.	
200	94.4	1.3	99.2	0.1	-4.7
400	88.0	1.2	92.8	0.1	-4.7
630	83.7	1.2	88.4	0.1	-4.7
1000	79.1	1.2	83.8	0.1	-4.8
2000	71.6	1.0	76.4	0.2	-4.8
4000	63.1	0.8	67.8	0.4	-4.7
6300	56.8	0.7	61.3	0.6	-4.5
10000	49.6	0.6	53.7	0.9	-4.1
16000	41.5	0.5	45.0	1.3	-3.5
25000	32.5	0.2	36.0	1.9	-3.5

Table 11. L_{AE} Comparison of Left and Right Side Noise Levels of the DHC-2

L_{AE} @ 160 kts					
	Aircraft Left		Aircraft Right		Delta (Left - Right)
Dist. (ft)	Average	Std. Dev.	Average	Std. Dev.	
200	95.1	0.5	98.2	0.6	-3.0
400	91.0	0.4	94.1	0.6	-3.1
630	88.1	0.4	91.2	0.6	-3.1
1000	85.0	0.4	88.1	0.6	-3.1
2000	79.8	0.2	82.9	0.6	-3.1
4000	73.5	0.3	76.5	0.9	-3.0
6300	68.7	0.6	71.5	1.1	-2.8
10000	63.1	0.9	65.5	1.5	-2.4
16000	56.5	0.9	58.3	1.9	-1.8
25000	48.9	0.8	50.7	2.5	-1.8

Table 12. L_{PNTSmx} Comparison of Left and Right Side Noise Levels of the DHC-2

L_{PNTSmx} @ 160 kts					
	Aircraft Left		Aircraft Right		Delta (Left - Right)
Dist. (ft)	Average	Std. Dev.	Average	Std. Dev.	
200	107.4	0.4	111.6	1.5	-4.2
400	100.9	0.3	105.0	1.4	-4.1
630	96.4	0.3	100.4	1.4	-4.1
1000	91.5	0.4	95.5	1.4	-4.0
2000	83.7	0.5	87.5	1.4	-3.8
4000	74.9	0.7	78.3	1.6	-3.4
6300	69.0	1.0	71.6	1.7	-2.6
10000	62.9	1.4	64.7	1.7	-1.8
16000	56.6	2.0	58.0	2.4	-1.5
25000	50.6	2.5	51.7	3.1	-1.2

Table 13. L_{EPN} Comparison of Left and Right Side Noise Levels of the DHC-2

L_{EPN} @ 160 kts					
	Aircraft Left		Aircraft Right		Delta (Left - Right)
Dist. (ft)	Average	Std. Dev.	Average	Std. Dev.	
200	99.0	0.3	101.3	2.0	-2.3
400	94.7	0.3	97.0	2.0	-2.3
630	91.7	0.3	93.9	1.9	-2.2
1000	88.4	0.4	90.5	1.9	-2.1
2000	82.8	0.6	84.7	2.0	-1.9
4000	76.3	0.8	77.8	2.1	-1.5
6300	71.8	1.1	72.5	2.2	-0.8
10000	67.2	1.5	67.1	2.2	0.1
16000	62.4	2.1	62.0	2.9	0.4
25000	57.9	2.6	57.2	3.6	0.7

It is believed that DHC-2 exhibited louder noise levels on the right side of the aircraft because of the placement of the engine exhaust system. In Figure 21 below, it can be seen the measured DHC-2 aircraft has the exhaust system installed on the bottom, right side of the aircraft. A review of the DHC-2 NPD plots (Appendix D.4) revealed that at distances of 1,000 feet and lower, the centerline noise levels were higher than that of the sideline. However, at distances of 2,000 feet and greater the sideline noise data exhibited higher noise levels than the centerline. This is a typical phenomenon when the measured noise source is dominated by a low frequency noise source, such as that of an aircraft exhaust system. Further investigation was conducted by comparing the spectral data from a pair of left and right side events. Figure 22 is a comparison of the averaged, un-weighted spectra taken at time of L_{ASmx}. Both spectra are corrected to an altitude of 1,000 feet and standard reference speed and atmospheric conditions. It be seen in this pot of the spectra that the two spectral shapes are very similar except at the 125 hertz third octave band, where the right side of the aircraft was approximately 11 decibels higher than the left. This low frequency tone is believed to be a product of the aircraft engine exhaust and contributed to the louder noise values seen from the right side of the aircraft.

Figure 21. Exhaust System of the DHC-2 Installed on Right Side of the Aircraft

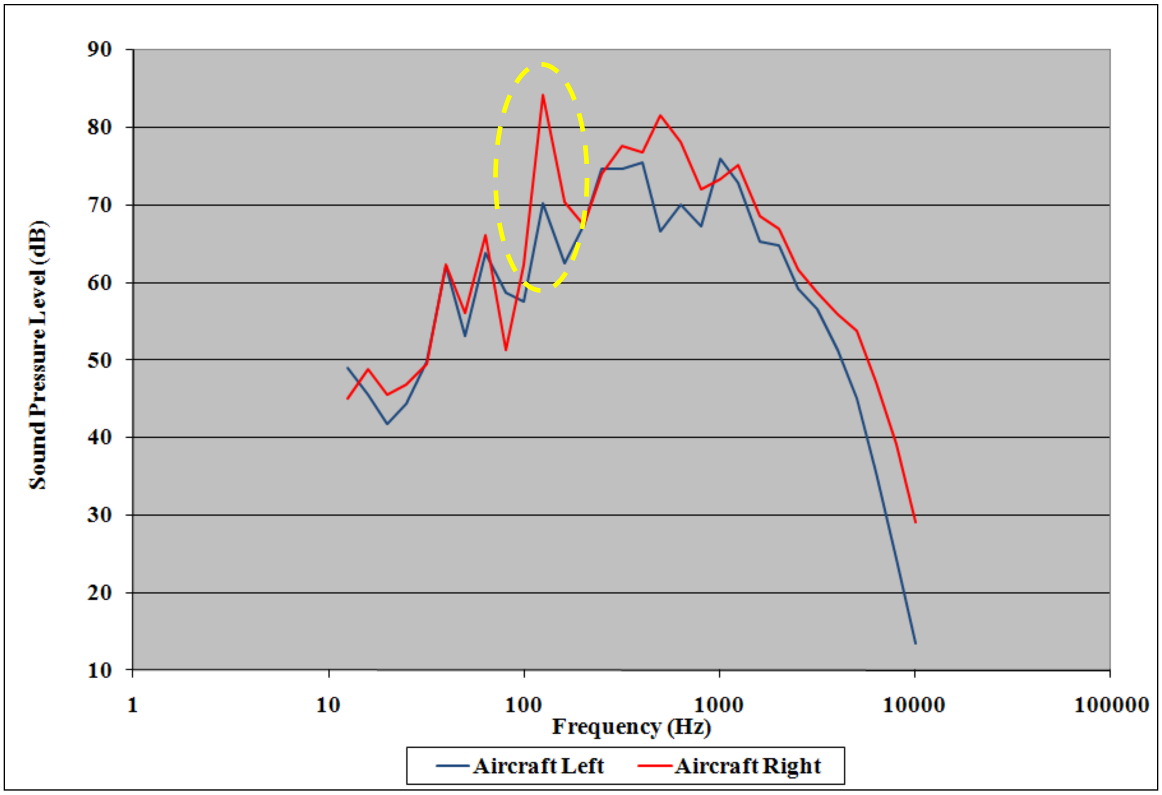

Figure 22. Spectral Comparison of Left and Right Side of the DHC-2

APPENDIX A: AIRCRAFT PERFORMANCE DATA

Appendix A presents the aircraft performance data necessary to build the INM / AEDT database tables for the Cessna 182S and De Havilland DHC-2. The calculation of INM input data, performance and aerodynamic parameters for both departures and approaches are explained in the following sections. Information on the aircraft was taken from their respective flight manuals unless otherwise stated.

A.1 Cessna 182S

A.1.1 Aircraft Descriptions and Performance Data

The Cessna 182S is equipped with a Textron Lycoming IO-540-AB1A5 and a 6-cylinder engine[14,15]. The rated full power of the engine is 230 brake horse power (BHP) at 2400 revolutions per minute (RPM). The maximum take-off weight (MTOW) of this aircraft is 3100 pounds (lbs). The maximum landing weight used for the analysis was 2950 lbs.

For this analysis, data from the flight test was provided by the TSPI system, meteorological data from the TAMS unit, the Lycoming 0-540, IO-540 Operator's Manual, and the Pilots Operators Handbook (POH). Equations provided in the INM Technical Manual[4] were used to compute the coefficients. A summary of the 182S's performance parameters used during flight tests for each series are shown in Table 14 below.

Table 14. Summary of Performance Parameters During 182S Flight Tests

Series	Series no.	Flap setting (deg)	RPM	MP (in-HG)	BHP	KTAS	Thrust (lb_f)	Efficiency
Tour Cruise	100	0	2250	23	161	106.9	402.0	0.82
Normal Cruise	200	0	2490	23	169	109.1	396.0*	0.78
Departure	300	20	2400	28.3	222	80.1	683.0	0.76
Cruise Climb	400	10	2383	23	164	88.3	479.0	0.79
Approach Flaps 10	500	10	2217	13.7	72	83.3	191.0	0.68
Approach Flaps 20	600	20	2400	17.7	110	90.0	318.0	0.73
Take Off Land	-	20	2400	28.5	224	69.0	740.0	0.71
Take Off Water	-	20	2400	28.5	226.2	59	825	0.66

The Cessna is equipped with a 3-bladed McCauley 84.0 inches diameter, constant speed, and hydraulically actuated propeller. Hartzell provided the proprietary information necessary to calculate thrust and propeller efficiency. The thrust and efficiency are functions of flight speed, altitude, engine horsepower, and engine RPM settings. Hartzell

* The normal cruise used more engine horsepower, but less thrust due to the lower propeller efficiency and higher airspeed. The R values are also slightly different to take this into account.

gives two associated thrust values for each input flight condition. One is based on the thrust coefficient *Ct* and the other is based on thrust coefficient η. An average value of 935 lbs of thrust based on the coefficient *Ct* was used to compute static thrust.

A.1.2 Aerodynamic Coefficients (B, C, D)

In order for the INM to calculate the procedural profiles, several coefficients need to be calculated. The calculations of aerodynamic coefficients *B, C* and *D* for the 182S are explained in this section.

Coefficient *B* is the ground roll-coefficient B_f, that depends on the flap settings. It is taken from the following INM equation (2.16)[4]:

$$S_g = \frac{B_f \cdot \theta \cdot \left(\frac{W}{\delta}\right)^2}{\left[N \cdot \left(\frac{F_n}{\delta}\right)_2\right]} \qquad \text{[Eq. 2]}$$

Where,

S_g	ground-roll distance (ft),
Θ	temperature ratio at the airport elevation,
W	departure profile weight (lb),
δ	pressure ratio at the airport,
N	number of engines, and
$(F_n/\ \delta)_2$	corrected net thrust per engine (lb) at take-off rotation.

Coefficient *C* is the take-off speed coefficient, C_f, which depends on flap settings. It is found in the INM equation (2.15):

$$v_2 = C_f \cdot W^{1/2} \qquad \text{[Eq. 3]}$$

Where,

v_2	calibrated airspeed (knots), at rotation take-off and
W	departure profile weight (lb); weight is assumed constant for the entire departure profile.

Coefficient *D* is the landing speed coefficient, D_f, which depends on flap and gear settings. It is found in the INM equation (2.60):

$$v_1 = D_f \cdot W^{1/2} \qquad \text{[Eq. 4]}$$

Where,

v_1	calibrated airspeed (knots), just before landing and
W	approach profile weight (lb); weight is assumed constant for the entire approach profile.

A.1.2.1 Departure Coefficients

Coefficient C

There were several take-off events from water and land during the 182S flight tests. All take-offs were done with flaps set to 20˚ and maximum take-off weight. In order to compute the take-off distance, *Sg*, and velocity, position data from the TSPI were plotted providing a visual clue as to the time the aircraft was beginning its climb (See Figure 23). The velocity data was inspected to find the beginning of the take-off. The aircraft had some residual speed from the touch-and-goes, roughly around 40 knots. The first take-off roll from water provided the clue to the distance travelling as the aircraft accelerated to 40 knots. A distance value of 50 feet was added to each take-off roll on water. In order to calculate the rest of the run, the time stamp was noted as soon as the velocity data showed signs of acceleration. The time stamp provided the clue to where the aircraft began the take-off run on the position data. The distance formula was then utilized to calculate the take-off roll.

$$\text{Distance formula: } \sqrt{(x_2 - x_1)^2 + (y_2 - y_1)^2} \qquad \text{[Eq. 5]}$$

The take-off distance from land was 1780 feet. The airspeed had to be extrapolated due to the velocity data having larger time increments than the position data. The calculated value for velocity was 69.0 knots. Take-off rolls recorded were 1601, 1803, 1706, and 1793 feet. The average roll computed was 1736 feet. There was a head wind associated with each run, indicated by the meteorological data, and was added to the respective take-off speed. The average take-off speed on water, with head winds factored in, was 59.0 knots. It was necessary to correct ground roll distance due to the presence of headwind. With this computed data, the INM equation (2.39) was used to compute the ground-roll distance:

$$S_{gw} = \frac{S_g \cdot (v_2 - w)^2}{(v_2 - 8)^2} \qquad \text{[Eq. 6]}$$

Where

S_{gw} ground-roll distance (feet) corrected for headwind,
S_g ground-roll distance (feet) uncorrected,
v_2 calibrated speed (knots) at take-off rotation, and
w headwind (knots).

The final value for ground roll take-off from the water is 1900 feet.

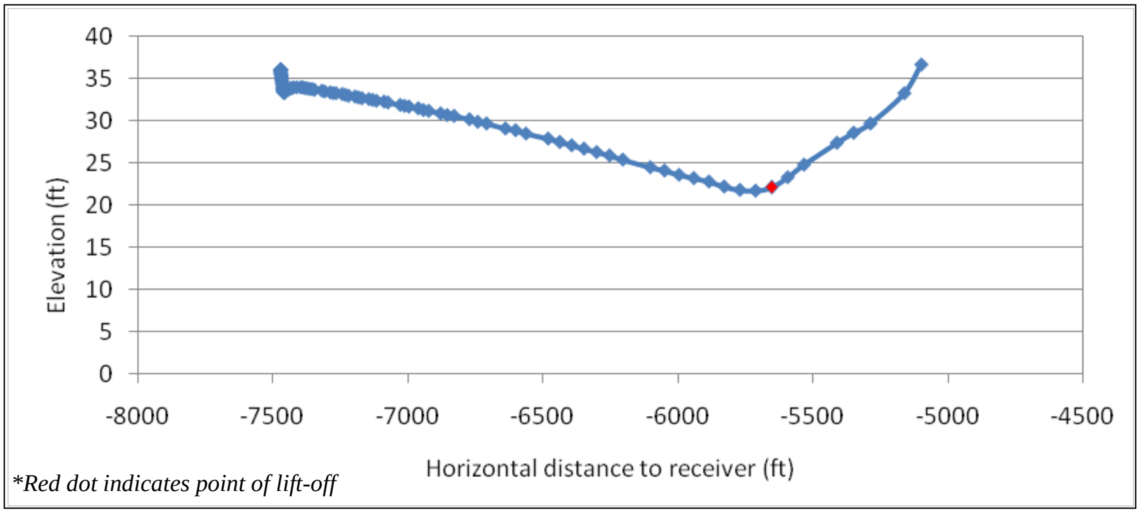

Figure 23. TSPI Plot of an 182S Simulated Departure from Land

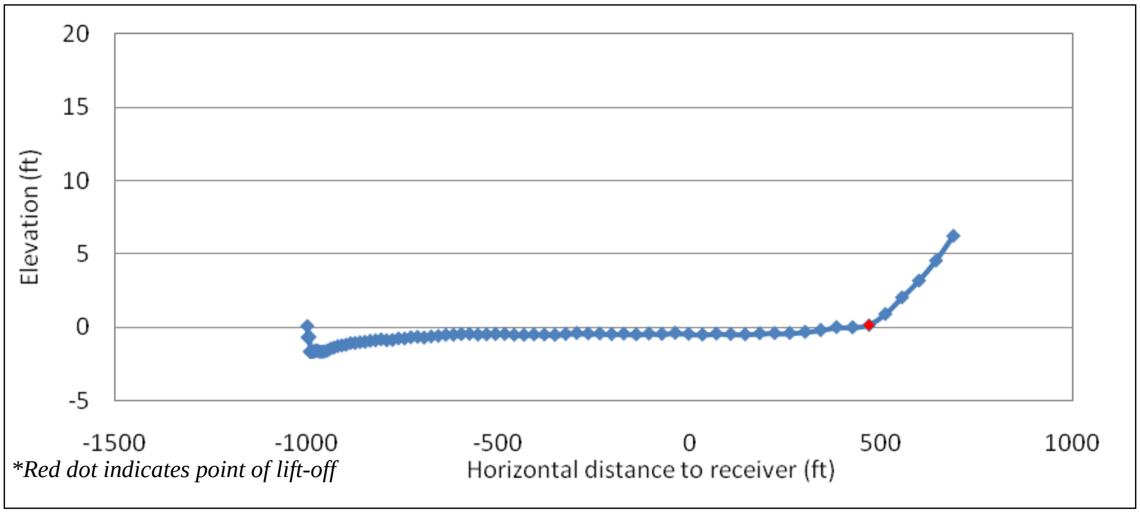

Figure 24. TSPI Plot of Departure from Water

The following equations were then used to calculate departure coefficients *B* and *C* for the water and ground take-offs:

Land:

$$C_{F-20\ land} = \frac{V_{C\ F-20}}{\sqrt{W}} = \frac{69.0KTAS}{\sqrt{3100\ lbs}} = 1.2393\frac{kts}{lb^{0.5}} \quad \text{[Eq. 7]}$$

Water:

$$C_{F-20\ water} = \frac{V_{C\ F-0}}{\sqrt{W}} = \frac{59.0KCAS}{\sqrt{3100\ lbs}} = 1.0597\frac{kts}{lb^{0.5}} \quad \text{[Eq. 8]}$$

Coefficient B

Land:

$$B_{F-20\ \ land} = \frac{s_g\left(N\, {F_N}/{\delta}\right)}{\theta\left({W}/{\delta}\right)^2} = \frac{(1780\,ft)\left({740lbs}/{0.994}\right)}{0.996\left({3100}/{0.994}\right)^2} = 0.1304 \qquad \text{[Eq. 9]}$$

Water:

$$B_{F-20\ \ water} = \frac{s_g\left(N\, {F_N}/{\delta}\right)}{\theta\left({W}/{\delta}\right)^2} = \frac{(1900\,ft)\left({825lbs}/{0.996}\right)}{0.985\left({3100}/{0.996}\right)^2} = 0.1551 \qquad \text{[Eq. 10]}$$

A.1.2.2 Approach Coefficients

Coefficient D

Approach speeds were calculated from the parameters used during the flight tests. The maximum landing weight was used for all coefficient *D* calculations. Knots indicated air speed, or KIAS, was left uncorrected, since there was no available data for airspeed calibrations. The following equations were used to calculate coefficient *D* for approach events:

$$D_{F-10} = \frac{V_{CA\,F-10}}{\sqrt{W}} = \frac{83.3KIAS}{\sqrt{2950}\ lbs} = \frac{83.3KCAS}{\sqrt{2950}\ lbs} = 1.5337\frac{kts}{lb^{0.5}} \qquad \text{[Eq. 11]}$$

$$D_{F-20} = \frac{V_{CA\,F-20}}{\sqrt{W}} = \frac{90KIAS}{\sqrt{2950}\ lbs} = \frac{90KCAS}{\sqrt{2950}\ lbs} = 1.6754\frac{kts}{lb^{0.5}} \qquad \text{[Eq. 12]}$$

A.1.3 Aerodynamic Coefficients (R)

Coefficient R is the drag-over-lift coefficient R_f that depends on flap settings. It is taken from the following INM equation (2.29):

$$\gamma = \left(K \cdot \left[\frac{N \cdot \left(\frac{F_n}{\delta} \right)}{\left(\frac{W}{\delta} \right)} - R_f \right] \right) \qquad \text{[Eq. 13]}$$

Where,

γ	average climb angle,
K	speed dependent constant, K=1.01 when climb speed ≤ 200 knots, And K=0.95 otherwise,
N	number of engines,
δ	pressure ratio at the airport,
N	number of engines,
F_n/δ	nominal value of corrected net thrust per engine (lb), and
W	departure profile weight (lb).

A.1.3.1 Departure Coefficients

The angles flown in each series, departure and approach, was found using the TSPI position data. The recorded aircraft parameters were matched to the TSPI data by time. The point the aircraft crossed the receiver was identified by the zero position on the horizontal axis (see Figure 25). Figure 26 illustrates the regression line to derive the departure angle. Once the area was narrowed down from what looked like a constant angle, a best fit linear line was added to compute the climb angle from the inverse tangent of the slope. The angle for Series 300 Standard Departure events, $R_{F\text{-}20}$, was calculated from an average of three departures events. The following equation was then used to compute $R_{F\text{-}20}$:

$$R_{F-20} = \frac{F_n / \delta_{am}}{W / \delta_{am}} - \frac{\sin\gamma}{1.01} = \frac{683lbs / 0.996}{3100 / 0.996} - \frac{\sin(3.70^o)}{1.01} = 0.1564 \qquad \text{[Eq. 14]}$$

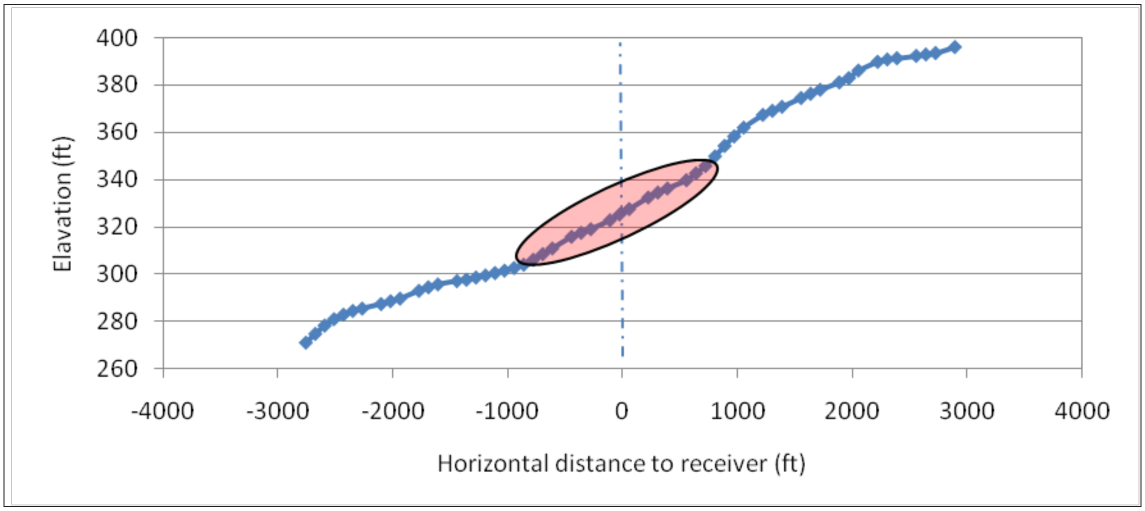

Figure 25. TSPI Plot of a Series 400 Departure Cruise Climb

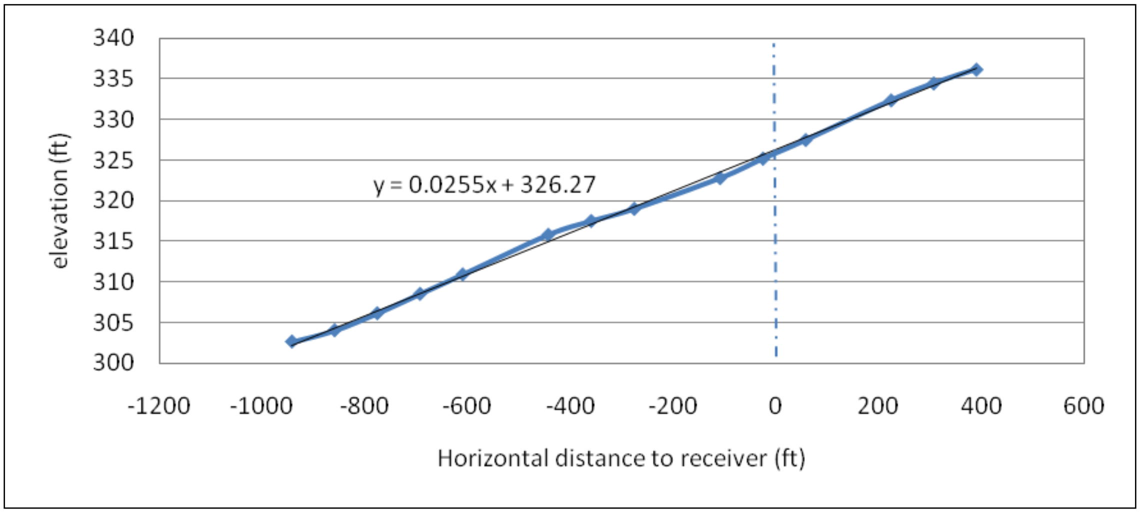

Figure 26. Regression Line Used to Define Angle of Departure for the 182S

The angle for Series 400 Cruise Climb events, $R_{F\text{-}10}$, were calculated from an average of three different departures. The following equation was then used to compute $R_{F\text{-}10}$:

$$R_{F-10} = \frac{F_n / \delta_{am}}{W / \delta_{am}} - \frac{\sin\gamma}{1.01} = \frac{479lbs / 0.989}{3100 / 0.989} - \frac{\sin(1.65^o)}{1.01} = 0.1260 \qquad \text{[Eq. 15]}$$

A.1.3.2 Approach Coefficients

Three different approach angles derived from the TSPI data were used to calculate averaged values for $R_{F\text{-}10}$ and $R_{F\text{-}20}$. The following equations were then used to compute $R_{F\text{-}10}$ and $R_{F\text{-}20}$:

$$R_{F-10} = \frac{F_n / \delta_{am}}{W / \delta_{am}} - \frac{\sin\gamma}{0.95} = \frac{191/0.989}{2950/0.989} + \frac{\sin(2.36^o)}{1.03} = 0.1047 \qquad \text{[Eq. 16]}$$

$$R_{F-20} = \frac{F_n / \delta_{am}}{W / \delta_{am}} - \frac{\sin\gamma}{0.95} = \frac{318/0.990}{2950/0.990} + \frac{\sin(3.41^o)}{1.03} = 0.1655 \qquad \text{[Eq. 17]}$$

A.1.3.3 Tour Cruise Coefficients

Coefficient $R_{Tour\text{-}Cruise}$ was calculated using the test day flight parameters and the following equation:

$$R_{Tour\ \ Cruise} = \frac{F_n / \delta_{am}}{W / \delta_{am}} - \frac{\sin\gamma}{0.95} = \frac{402lbs/0.989}{3100/0.989} - \frac{\sin(0^o)}{0.95} = 0.1297 \qquad \text{[Eq. 18]}$$

A.1.3.4 Normal Cruise Coefficients

Coefficient $R_{Normal\text{-}Cruise}$ was calculated using the test day flight parameters and the following equation:

$$R_{Normal\ \ Cruise} = \frac{F_n / \delta_{am}}{W / \delta_{am}} - \frac{\sin\gamma}{0.95} = \frac{396lbs/0.989}{3100/0.989} - \frac{\sin(0^o)}{0.95} = 0.1277 \qquad \text{[Eq. 19]}$$

A.1.4 INM Data

Table 15 summarizes the resulting performance summary data that will be imported into INM.

Table 15. Summary of 182S INM Coefficients

Parameter	Value	Units
MTOGW	3100	lbs
MLW	2950	lbs
Approach		
$D_{F\text{-}10}$	1.5337	kt / lb$^{1/2}$
$D_{F\text{-}20}$	1.6754	kt / lb$^{1/2}$
$R_{Approach,\ F\text{-}10}$	0.1047	-
$R_{Approach,\ F\text{-}20}$	0.1655	-
Departure		
$B_{F\text{-}20}$ (Land)	0.1304	kt / lb$^{0.5}$
$B_{F\text{-}20}$ (Water)	0.1551	kt / lb$^{0.5}$
$C_{F\text{-}20}$ (Land)	1.1293	kt / lb$^{0.5}$
$C_{F\text{-}20}$ (Water)	1.0597	kt / lb$^{0.5}$
$R_{Departure,\ F\text{-}10}$	0.1260	-
$R_{Departure,\ F\text{-}20}$	0.1564	-
Level Flyover		
$R_{Tour\ Cruise}$	0.1297	-
$R_{Normal\ Cruise}$	0.1277	-

A.2 De Havilland DHC-2

A.2.1 Aircraft Description and Performance Data

The DHC-2 test aircraft is equipped with a Pratt & Whitney R-985-39A, and a 9-cylinder engine with a normal rated power of 400 HP at 2200 RPM and a manifold setting of 34.5 in-Hg[16]. Maximum take-off RPM is set to 2300 with a manifold pressure 36.5 in-Hg[17]. The propeller is a Hartzell 3-bladed, 95.5 inch diameter, constant speed propeller. The MTOW of this aircraft (seaplane version) is 5090 lbs. The maximum landing weight used for the analysis was set at the same value as the take-off weight of 5091 lbs.

To conduct the analysis, data from the flight test was provided by the TSPI system. Equations provided by the INM were used to compute the coefficients. In addition, the meteorological data, Pratt & Whitney Aircraft R-985-39A Engine Technical Manual, and DHC-2 Beaver 1952 Flight Manual were used to compute the coefficients. A summary of the DHC-2's performance parameters used during flight tests for each series are shown in Table 16.

Table 16: Summary of Performance Parameters During DHC-2 Flight Tests

Series	Series no.	Flap setting (deg)	RPM	MP (in-HG)	BHP	KTAS	Thrust (lb_f)	Efficiency
Tour Cruise*	100	Up	1900	27.5	305	82.7	874	0.73
Cert. F Full Power	200	Up	2300	35	445	100.0	1100	0.76
Departure	300	T/O	2300	34.4	440	66.4	1321	0.61
Cruise Climb	400	Climb	2000	29.7	338	78.4	990	0.71
Approach Flaps UP	500	Up	1900	19.3	232	101.6	606	0.82
Approach Flaps Final	600	Landing	1750	15.1	157	78.5	506	0.78
Take Off Water	-	T/O	2300	35.5	450	61.0	1392	0.58

Hartzell provided the proprietary information necessary to calculate thrust and propeller efficiency. The thrust and propeller efficiency are functions of flight speed, altitude, engine horsepower, and engine RPM setting. Hartzell gives two associated thrust values for each input flight condition; one based on the thrust coefficient *Ct* and the other based on thrust coefficient η. An average value of 1884 lbs of thrust based on the coefficient *Ct* was used to compute static thrust.

A.2.2 Aerodynamic Coefficients (B, C, D)

In order for the INM to calculate the procedural profiles, several coefficients need to be calculated. The calculations of aerodynamic coefficients *B*, *C* and *D* for the DHC-2 are explained in this section.

Coefficient *B* is the ground roll-coefficient B_f, that depends on the flap settings. It is taken from the following INM equation (2.16):

$$S_g = \frac{B_f \cdot \theta \cdot \left(\frac{W}{\delta}\right)^2}{\left[N \cdot \left(\frac{F_n}{\delta}\right)_2\right]} \qquad \text{[Eq. 2]}$$

Where,

S_g	ground-roll distance (feet),
θ	temperature ratio at the airport elevation,
W	departure profile weight (lb),
δ	pressure ratio at the airport,
N	number of engines, and
$(F_n/\delta)_2$	corrected net thrust per engine (lb) at take-off rotation.

* Note that no normal cruise performance parameters were developed for the DHC-2 with floats. For this aircraft, tour cruise and normal cruise operations are one and the same.

Coefficient C is the take-off speed coefficient C_f that depends on flap settings. It is found in the INM equation (2.15):

$$v_2 = C_f \cdot W^{1/2} \qquad \text{[Eq. 3]}$$

Where,

v_2 calibrated airspeed (knots), at rotation take-off and

W departure profile weight (lb); weight is assumed constant for the entire departure profile.

Coefficient D is the landing speed coefficient D_f that depends on flap and gear settings. It is found in the INM equation (2.60):

$$v_1 = D_f \cdot W^{1/2} \qquad \text{[Eq. 4]}$$

Where,

v_1 calibrated airspeed (knots), just before landing and

W approach profile weight (lb); weight is assumed constant for the entire approach profile.

A.2.2.1 Departure Coefficients

Coefficient C

Take-off ground roll distance, S_g, information was extracted from the TSPI data, where an average was computed. Flaps were set to take-off position at MTOW. In order to compute the take-off distance, S_g, and velocity, position data from the TSPI were plotted providing a visual clue as to the time the aircraft was beginning its climb (See Figure 27).

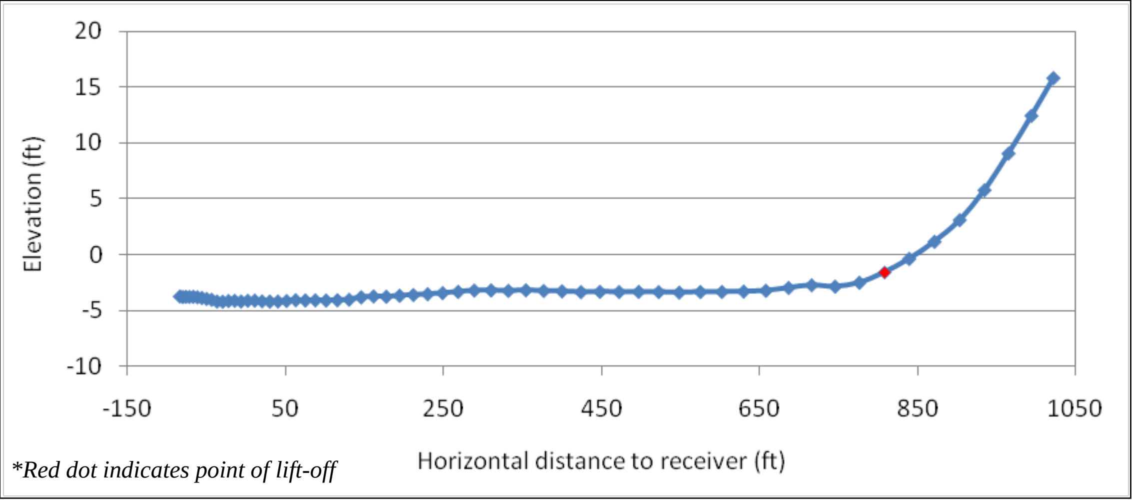

Figure 27. TSPI Plot of a DHC-2 Departure

The velocity data from TSPI was used to find the beginning of the take-off roll. The aircraft had some residual speed from the touch-and-goes, roughly around 40 knots. The first take-off run from water provided the clue to the distance travelling, as the aircraft accelerated to 40 knots. A distance value of 50 feet was added to each take-off roll on water. In order to calculate the rest of the run, the time stamp was noted as soon as the velocity data showed signs of acceleration. The time stamp indicated where the aircraft began the run on the position data. The distance formula was utilized to calculate the take-off roll.

$$\text{Distance formula: } \sqrt{(x_2 - x_1)^2 + (y_2 - y_1)^2} \qquad \text{[Eq. 5]}$$

The take-off rolls computed were 1272, 1296, 1411, 1557, 1599, and 1464 feet. This provided an average take-off roll of 1433 feet. There was a head wind associated with each run and was added to the respective take-off speed. The average take-off speed on water, with head winds factored in, is 61.0 knots. It was necessary to correct ground roll distance due to the presence of headwind. Using the INM equation (2.39):

$$S_{gw} = \frac{S_g \cdot (v_2 - w)^2}{(v_2 - 8)^2} \qquad \text{[Eq. 6]}$$

Where

- S_{gw} ground-roll distance (ft) corrected for headwind,
- S_g ground-roll distance (ft) uncorrected,
- v_2 calibrated speed (knots) at take-off rotation, and
- w headwind (knots).

The final value for ground roll take-off from the water, calculated using Equation 20 below, is 1630 feet.

$$C_{F-T/O\ \ water} = \frac{V_{C\,F-T/O}}{\sqrt{W}} = \frac{61KCAS}{\sqrt{5090}\ lbs} = 0.8550\frac{kts}{lb^{0.5}} \qquad \text{[Eq. 20]}$$

Coefficient B

Coefficient *B* was then calculated using Equation 21 below, giving the value of 0.0883.

$$B_{F-T/O\ \ water} = \frac{s_g\left(N\, {F_N}/{\delta}\right)}{\theta\left({W}/{\delta}\right)^2} = \frac{(1630\,ft)\left(1392lbs/0.998\right)}{0.9896\left(5090/0.998\right)^2} = 0.0883 \qquad \text{[Eq. 21]}$$

A.2.2.2 Approach Coefficients

Coefficient D

Approach speeds were calculated from the parameters used during the flight tests. The MTOW was used to calculate all coefficients. KIAS was left uncorrected since there was no available data for airspeed calibrations. Coefficient *D* was calculated by the following equations:

$$D_{F-UP} = \frac{V_{CA\,F-UP}}{\sqrt{W}} = \frac{101.6KIAS}{\sqrt{5090}\ lbs} = \frac{101.4KCAS}{\sqrt{5090}\ lbs} = 1.4213\frac{kts}{lb^{0.5}} \qquad \text{[Eq. 22]}$$

$$D_{F-Landing} = \frac{V_{CA\,F-Landing}}{\sqrt{W}} = \frac{78.5KIAS}{\sqrt{5090}\ lbs} = \frac{78.2KCAS}{\sqrt{5090}\ lbs} = 1.0961\frac{kts}{lb^{0.5}} \qquad \text{[Eq. 23]}$$

A.2.3 Aerodynamic Coefficients (R)

Coefficient *R* is the drag-over-lift coefficient R_f that depends on the flap setting. It is taken from the following INM equation (2.29):

$$\gamma = \left(K \cdot \left[\frac{N \cdot \left(\frac{F_n}{\delta}\right)}{\left(\frac{W}{\delta}\right)} - R_f\right]\right) \qquad \text{[Eq. 24]}$$

Where,

γ average climb angle,

K speed dependent constant, K=1.01 when climb speed ≤ 200 knots, and K=0.95 otherwise,

N number of engines,

δ pressure ratio at the airport,

N number of engines,

F_n/δ nominal value of corrected net thrust per engine (lb), and

W departure profile weight (lb).

A.2.3.1 Departure Coefficients

The angles flown in each series, departure and approach, was found using the TSPI position data. The flight test logs provided the information for the time each event occurred. The time was matched to the time stamp on the TSPI data. The point the aircraft crossed the receiver was identified by the zero position on the horizontal axis (See Figure 28). Once the area was narrowed down from what looks like a constant angle, a best fit linear line was added to compute the climb angle from the inverse tan of the slope. Figure 29 illustrates the best fit line used to compute the departure angle.

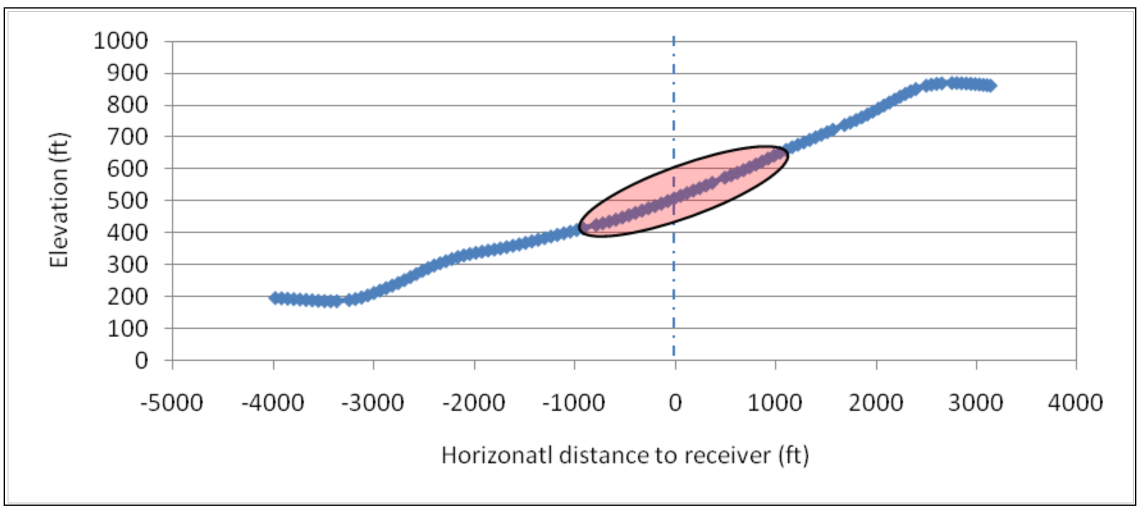

Figure 28. TSPI Plot of a Series 300 Standard Departure

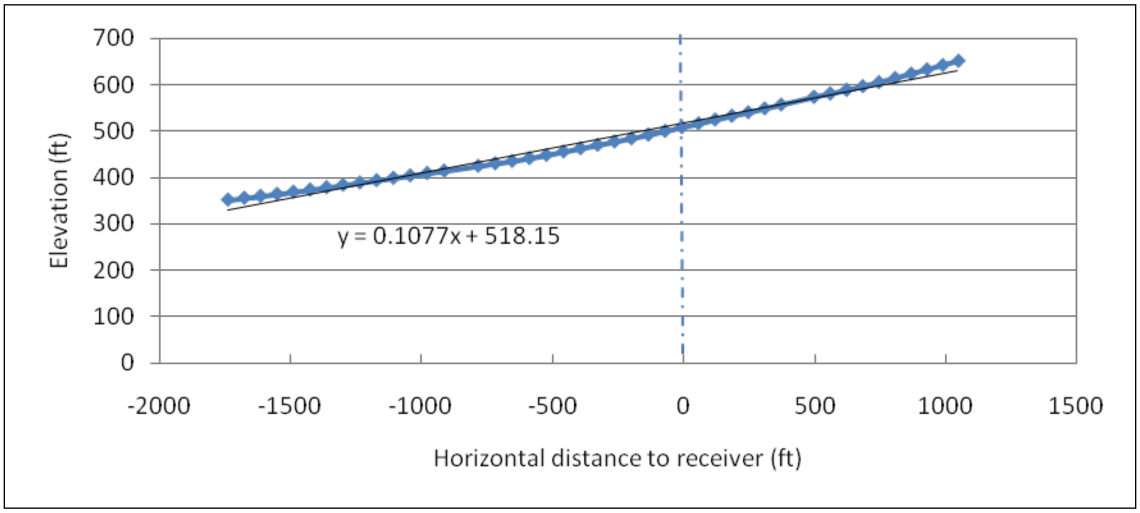

Figure 29. Regression Line Used to Derive Angle of Departure for the DHC-2

The angle for the series 300 standard departure events, $R_{f\text{-}T/O}$, was calculated from an average of four different departures. The following equation was then used to compute $R_{F\text{-}T/O}$:

$$R_{F-T/O} = \frac{F_n/\delta_{am}}{W/\delta_{am}} - \frac{\sin\gamma}{1.01} = \frac{1321lbs/0.987}{5090/0.987} - \frac{\sin(6.74^o)}{1.01} = 0.1433 \qquad \text{[Eq. 25]}$$

This rate of climb was lower than expected even with a relatively steep gradient. This is a result of the 'tractor' effect, i.e., the aircraft performs well at low airspeeds, while the performance at higher speeds falls off markedly.

The angle for the series 400 cruise climb events, $R_{f\text{-}Cruise\ Climb}$, was calculated from an average of two cruise climbs. The following equation was then used to compute $R_{F\text{-}Cruise\ \mathrm{Climb}}$:

$$R_{F-cruise\_\mathrm{climb}} = \frac{F_n/\delta_{am}}{W/\delta_{am}} - \frac{\sin\gamma}{1.01} = \frac{990lbs/0.987}{5090/0.987} - \frac{\sin(0.65^o)}{1.01} = 0.1833 \qquad \text{[Eq. 26]}$$

A.2.3.3 Approach Coefficients

The angles for $R_{f\text{-}UP}$ and $R_{f\text{-}Landing}$ were calculated from an average of two different approaches. Then the following equations were to compute $R_{f\text{-}UP}$ and $R_{f\text{-}Landing}$:

$$R_{F-UP} = \frac{F_n/\delta_{am}}{W/\delta_{am}} - \frac{\sin\gamma}{0.95} = \frac{606/0.987}{5090/0.987} + \frac{\sin(4.84^o)}{1.03} = 0.2010 \qquad \text{[Eq. 26]}$$

$$R_{F-Landing} = \frac{F_n/\delta_{am}}{W/\delta_{am}} - \frac{\sin\gamma}{0.95} = \frac{506/0.986}{5090/0.986} + \frac{\sin(4.92^o)}{1.03} = 0.1827 \qquad \text{[Eq. 27]}$$

A.2.3.3 Tour Cruise Coefficients

Coefficient $R_{Tour\text{ -}Cruise}$ was calculated using the test day flight parameters and the following equation:

$$R_{Tour\quad Cruise} = \frac{F_n/\delta_{am}}{W/\delta_{am}} - \frac{\sin\gamma}{0.95} = \frac{874lbs/0.987}{5090/0.987} - \frac{\sin(0^o)}{0.95} = 0.1717 \qquad \text{[Eq. 28]}$$

A.2.4 INM Data

Table 19 below summarizes the resulting performance summary data, which will be imported into INM.

Table 17. Summary of DHC-2 INM Parameters

Parameter	Value	Units
MTOGW	5090	lbs
MLW	5090	lbs
Approaches		
$D_{\text{F- up}}$	1.4213	$Kt / lb^{0.5}$
$D_{\text{F-Landing}}$	1.0961	$Kt / lb^{0.5}$
$R_{\text{Approach, F-0}}$	0.2010	-
$R_{\text{Approach, F-Landing}}$	0.1827	-
Departures		
$B_{\text{F-T/O}}$ (Water)	0.0884	$Kt / lb^{0.5}$
$C_{\text{F-T/O}}$ (Water)	0.8550	$Kt / lb^{0.5}$
$R_{\text{Departure, F-T/O}}$	0.1433	-
$R_{\text{Cruise Climb, F-Cruise Climb}}$	0.1833	-
Level Flyover		
$R_{\text{Tour Cruise}}$	0.1717	-

APPENDIX B: METEOROLOGICAL DATA

This Appendix presents the test day meteorological data used in the processing of the acoustic data. Temperature in degrees Fahrenheit and relative humidity in percent taken at the aircraft's time at maximum sound pressure level during flyover, along with average wind speed in knots over the duration of the event are presented for each event in Tables 18 and 19. Changes in outdoor temperature and relative humidity are assumed to be negligible over short periods of time; accordingly, for the purpose of data processing, temperature and relative humidity were assumed to be constant over the ten-decibel up and down period of each aircraft event. Note that only meteorological data for events that passed the Quality Assurance test outlined in Section 9 are provided.

All acoustic data presented herein were analyzed in accordance with wind speed and direction criteria as specified in FAR 36 / Annex 16. As described in Section 0, test day meteorological data were used to correct the acoustic data to the SAE-AIR-1845 reference day atmospheric conditions.

Table 18. Cessna 182S Event Meteorological Data

Event	Date	Time of Day	Air Temp (^{o}F)	Relative Humidity (%)	Average Wind Speed (kts)
110	9/21/2010	11:17:33	59.2	68	4.3
120	9/21/2010	11:24:01	58.2	66	5.4
130	9/21/2010	11:32:45	59.2	66	3.5
210	9/21/2010	11:40:07	60.1	65	2.7
240	9/21/2010	11:54:53	56.7	68	4.3
250	9/21/2010	11:58:24	56.7	70	6.4
320	9/21/2010	12:08:05	58.3	68	5.1
330	9/21/2010	12:12:22	57.7	69	3.1
340	9/21/2010	12:16:13	59	67	3.7
420	9/21/2010	12:25:18	60.3	68	3.1
430	9/21/2010	12:30:36	57.7	68	2.5
440	9/21/2010	12:34:52	58.3	68	4.7
520	9/21/2010	12:44:00	57	71.4	2.3
530	9/21/2010	12:48:31	57.9	72	4.9
540	9/21/2010	12:53:10	56.1	72	3.7
610	9/21/2010	12:59:12	59	72	5.6
620	9/21/2010	13:06:05	57.9	72	4.3
640	9/21/2010	13:14:55	58.3	71	3.5
810	9/21/2010	10:51:01	57.1	70	3.1
830	9/21/2010	11:03:18	57.7	71	3.7
840	9/21/2010	11:08:24	58.5	67	2.9
910	9/23/2010	09:56:13	51.1	90	2.6

Table 19. De Havilland DHC-2 Event Meteorological Data

Event	Date	Time of Day	Air Temp (^{o}F)	Relative Humidity (%)	Average Wind Speed (kts)
130	9/22/2010	13:44:30	57.2	66	2.1
140	9/22/2010	13:47:49	57.6	65	2.9
150	9/22/2010	13:51:13	56.5	65	2.1
210	9/22/2010	13:18:51	57.6	61	3.1
220	9/22/2010	13:22:57	57.2	62	1.6
230	9/22/2010	13:28:46	57	62	2.7
320	9/22/2010	13:59:32	59.9	61	1.2
330	9/22/2010	14:05:42	60.1	57	2.3
340	9/22/2010	14:19:07	59.2	58	1.4
350	9/22/2010	16:08:13	60.1	61	2.1
410	9/22/2010	14:23:29	59	57	2.1
420	9/22/2010	14:28:23	59.2	59	3.3
430	9/22/2010	14:35:21	58.5	58	2.7
440	9/22/2010	14:39:35	58.5	57	2.9
510	9/22/2010	14:53:14	58.3	60	3.1
530	9/22/2010	15:06:40	58.5	61	2.9
540	9/22/2010	15:12:31	59.3	59	2.5
610	9/22/2010	15:21:28	59	61	3.1
620	9/22/2010	15:27:37	60.6	60	3.1
640	9/22/2010	15:53:48	60.6	58	3.9
940	9/23/2010	12:06:30	54	84	2.2

APPENDIX C: TIME SPACE POSITION INFORMATION (TSPI)

This Appendix presents a summary of the TSPI data used in the processing of the acoustic data. The data includes the test aircrafts' altitude and speed at time of L_{ASmx} for each event. Also included are the test aircrafts' rate of climb (ROC) and gradient for departure and approach events. LFO events, which do not have a ROC or gradient, are denoted with "N/A" (not applicable). Data presented in Tables 20 and 21 include aircraft-specific test and reference conditions. For completeness, values of DUR_{ADJ}, used to adjust exposure-based metrics from these conditions to the appropriate reference speed required for inclusion in the INM, are provided in the last column. Note that only TSPI data for events that passed the Quality Assurance test outlined in Section 9 are provided.

Table 20. Cessna 182S Event TSPI Data

Event	Event Description	Time at L_{ASmx}	Test Altitude (ft, AGL)	Rate of Climb (ft/min)	Gradient	Test Speed (kts)	Reference Speed (kts)	DUR_{ADJ} (dB)
110	LFO: Tour Cruise @ 500 ft	11:17:29	501.2	N/A	N/A	108.0	160	1.7
120	LFO: Tour Cruise @ 500 ft	11:23:57	512.6	N/A	N/A	109.0	160	1.7
130	LFO: Tour Cruise @ 500 ft	11:32:41	509.5	N/A	N/A	109.5	160	1.6
210	LFO: Normal Cruise @ 500 ft	11:40:04	482.4	N/A	N/A	110.5	160	1.6
240	LFO: Normal Cruise @ 500 ft	11:54:49	507.2	N/A	N/A	110.6	160	1.6
250	LFO: Normal Cruise @ 500 ft	11:58:22	492.1	N/A	N/A	109.9	160	1.6
320	DEP: Standard	12:08:05	524.6	493.0	-0.05695	87.8	160	2.6
330	DEP: Standard	12:12:22	552.3	579.1	-0.07415	88.5	160	2.6
340	DEP: Standard	12:16:13	458.0	525.2	-0.05708	88.7	160	2.6
420	DEP: Cruise Climb	12:25:18	457.8	472.2	-0.05130	86.0	160	2.7
430	DEP: Cruise Climb	12:30:36	687.5	322.4	-0.03550	84.2	160	2.8
440	DEP: Cruise Climb	12:34:52	508.7	253.9	-0.02638	85.9	160	2.7
520	APP: Flaps Initial	12:44:00	503.0	-347.1	0.04033	80.3	160	3.0
530	APP: Flaps Initial	12:48:31	512.7	-272.4	0.02798	79.8	160	3.0
540	APP: Flaps Initial	12:53:10	492.6	-227.7	0.02651	80.2	160	3.0
610	APP: Flaps 20	12:59:12	559.8	-460.7	0.04845	83.4	160	2.8
620	APP: Flaps 20	13:06:05	526.4	-733.2	0.07689	83.6	160	2.8
640	APP: Flaps 20	13:14:55	510.6	-474.7	0.04761	83.1	160	2.8
810	LFO: Appendix F Certification	10:50:54	1025.3	N/A	N/A	124.1	160	1.1
830	LFO: Appendix F Certification	11:03:12	1031.9	N/A	N/A	124.0	160	1.1
840	LFO: Appendix F Certification	11:08:18	952.7	N/A	N/A	123.3	160	1.1
910	Water Landing	09:56:13	0	N/A	N/A	51.2	160	4.9

Table 21. De Havilland DHC-2 Event TSPI Data

Event	Event Description	Time at L_{ASmx}	Test Altitude (ft, AGL)	Rate of Climb (ft/min)	Gradient (ft)	Test Speed (kts)	Reference Speed (kts)	DUR_{ADJ} (dB)
130	LFO: Tour Cruise @ 500 ft	13:44:30	496.5	N/A	N/A	97.5	160	2.2
140	LFO: Tour Cruise @ 500 ft	13:47:49	511.3	N/A	N/A	96.5	160	2.2
150	LFO: Tour Cruise @ 500 ft	13:51:13	494.9	N/A	N/A	97.6	160	2.1
210	LFO: Appendix F Certification	13:18:51	1028.4	N/A	N/A	116.7	160	1.4
220	LFO: Appendix F Certification	13:22:57	989.6	N/A	N/A	117.6	160	1.3
230	LFO: Appendix F Certification	13:28:46	990.5	N/A	N/A	118.8	160	1.3
320	DEP: Standard	13:59:32	620.3	820.8	-0.11027	70.6	160	3.6
330	DEP: Standard	14:05:42	668.2	723.6	-0.11137	62.9	160	4.1
340	DEP: Standard	14:19:07	491.8	920.9	-0.11977	76.4	160	3.2
350	DEP: Standard	16:08:13	551.3	897.6	-0.12609	70.6	160	3.6
410	DEP: Cruise Climb	14:23:29	359.7	82.3	-0.00958	84.9	160	2.8
420	DEP: Cruise Climb	14:28:23	269.7	419.5	-0.04808	86.2	160	2.7
430	DEP: Cruise Climb	14:35:21	310.7	255.3	-0.03216	88.2	160	2.6
440	DEP: Cruise Climb	14:39:35	257.4	25.6	-0.00292	86.9	160	2.7
510	APP: Flaps Initial	'14:53:14	475.5	-6.2	0.04122	87.7	160	2.6
530	APP: Flaps Initial	15:06:40	481.2	-1031.2	0.09083	112.5	160	1.5
540	APP: Flaps Initial	15:12:31	505.7	-971.3	0.08580	111.8	160	1.6
610	APP: Flaps Final	15:21:28	487.0	-787.1	0.08978	86.5	160	2.7
620	APP: Flaps Final	15:27:37	502.1	-698.8	0.08206	87.5	160	2.6
640	APP: Flaps Final	15:53:48	505.3	-673.5	0.07816	84.9	160	2.8
940	Water Landing	12:06:30	0.0	N/A	N/A	42.4	160	5.8

APPENDIX D: AIRCRAFT NOISE POWER DISTANCE DATA

Sections D.1 and D.2 present center and sideline NPDs for the 182S and DHC-2 test aircraft. As can be seen in Figure 3 and Figure 10, sideline data represents the left-side of the test aircraft (relative to the direction of travel). Data presented include tabular NPD results generated for four noise metrics: sound exposure level (SEL), denoted by the ANSI symbol L_{AE}, maximum, slow time- and A-weighted sound level (MXSA), denoted by the ANSI symbol L_{ASmx}, effective perceived noise level (EPNL), denoted by the ANSI symbol L_{EPN}, and tone-adjusted maximum, slow time-weighted, perceived noise level (MXSPNT), denoted by the symbol L_{PNTSmx}. All NPD data are corrected to the SAE-AIR-1845 reference day atmospheric conditions and reference speed of 160 knots.

Sections D.3 and D.4 present graphical representations of the L_{AE} NPDs derived using the simplified procedure for each aircraft measured. Only events that passed the Quality Assurance test outlined in Section 9 are included in this Appendix.

D.1 Cessna 182S Noise Power Distance Tables

Table 22. Cessna 182S L_{AE} NPDs

Dist. (ft)	100 Series LFO: Tour Cruise @ 500 ft		200 Series LFO: Normal Cruise @ 500 ft		300 Series DEP: Departure		400 Series DEP: Cruise Climb		500 Series APP: Flaps-initial		600 Series APP: Flaps 20	
	L_{AE} @ 160 kts		L_{AE} @ 160 kts		L_{AE} @ 160 kts		L_{AE} @ 160 kts		L_{AE} @ 160 kts		L_{AE} @ 160 kts	
	Center	Sideline	Center	Sideline	Center	Sideline	Center	Sideline	Center	Sideline	Center	Sideline
200	88.0	86.8	89.0	88.8	91.0	89.9	89.0	88.0	82.6	81.7	86.7	86.8
400	83.9	82.7	85.0	84.8	87.0	85.8	85.0	84.0	78.7	77.7	82.8	82.8
630	81.2	80.0	82.3	82.0	84.2	83.0	82.3	81.2	76.1	75.0	80.1	80.1
1000	78.3	77.0	79.4	79.1	81.3	80.0	79.4	78.3	73.3	72.2	77.4	77.2
2000	73.7	72.4	74.9	74.2	76.7	75.1	74.9	73.5	69.0	67.6	72.9	72.4
4000	68.8	67.3	69.9	68.6	71.6	69.3	70.0	68.0	64.4	62.4	68.0	66.7
6300	65.3	63.5	66.5	64.3	68.1	64.9	66.5	63.7	61.0	58.5	64.5	62.4
10000	61.5	59.3	62.7	59.3	64.3	59.8	62.7	58.7	57.3	53.9	60.6	57.2
16000	57.3	54.4	58.4	53.6	60.1	53.8	58.4	52.7	53.1	48.7	56.1	51.3
25000	52.7	48.8	53.8	47.3	55.4	47.4	53.7	46.1	48.4	43.0	51.1	45.1

Table 23. Cessna 182S L_{ASmx} NPDs

Dist. (ft)	100 Series LFO: Tour Cruise @ 500 ft		200 Series LFO: Normal Cruise @ 500 ft		300 Series DEP: Departure		400 Series DEP: Cruise Climb		500 Series APP: Flaps-initial		600 Series APP: Flaps 20	
	L_{ASmx} @ 160 kts		L_{ASmx} @ 160 kts		L_{ASmx} @ 160 kts		L_{ASmx} @ 160 kts		L_{ASmx} @ 160 kts		L_{ASmx} @ 160 kts	
	Center	Sideline	Center	Sideline	Center	Sideline	Center	Sideline	Center	Sideline	Center	Sideline
200	87.3	85.9	89.0	89.0	90.7	90.6	89.3	88.0	83.2	81.6	87.6	88.6
400	81.0	79.6	82.8	82.7	84.5	84.2	83.0	81.7	77.1	75.4	81.4	82.3
630	76.8	75.3	78.6	78.4	80.2	80.0	78.8	77.5	72.9	71.2	77.2	78.1
1000	72.4	70.9	74.2	74.0	75.8	75.5	74.5	73.1	68.7	66.9	72.9	73.7
2000	65.6	64.0	67.4	66.9	68.9	68.3	67.7	66.1	62.1	60.0	66.2	66.6
4000	58.4	56.6	60.2	59.0	61.6	60.3	60.6	58.3	55.2	52.6	59.1	58.7
6300	53.4	51.4	55.3	53.2	56.6	54.4	55.6	52.5	50.4	47.2	54.1	52.9
10000	48.1	45.7	50.0	46.7	51.3	47.7	50.2	46.0	45.2	41.1	48.6	46.3
16000	42.3	39.2	44.2	39.4	45.5	40.2	44.4	38.4	39.4	34.3	42.6	38.8
25000	36.3	32.2	38.1	31.7	39.5	32.3	38.3	30.4	33.3	27.2	36.2	31.2

Table 24. Cessna 182S LEPN NPDs

Dist. (ft)	100 Series LFO: Tour Cruise @ 500 ft		200 Series LFO: Normal Cruise @ 500 ft		300 Series DEP: Departure		400 Series DEP: Cruise Climb		500 Series APP: Flaps-initial		600 Series APP: Flaps 20	
	L_{EPN} @ 160 kts		L_{EPN} @ 160 kts		L_{EPN} @ 160 kts		L_{EPN} @ 160 kts		L_{EPN} @ 160 kts		L_{EPN} @ 160 kts	
	Center	Sideline	Center	Sideline	Center	Sideline	Center	Sideline	Center	Sideline	Center	Sideline
200	94.4	92.9	96.0	93.6	97.5	94.8	95.8	92.9	90.4	87.8	93.7	91.9
400	90.2	88.6	91.8	89.3	93.3	90.5	91.6	88.7	86.2	83.5	89.6	87.7
630	87.2	85.6	88.9	86.3	90.4	87.5	88.7	85.7	83.3	80.5	86.8	84.7
1000	84.1	82.3	85.8	83.1	87.2	84.2	85.7	82.4	80.2	77.0	83.8	81.5
2000	79.0	76.7	80.8	77.6	82.2	78.6	80.8	76.9	74.9	71.4	78.9	76.1
4000	72.7	70.4	74.7	71.2	76.1	72.1	74.7	70.5	68.8	65.0	72.8	69.7
6300	68.2	66.0	70.2	66.4	71.6	67.1	70.3	65.6	64.4	60.5	68.5	65.0
10000	63.7	61.7	65.7	61.3	67.2	61.5	65.6	60.4	59.9	55.9	63.8	60.0
16000	59.2	57.3	61.2	56.1	63.1	55.8	60.8	55.2	55.2	51.3	59.0	54.9
25000	54.8	53.1	56.9	51.2	59.2	50.4	56.3	50.3	50.8	46.9	54.5	50.1

Table 25. Cessna 182S L_{PNTSmx} NPDs

Dist. (ft)	100 Series LFO: Tour Cruise @ 500 ft		200 Series LFO: Normal Cruise @ 500 ft		300 Series DEP: Departure		400 Series DEP: Cruise Climb		500 Series APP: Flaps-initial		600 Series APP: Flaps 20	
	L_{PNTSmx} @ 160 kts		L_{PNTSmx} @ 160 kts		L_{PNTSmx} @ 160 kts		L_{PNTSmx} @ 160 kts		L_{PNTSmx} @ 160 kts		L_{PNTSmx} @ 160 kts	
	Center	Sideline	Center	Sideline	Center	Sideline	Center	Sideline	Center	Sideline	Center	Sideline
200	105.6	101.8	107.1	103.7	108.5	105.3	106.8	102.9	101.1	97.3	104.8	103.0
400	99.1	95.3	100.6	97.2	102.1	98.8	100.4	96.4	94.6	90.8	98.4	96.6
630	94.7	90.8	96.2	92.8	97.7	94.3	96.1	91.9	90.2	86.2	94.1	92.1
1000	90.1	86.0	91.6	88.0	93.0	89.5	91.5	87.1	85.6	81.3	89.5	87.4
2000	82.7	78.1	84.4	80.3	85.7	81.6	84.3	79.3	78.0	73.4	82.4	79.7
4000	74.2	69.6	76.0	71.6	77.4	72.8	76.0	70.7	69.7	64.8	74.1	71.1
6300	68.2	63.7	70.1	65.3	71.4	66.4	70.1	64.3	63.8	58.8	68.2	64.9
10000	62.2	57.9	64.1	58.7	65.5	59.3	63.9	57.7	57.8	52.7	62.0	58.4
16000	56.1	51.9	58.1	52.0	59.9	52.0	57.6	50.9	51.6	46.5	55.8	51.7
25000	50.3	46.3	52.3	45.6	54.6	45.1	51.6	44.5	45.8	40.6	49.8	45.5

Table 26. Cessna 182S Water Landing NPDs

Dist. (ft)	Event 910 Water Landing			
	L_{AE} @ 160 kts	L_{ASmx} @ 160 kts	L_{EPN} @ 160 kts	L_{PNTSmx} @ 160 kts
	Center	Center	Center	Center
200	70.1	69.0	76.8	86.0
400	66.0	62.6	71.8	78.7
630	63.2	58.3	68.3	73.8
1000	60.2	53.9	64.5	68.5
2000	55.5	46.9	58.3	60.0
4000	50.4	39.6	51.1	50.5
6300	46.9	34.5	45.7	43.6
10000	43.2	29.3	40.1	36.6
16000	39.1	23.8	34.5	29.4
25000	35.0	18.2	29.2	22.7

D.2 De Havilland Canada DHC-2 Noise Power Distance Tables

Table 27. De Havilland Canada DHC-2 L_{AE} NPDs

Dist. (ft)	100 Series LFO: Tour Cruise @ 500 ft		300 Series DEP: Departure		400 Series DEP: Cruise Climb		500 Series APP: Flaps-initial		600 Series APP: Flaps-final	
	L_{AE} @ 160 kts		L_{AE} @ 160 kts		L_{AE} @ 160 kts		L_{AE} @ 160 kts		L_{AE} @ 160 kts	
	Center	Sideline	Center	Sideline	Center	Sideline	Center	Sideline	Center	Sideline
200	90.1	88.9	98.7	101.3	91.2	89.6	86.7	86.6	80.1	79.3
400	85.8	84.7	94.6	97.3	86.9	85.6	82.5	82.6	75.9	75.2
630	82.8	81.9	91.8	94.5	83.9	82.8	79.6	79.8	73.0	72.5
1000	79.5	78.9	88.7	91.6	80.7	79.9	76.5	76.9	70.0	69.7
2000	74.0	74.2	83.7	86.7	75.3	75.2	71.5	72.2	65.3	65.2
4000	67.7	69.0	77.8	80.9	69.0	69.9	65.7	67.0	60.1	60.3
6300	63.2	65.3	73.1	76.3	64.4	66.0	61.3	63.2	56.3	56.8
10000	58.1	61.3	67.5	70.8	59.2	61.5	56.3	58.8	52.0	52.7
16000	52.5	56.8	60.7	64.2	53.5	56.2	50.7	53.7	47.0	47.8
25000	46.7	51.8	53.6	56.9	47.7	50.1	44.6	47.9	41.5	42.1

Table 28. De Havilland Canada DHC-2 L_{ASmx} NPDs

Dist. (ft)	100 Series LFO: Tour Cruise @ 500 ft		300 Series DEP: Departure		400 Series DEP: Cruise Climb		500 Series APP: Flaps-initial		600 Series APP: Flaps-final	
	L_{ASmx} @ 160 kts		L_{ASmx} @ 160 kts		L_{ASmx} @ 160 kts		L_{ASmx} @ 160 kts		L_{ASmx} @ 160 kts	
	Center	Sideline	Center	Sideline	Center	Sideline	Center	Sideline	Center	Sideline
200	91.0	87.4	99.6	102.7	92.6	88.6	86.0	84.3	78.0	77.2
400	84.5	81.0	93.3	96.4	86.0	82.3	79.5	78.0	71.6	70.9
630	80.0	76.7	89.0	92.2	81.6	78.0	75.2	73.8	67.3	66.7
1000	75.2	72.2	84.4	87.7	76.8	73.6	70.6	69.4	62.8	62.4
2000	67.4	65.2	77.2	80.6	69.1	66.7	63.2	62.4	55.7	55.7
4000	58.9	57.8	69.0	72.5	60.6	59.2	55.2	55.0	48.3	48.5
6300	52.8	52.6	62.8	66.5	54.5	53.8	49.3	49.7	43.0	43.5
10000	46.3	47.1	55.7	59.5	47.8	47.8	42.8	43.8	37.2	37.9
16000	39.1	41.0	47.4	51.3	40.6	40.9	35.7	37.1	30.7	31.5
25000	31.8	34.6	38.8	42.5	33.3	33.4	28.2	29.9	23.8	24.4

Table 29. De Havilland Canada DHC-2 L_{EPN} NPDs

Dist. (ft)	100 Series LFO: Tour Cruise @ 500 ft		300 Series DEP: Departure		400 Series DEP: Cruise Climb		500 Series APP: Flaps-initial		600 Series APP: Flaps-final	
	L_{EPN} @ 160 kts		L_{EPN} @ 160 kts		L_{EPN} @ 160 kts		L_{EPN} @ 160 kts		L_{EPN} @ 160 kts	
	Center	Sideline	Center	Sideline	Center	Sideline	Center	Sideline	Center	Sideline
200	94.8	93.4	103.2	104.8	96.6	94.1	91.5	91.1	85.6	84.4
400	90.4	89.1	98.8	100.6	91.9	89.7	87.1	86.8	81.0	80.0
630	87.3	86.2	95.8	97.7	88.7	86.6	83.9	83.8	77.7	76.9
1000	83.9	82.9	92.4	94.4	85.1	83.3	80.4	80.5	74.1	73.4
2000	77.7	77.6	87.0	89.0	79.0	77.9	74.6	75.1	68.0	67.8
4000	70.9	71.2	80.4	82.7	72.0	71.7	68.0	68.7	61.6	61.5
6300	65.9	66.8	76.0	78.0	66.8	67.2	63.4	64.7	57.3	57.3
10000	61.4	62.5	71.8	72.6	61.5	62.1	58.9	60.6	53.0	52.9
16000	57.1	58.4	68.1	67.1	56.5	57.0	54.3	56.5	48.5	48.4
25000	52.9	54.4	64.5	61.8	51.8	52.2	50.0	52.6	44.3	44.2

Table 30. De Havilland Canada DHC-2 L_{PNTSmx} NPDs

Dist. (ft)	100 Series LFO: Tour Cruise @ 500 ft		300 Series DEP: Departure		400 Series DEP: Cruise Climb		500 Series APP: Flaps-initial		600 Series APP: Flaps-final	
	L_{PNTSmx} @ 160 kts		L_{PNTSmx} @ 160 kts		L_{PNTSmx} @ 160 kts		L_{PNTSmx} @ 160 kts		L_{PNTSmx} @ 160 kts	
	Center	Sideline	Center	Sideline	Center	Sideline	Center	Sideline	Center	Sideline
200	105.3	103.1	114.1	116.2	108.4	104.1	100.6	99.9	94.5	93.0
400	98.7	96.6	107.4	109.7	101.5	97.5	94.0	93.3	87.7	86.4
630	94.1	92.1	102.9	105.3	96.8	92.9	89.3	88.8	82.9	81.8
1000	89.2	87.4	98.1	100.5	91.7	88.1	84.3	84.1	77.7	76.8
2000	80.8	79.8	90.4	92.9	83.3	80.5	76.3	76.5	69.4	68.9
4000	71.7	71.2	81.6	84.3	74.0	72.1	67.4	67.8	60.8	60.4
6300	65.2	65.2	75.6	78.1	67.4	66.0	61.4	62.3	55.0	54.7
10000	59.3	59.5	70.0	71.3	60.6	59.4	55.3	56.7	49.1	48.8
16000	53.4	53.8	64.7	64.2	54.1	52.8	49.2	51.0	43.2	42.8
25000	47.8	48.4	59.7	57.5	47.9	46.5	43.4	45.7	37.5	37.1

Table 31. De Havilland Canada DHC-2 Water Landing NPDs

Dist. (ft)	Event 940 Water Landing			
	L_{AE} @ 160 kts	L_{ASmx} @ 160 kts	L_{EPN} @ 160 kts	L_{PNTSmx} @ 160 kts
	Center	Center	Center	Center
200	68.7	66.8	73.4	82.7
400	64.2	60.0	68.1	75.2
630	61.0	55.3	64.1	69.6
1000	57.5	50.3	59.2	63.2
2000	51.9	42.5	50.4	52.2
4000	45.6	34.0	40.8	40.3
6300	41.1	28.0	32.3	30.3
10000	36.3	21.6	23.6	20.2
16000	31.3	15.1	14.9	9.9
25000	26.4	8.7	6.5	0.1

D.3 Cessna 182S LAE NPD Plots

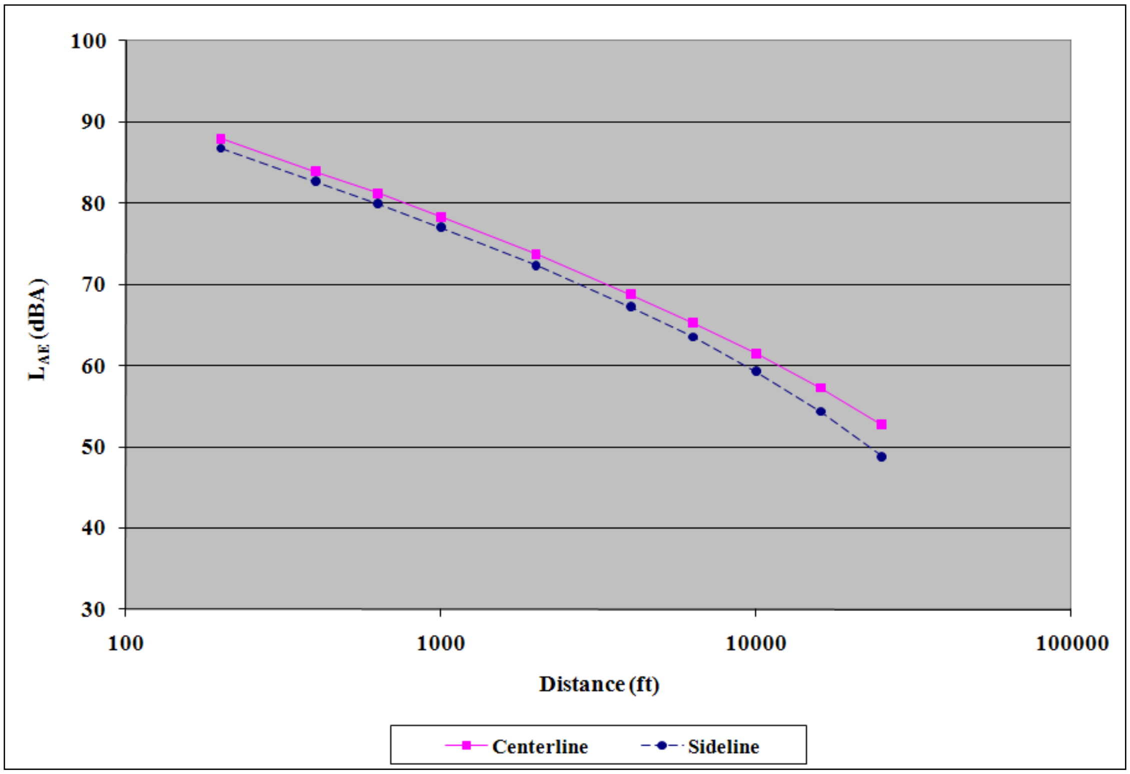

Figure 30. 182S 100 Series LAE Data (Ref. Spd. = 160 kts.)

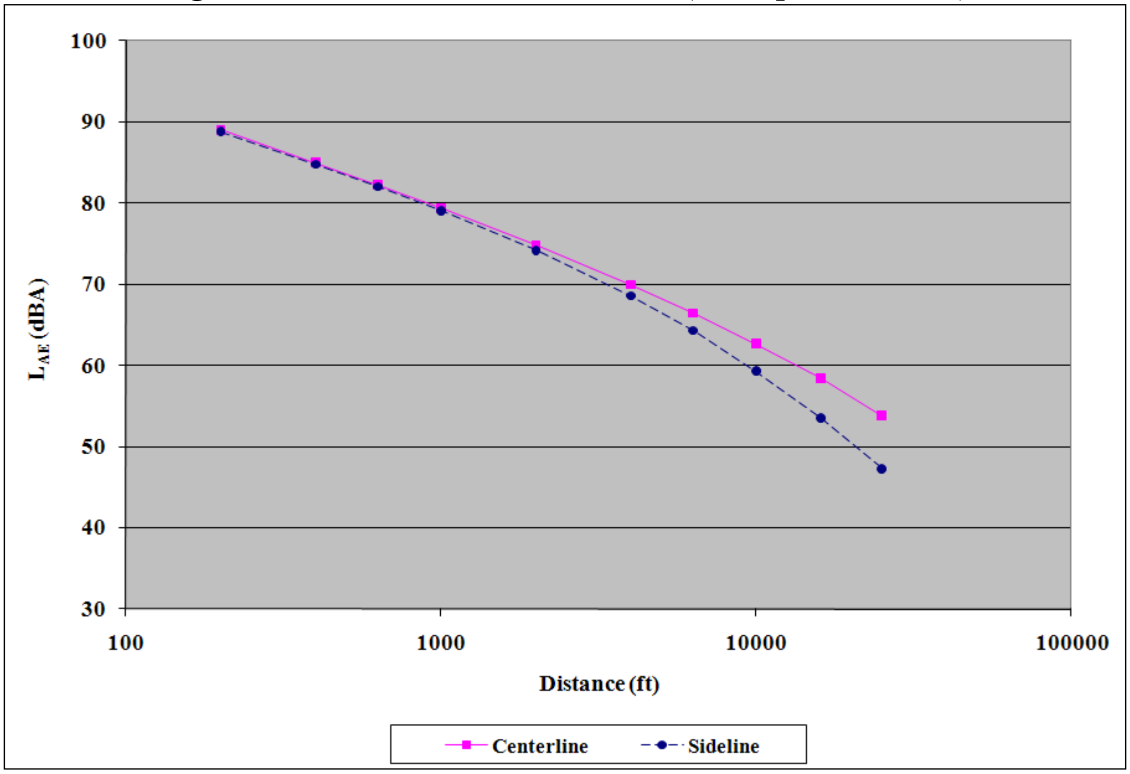

Figure 31. 182S 200 Series LAE Data (Ref. Spd. = 160 kts.)

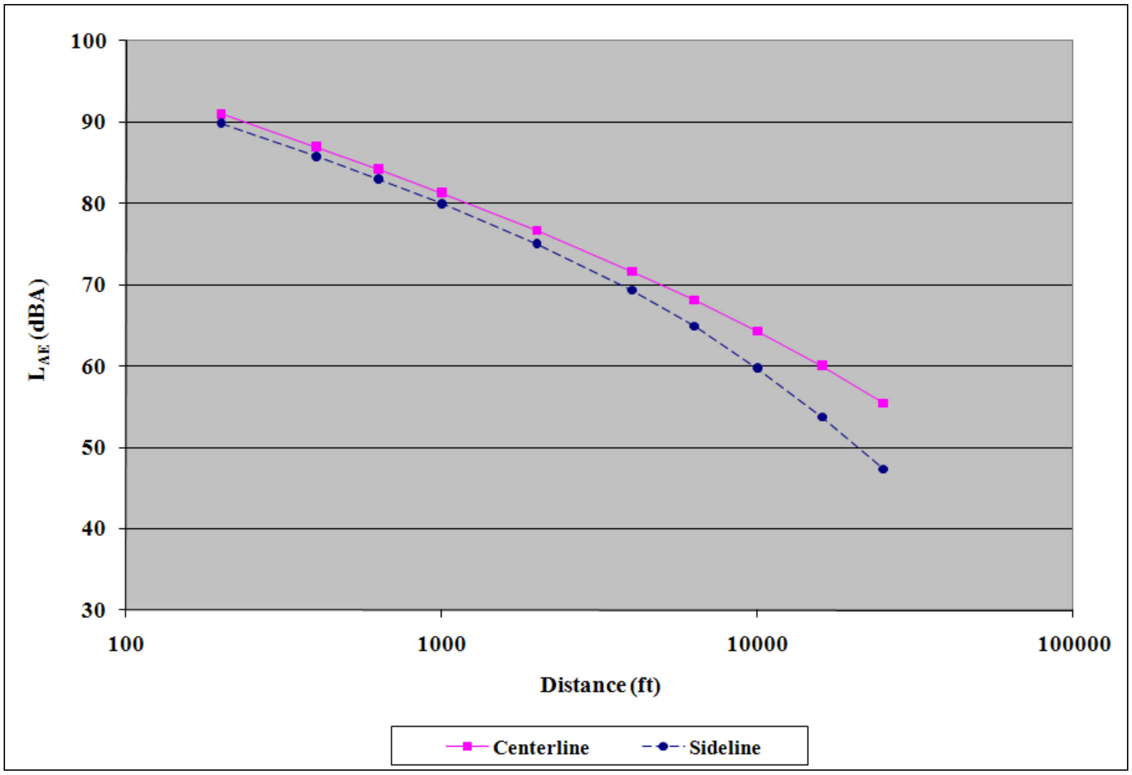

Figure 32. 182S 300 Series LAE Data (Ref. Spd. = 160 kts.)

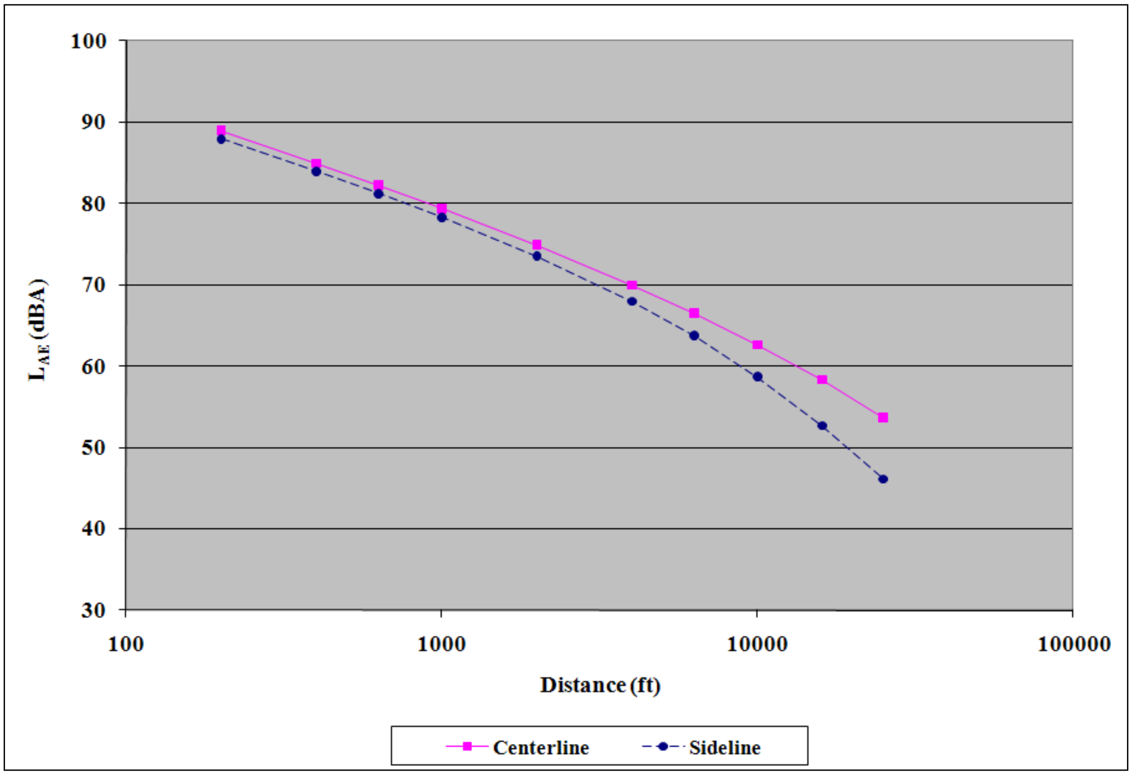

Figure 33. 182S 400 Series LAE Data (Ref. Spd. = 160 kts.)

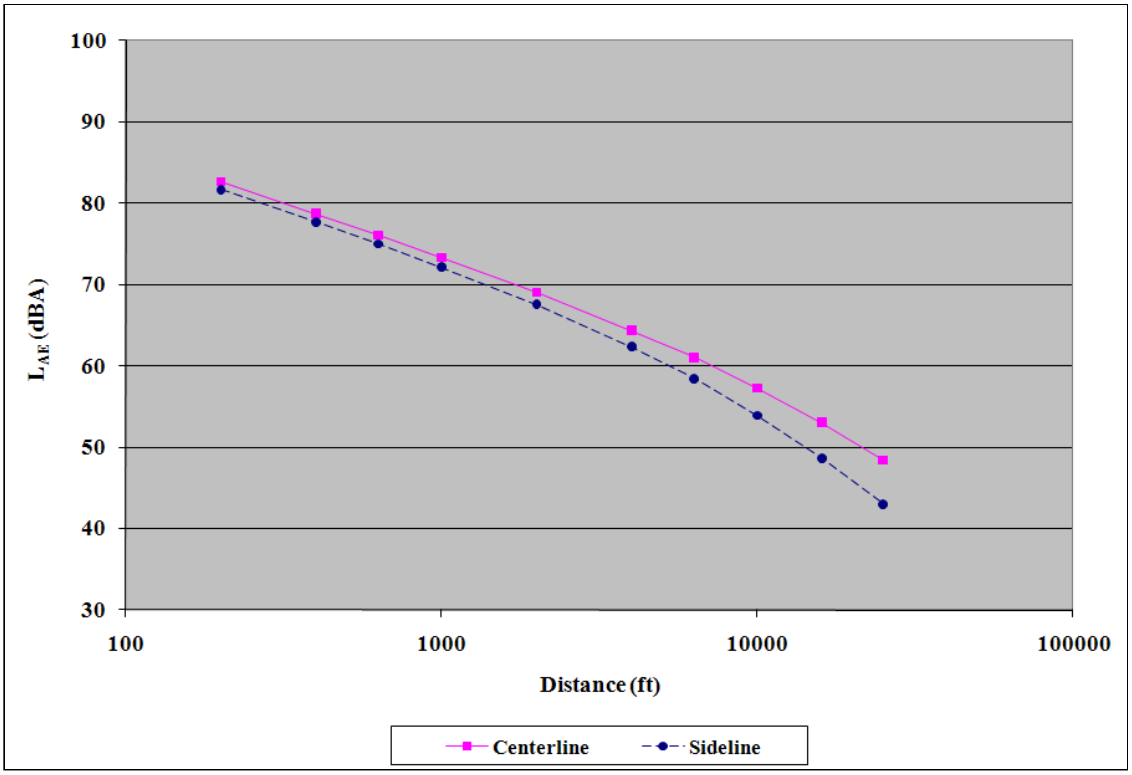

Figure 34. 182S 500 Series LAE Data (Ref. Spd. = 160 kts.)

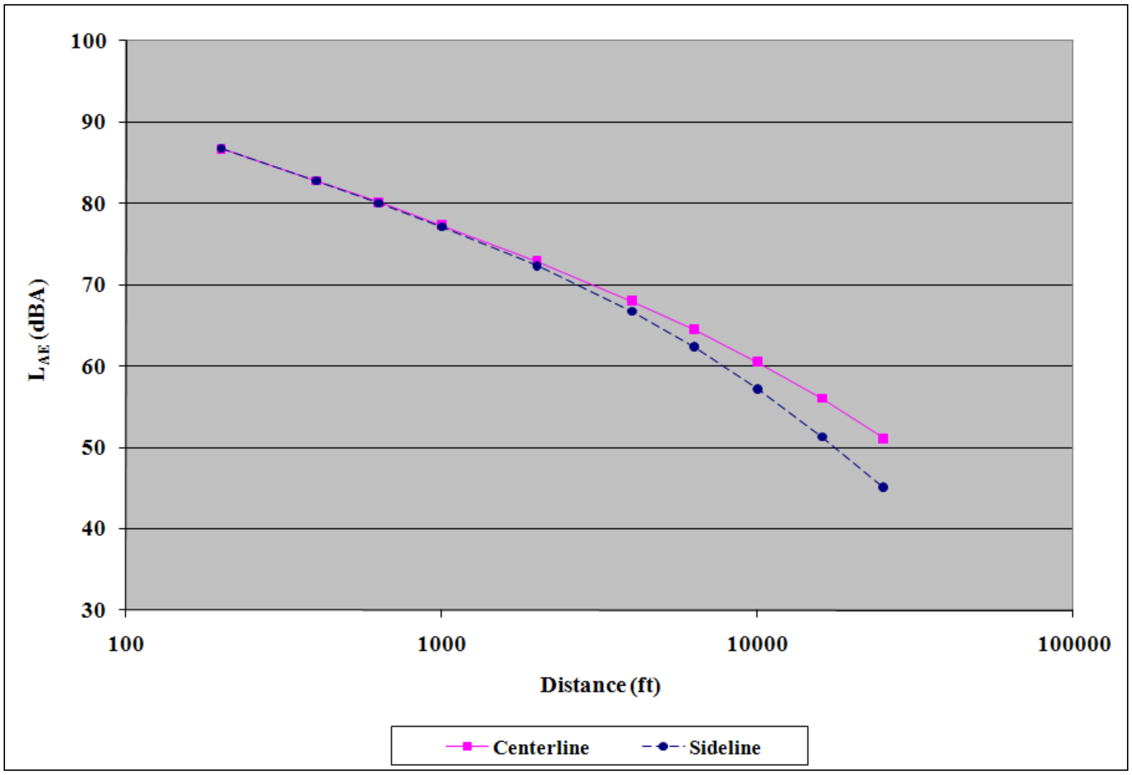

Figure 35. 182S 600 Series LAE Data (Ref. Spd. = 160 kts.)

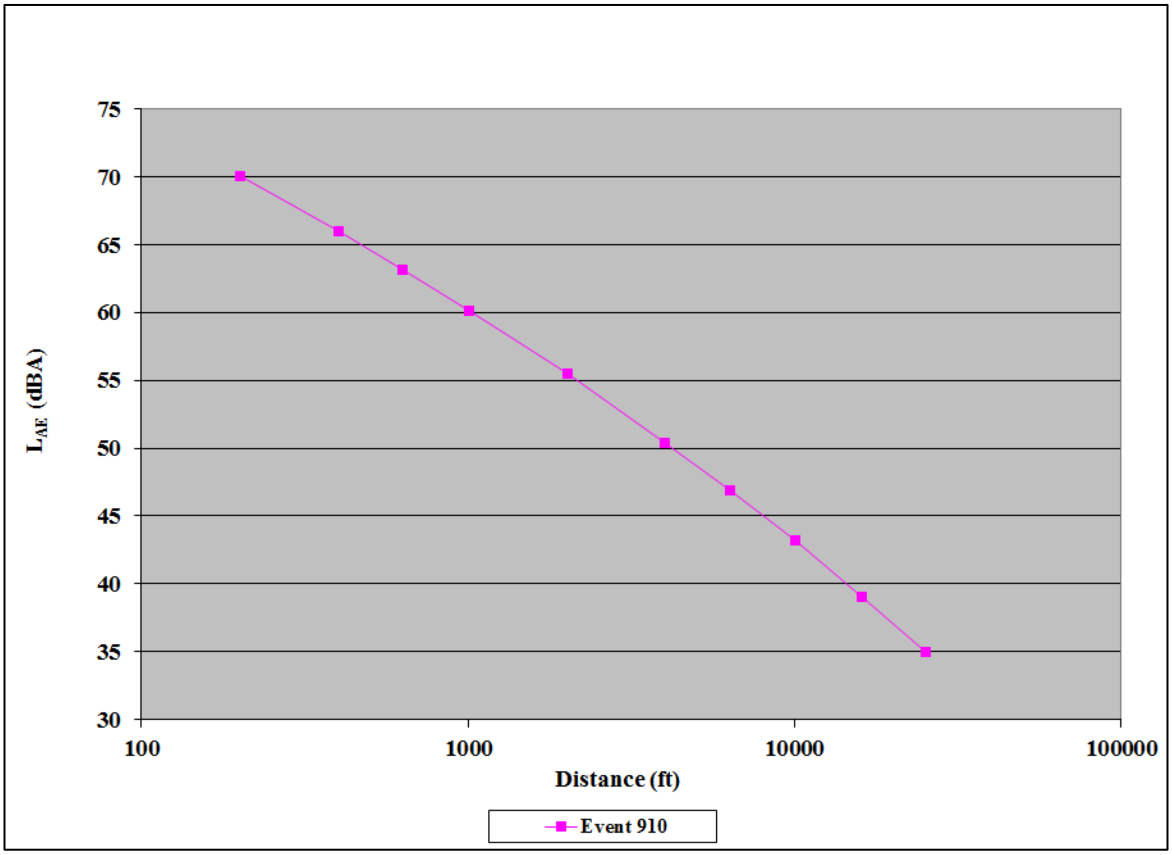

Figure 36. 182S Event 910 (Water Landing) LAE Data (Ref. Spd. = 160 kts.)

D.4 De Havilland Canada DHC-2 LAE NPD Plots

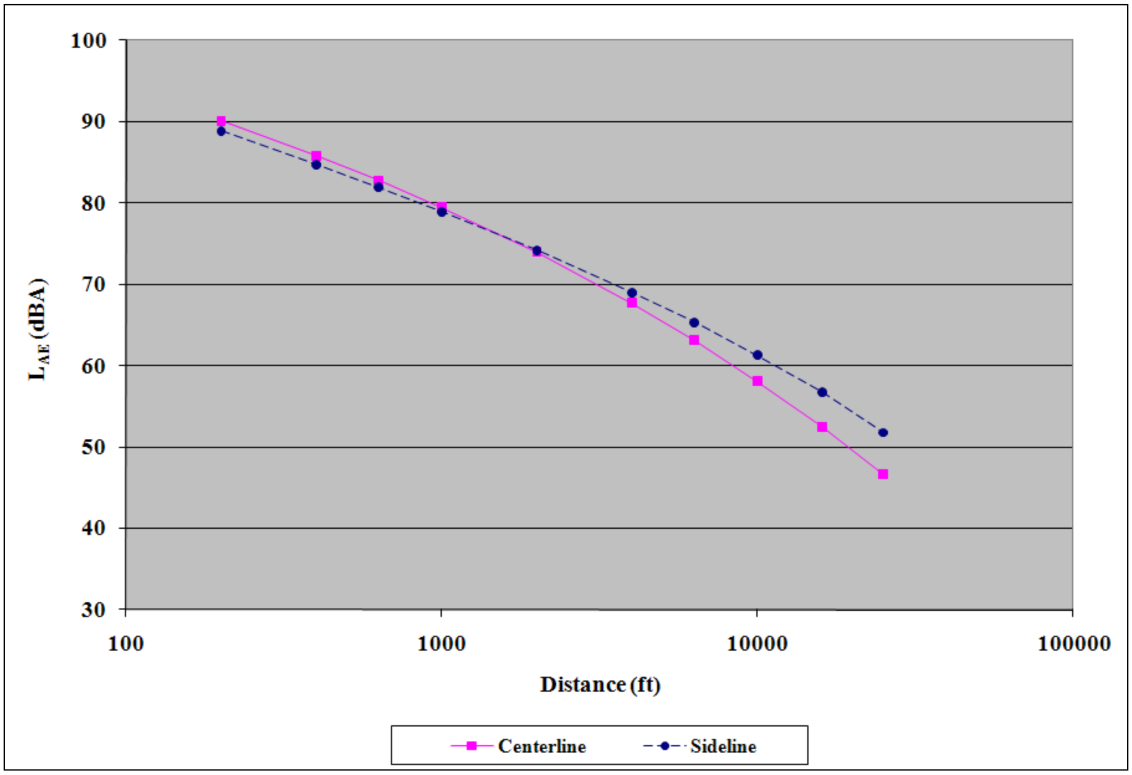

Figure 37. DHC-2 100 Series LAE Data (Ref. Spd. = 160 kts.)

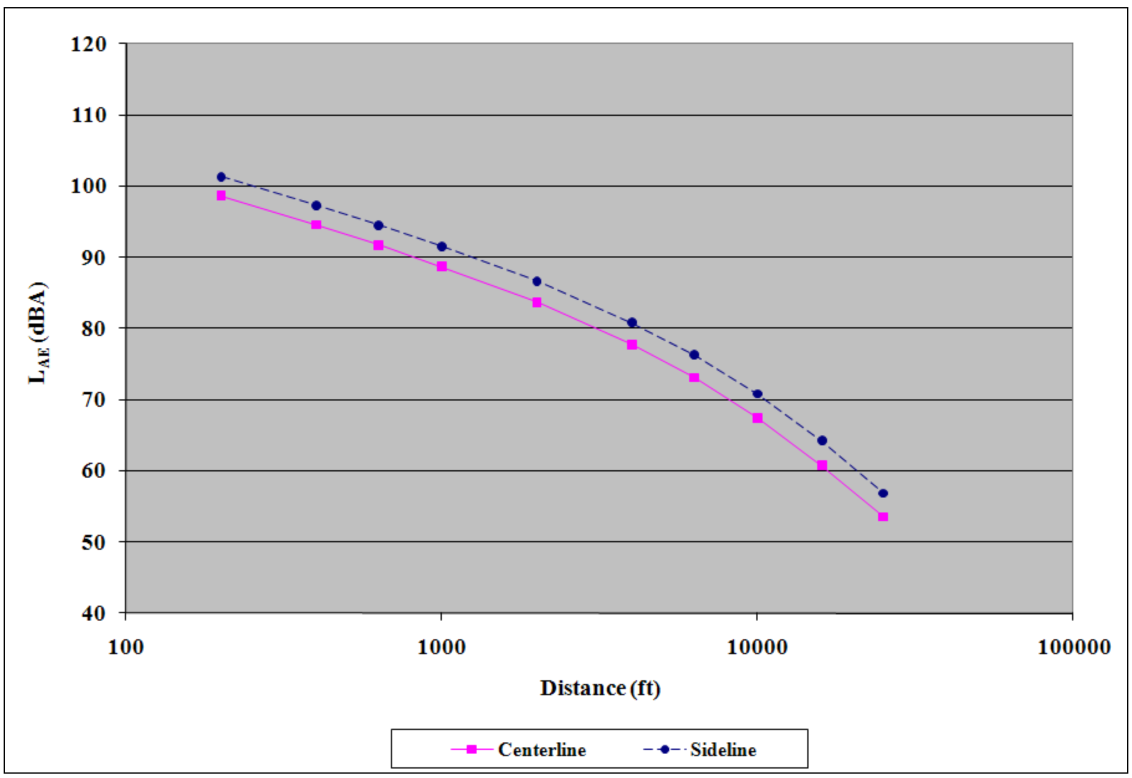

Figure 38. DHC-2 300 Series LAE Data (Ref. Spd. = 160 kts.)

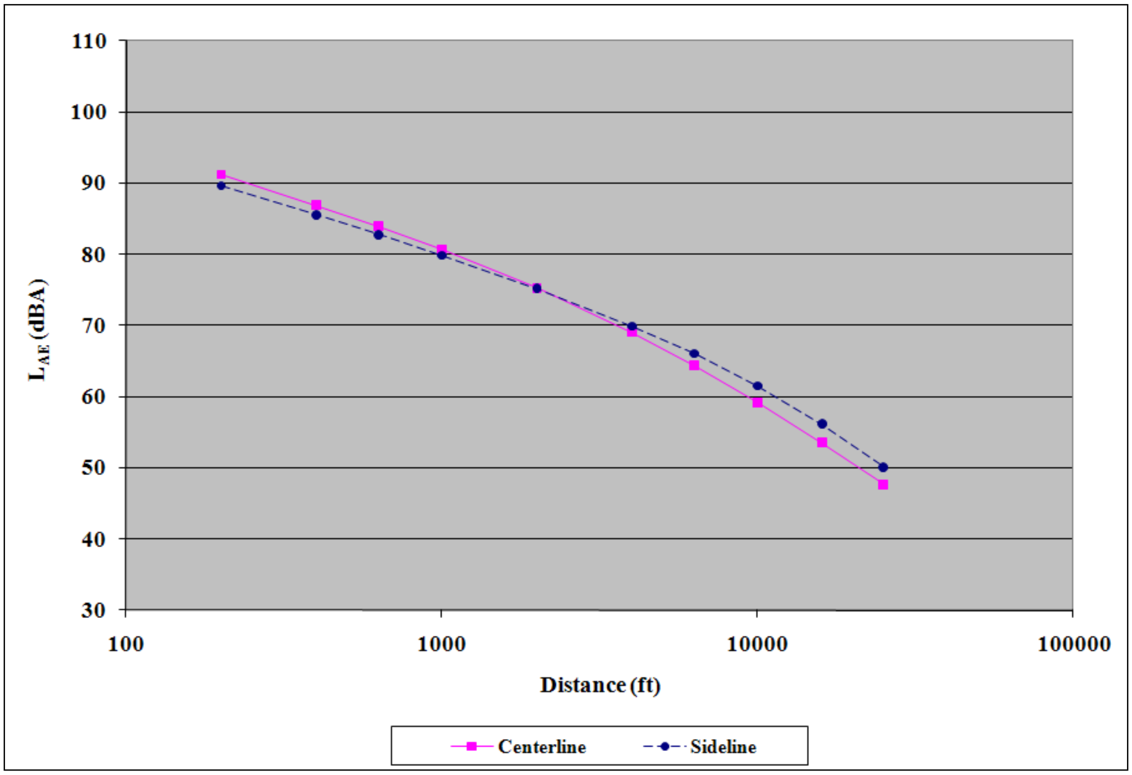

Figure 39. DHC-2 400 Series LAE Data (Ref. Spd. = 160 kts.)

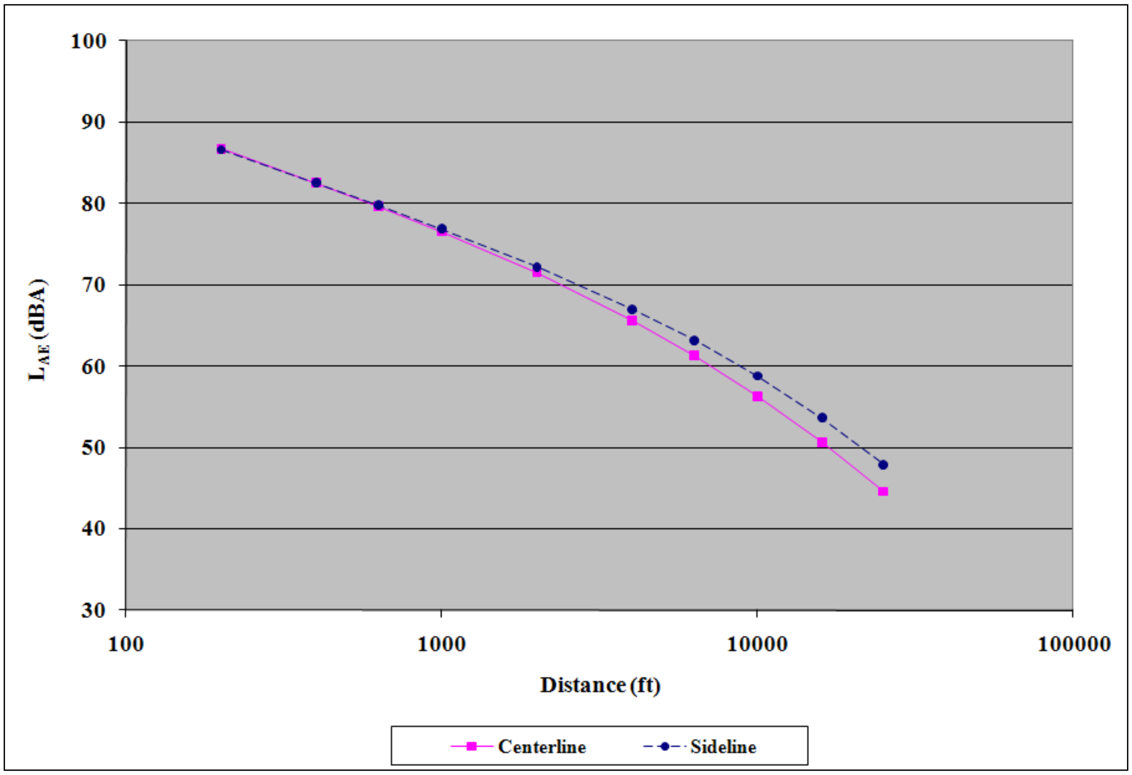

Figure 40. DHC-2 500 Series LAE Data (Ref. Spd. = 160 kts.)

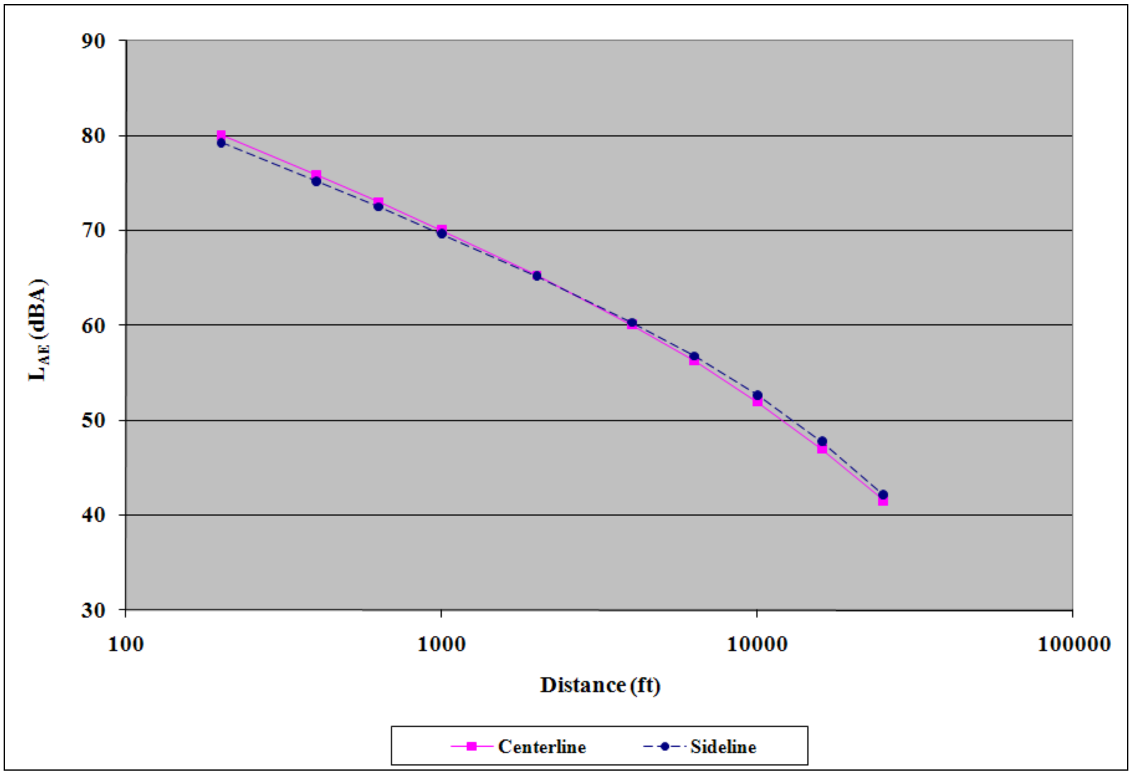

Figure 41. DHC-2 600 Series LAE Data (Ref. Spd. = 160 kts.)

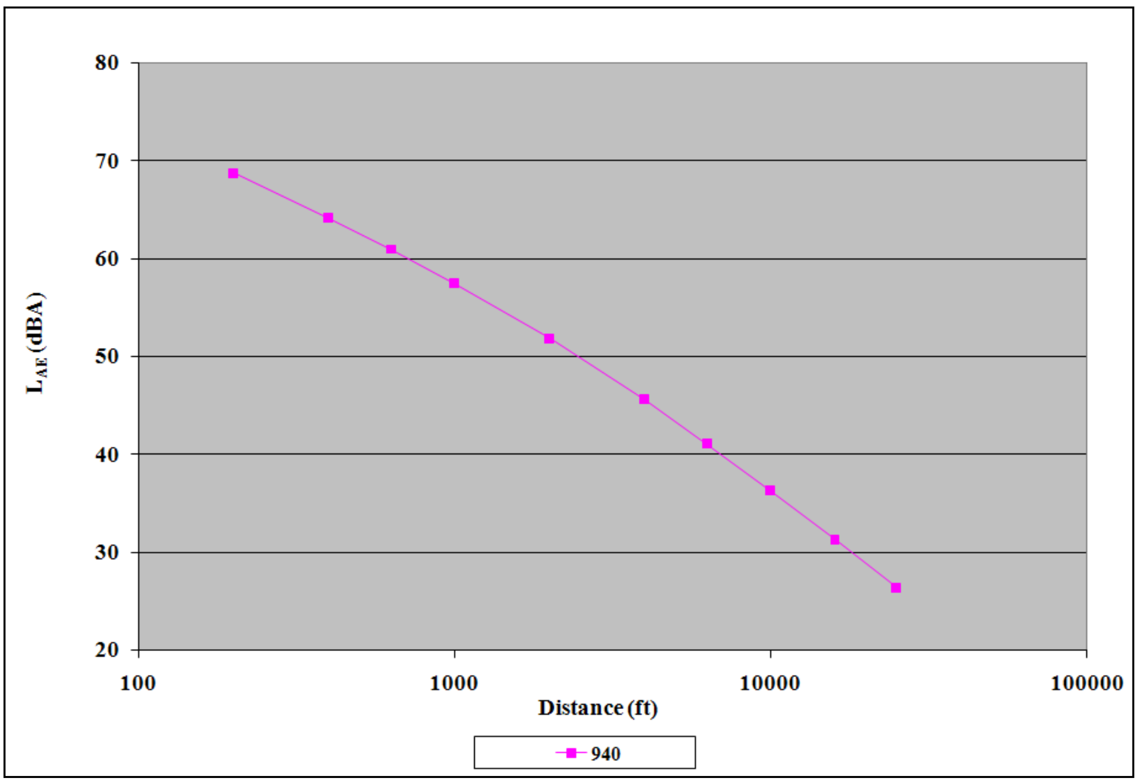

Figure 42. DHC-2 Event 940 (Water Landing) LAE Data (Ref. Spd. = 160 kts.)

APPENDIX E: SPECTRAL CLASS

The INM utilizes spectral data for some of its calculations, e.g., atmospheric absorption. Accordingly, representative spectral data are presented for each Dynamic Operations measurement series for which data were collected. Provided below is the 1,000 feet LFO, APP, and DEP adjusted spectral information used to determine each aircraft's LFO, APP, and DEP spectral classes. Each spectrum was generated from noise data collected during LFO, APP, and DEP events. These data were adjusted to 1,000 feet in Volpe Center's LCorrect processing software, grouped by configuration and power settings, and arithmetically averaged together. Each spectrum has been normalized to 70.0 dB at 1,000 Hz per the methodology employed in Reference 18, and is described in Section 8.5. The INM spectral class assignments determined for these aircraft are listed in Table 32.

Table 32. INM Spectral Class Assignments

Aircraft	Operation	Spectral Class Assignment
Cessna 182S	DEP	111
	APP	211
	LFO*	112
De Havilland Canada DHC-2	DEP	113†
	APP	213
	LFO*	105

* For fixed-wing aircraft in INM, only departure and approach spectral class assignments are used. Additional spectral class assignments are provided for use with research and non-standard modeling in INM.

† In INM, there is an engine location parameter associated with spectral classes. This engine location parameter is used in the lateral attenuation adjustment calculation, which takes into account different lateral directivity for 5 different types of aircraft in INM: jets with wing-mounted engines, jets with fuselage-mounted engines, propeller aircraft, military aircraft, and helicopters. The best spectral class match for the DHC-2 for departure operations is spectral class 113 in INM 7.0b. However, that spectral class is associated with the directivity for jets with fuselage-mounted engines in INM 7.0b. Therefore, a new spectral class was added to INM 7.0c, to best represent the DHC-2 departure spectrum with the directivity for propeller aircraft. That new departure special class is 135.

E.1 Cessna 182S Spectral Class Comparison

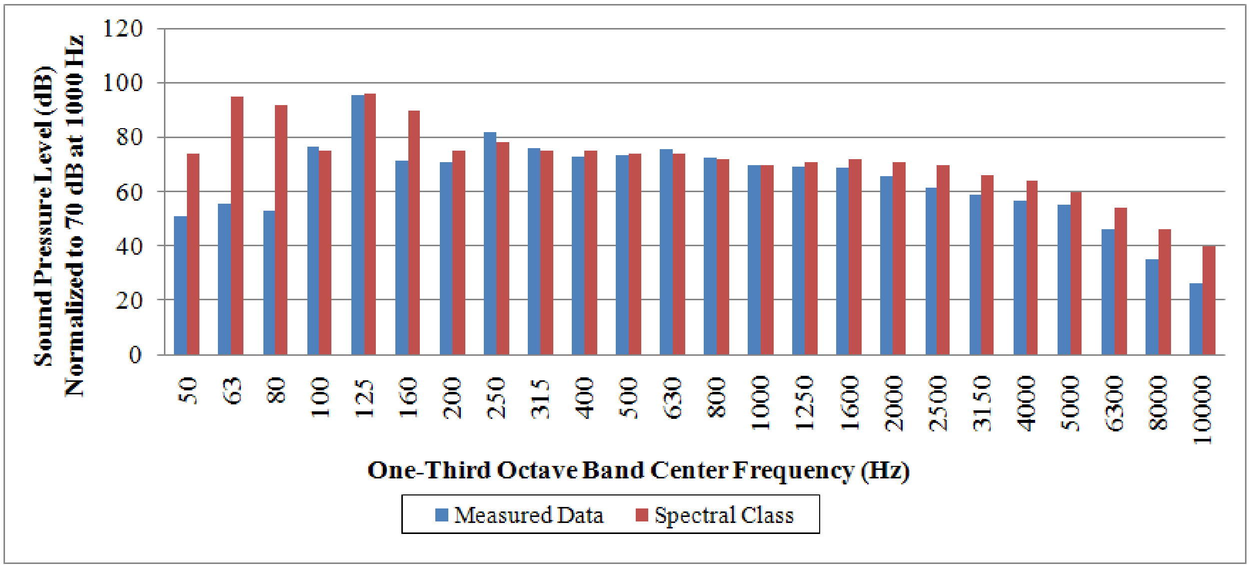

Figure 43. 182S Average 1000-ft 100 Series LFO Spectrum (normalized)

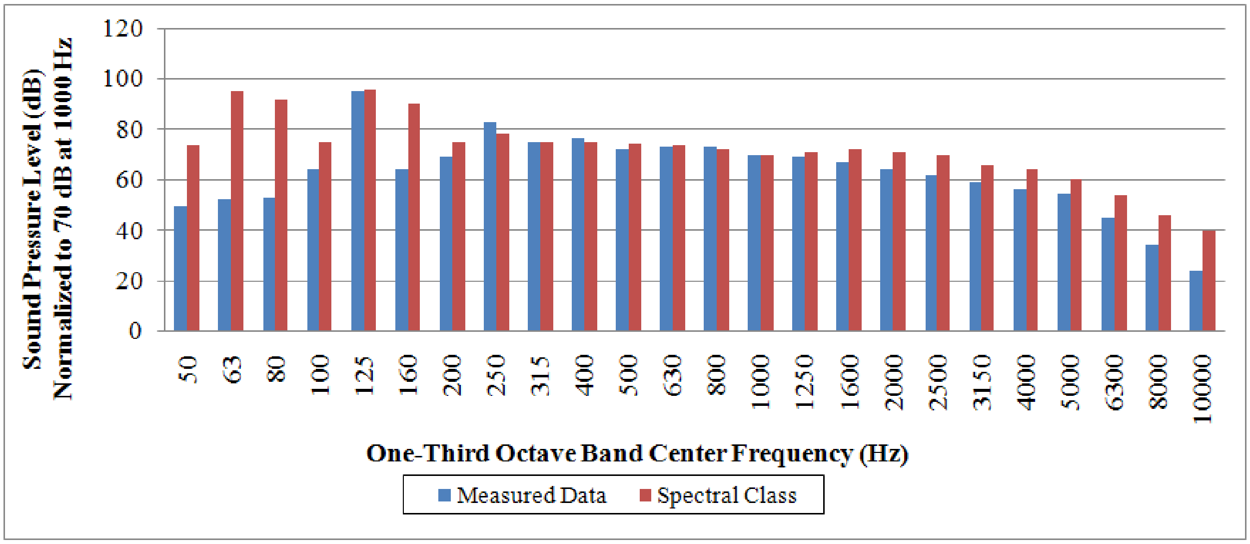

Figure 44. 182S Average 1000-ft 200 Series LFO Spectrum (normalized)

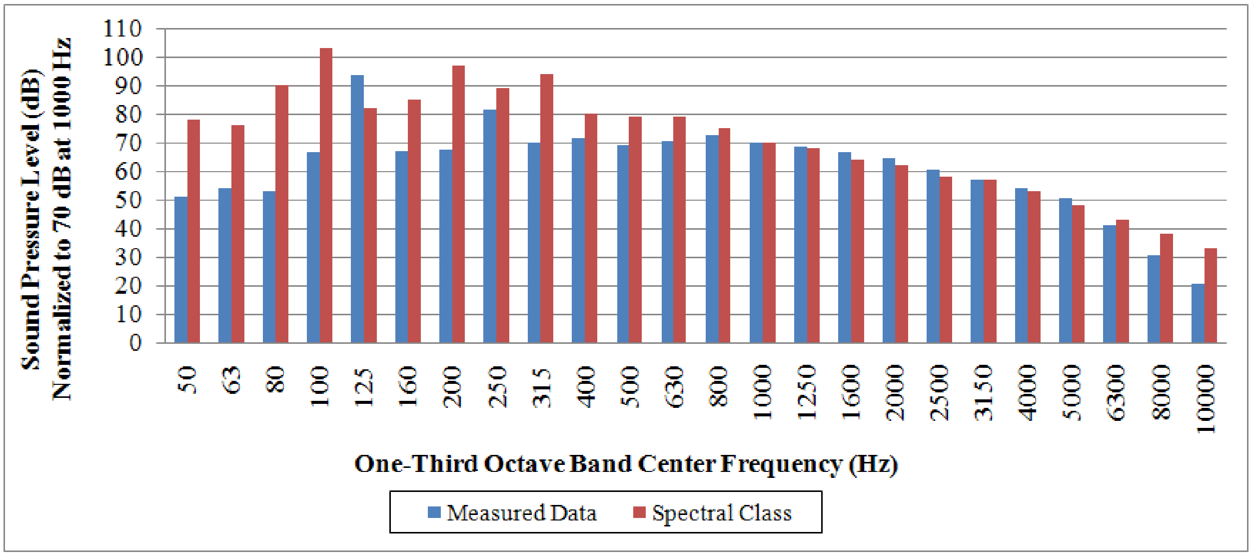

Figure 45. 182S Average 1000-ft 300 Series DEP Spectrum (normalized)

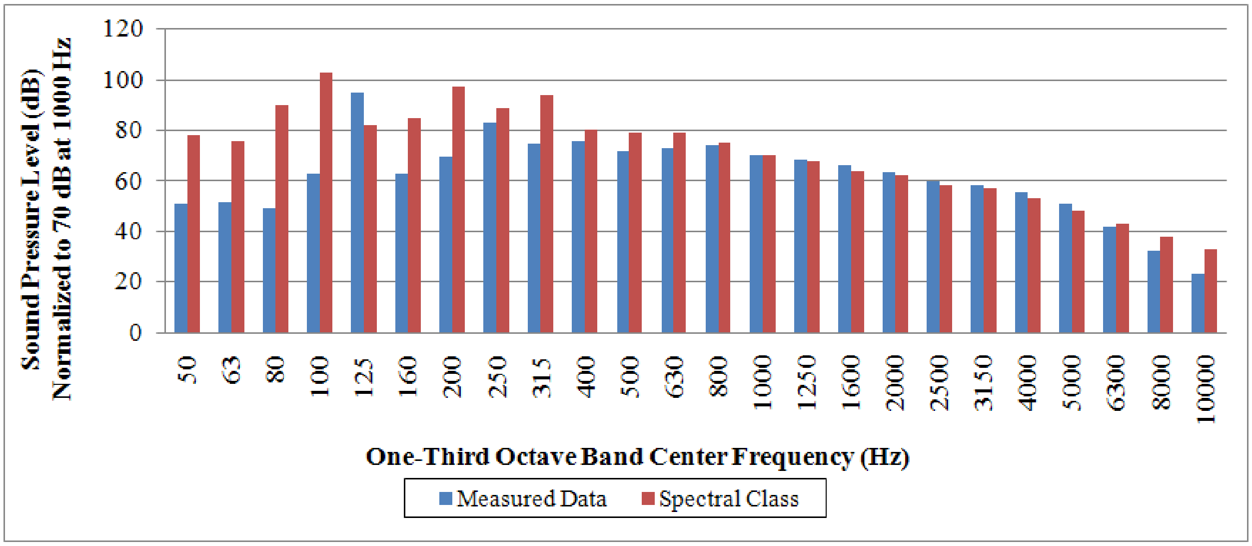

Figure 46. 182S Average 1000-ft 400 Series DEP Spectrum (normalized)

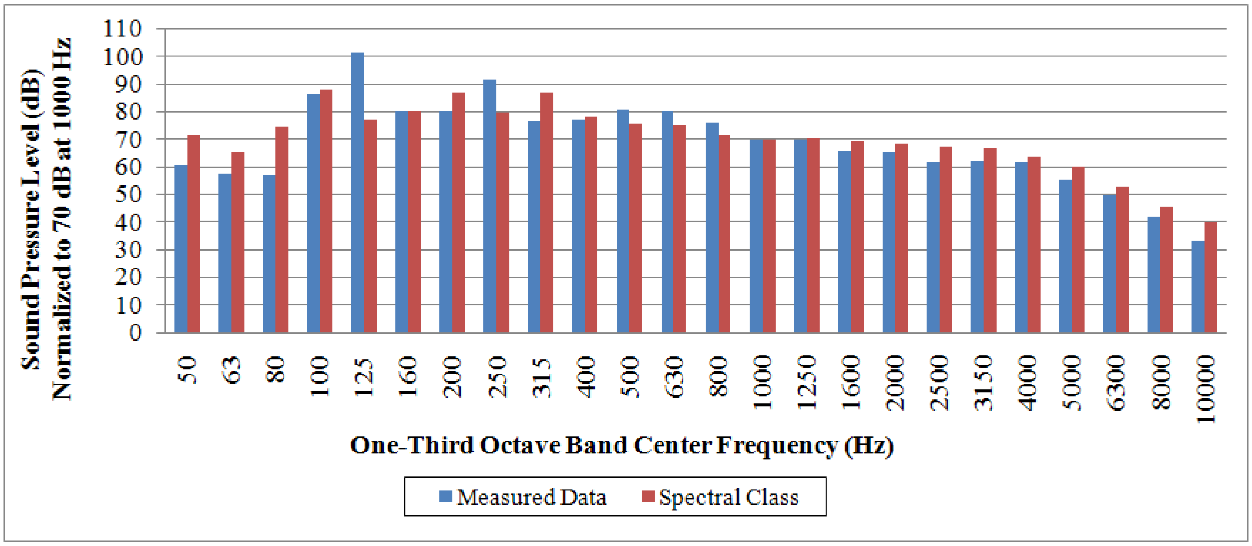

Figure 47. 182S Average 1000-ft 500 Series APP Spectrum (normalized)

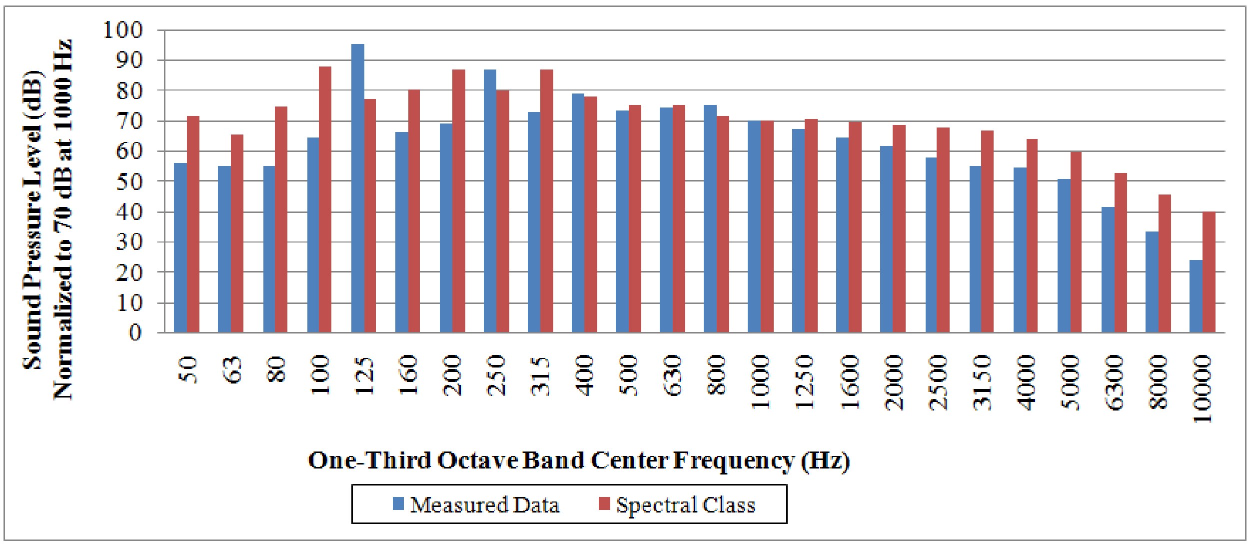

Figure 48. 182S Average 1000-ft 600 Series APP Spectrum (normalized)

E.2 DHC-2 Spectral Class Comparison

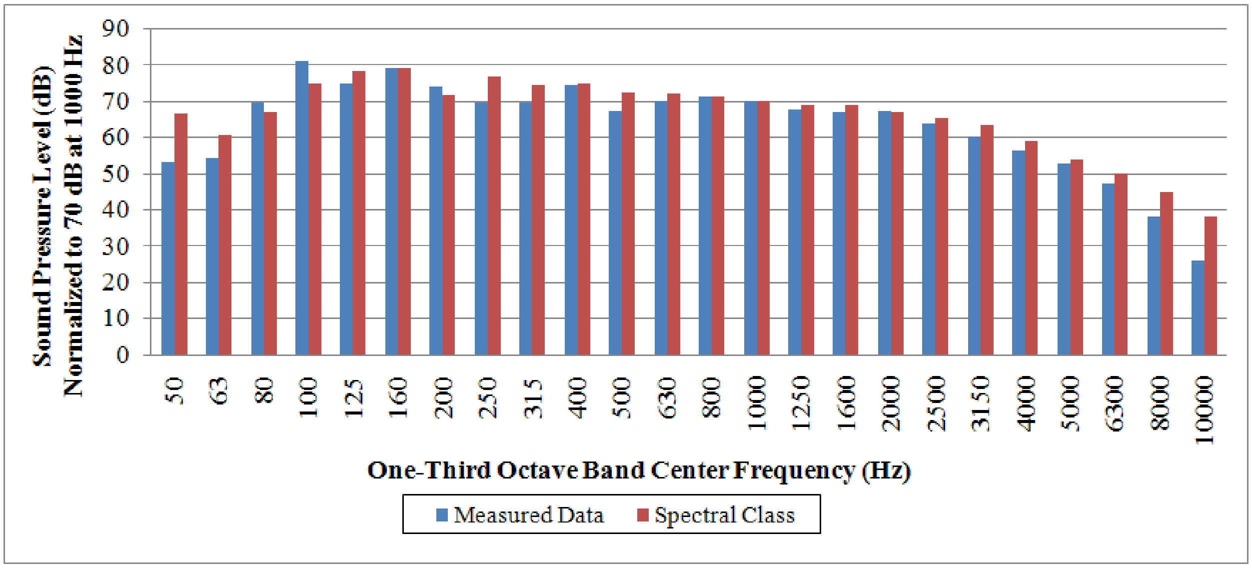

Figure 49. DHC-2 Average 1000-ft 100 Series LFO Spectrum (normalized)

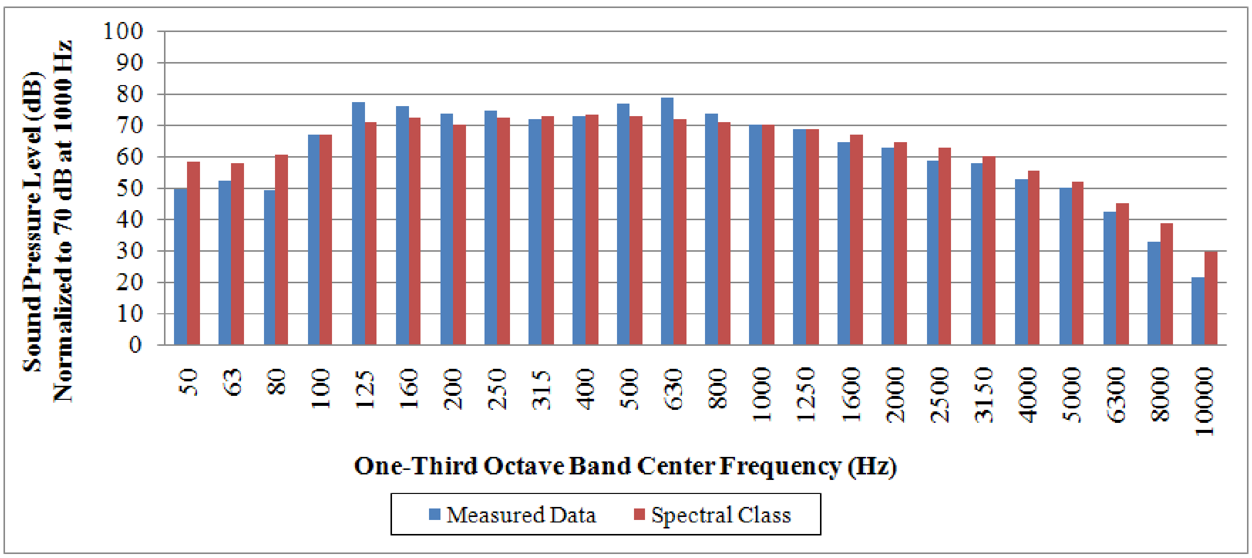

Figure 50. DHC-2 Average 1000-ft 300 Series DEP Spectrum (normalized)

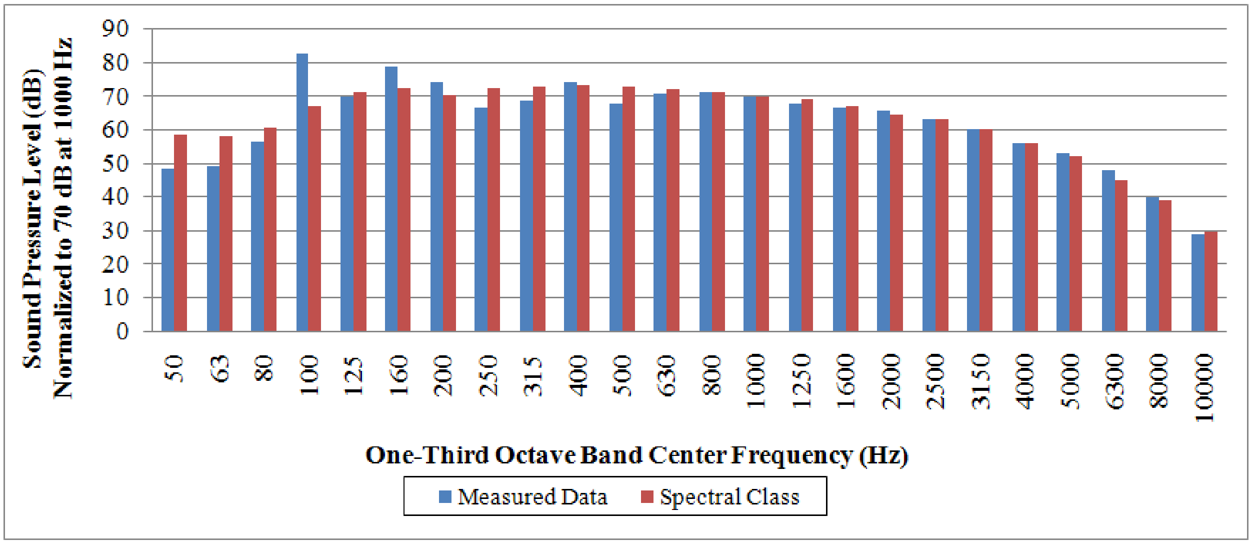

Figure 51. DHC-2 Average 1000-ft 400 Series DEP Spectrum (normalized)

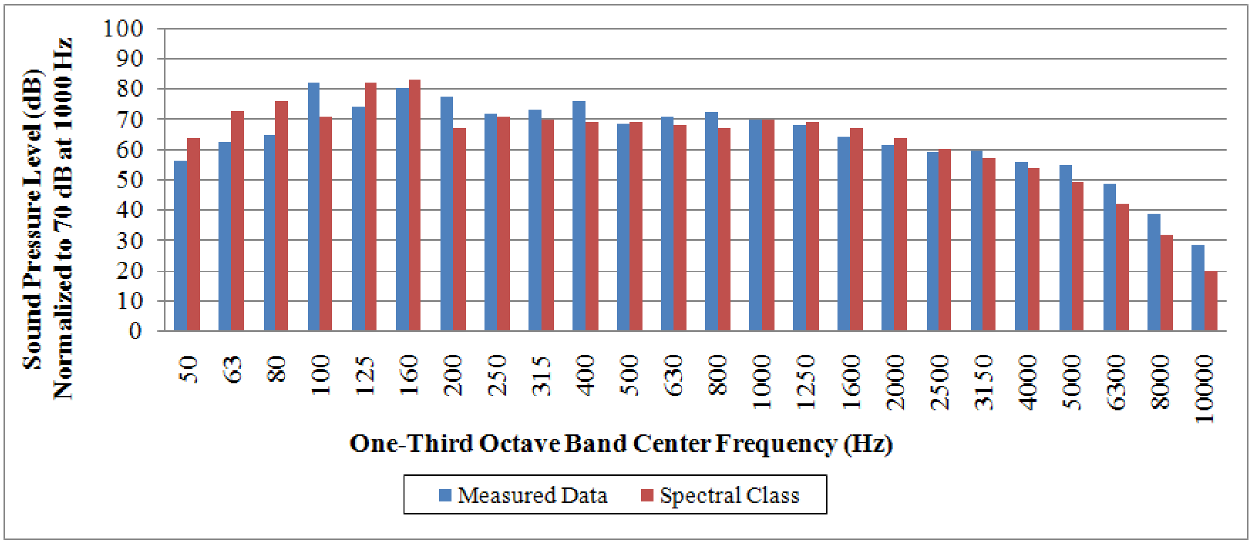

Figure 52. DHC-2 Average 1000-ft 500 Series APP Spectrum (normalized)

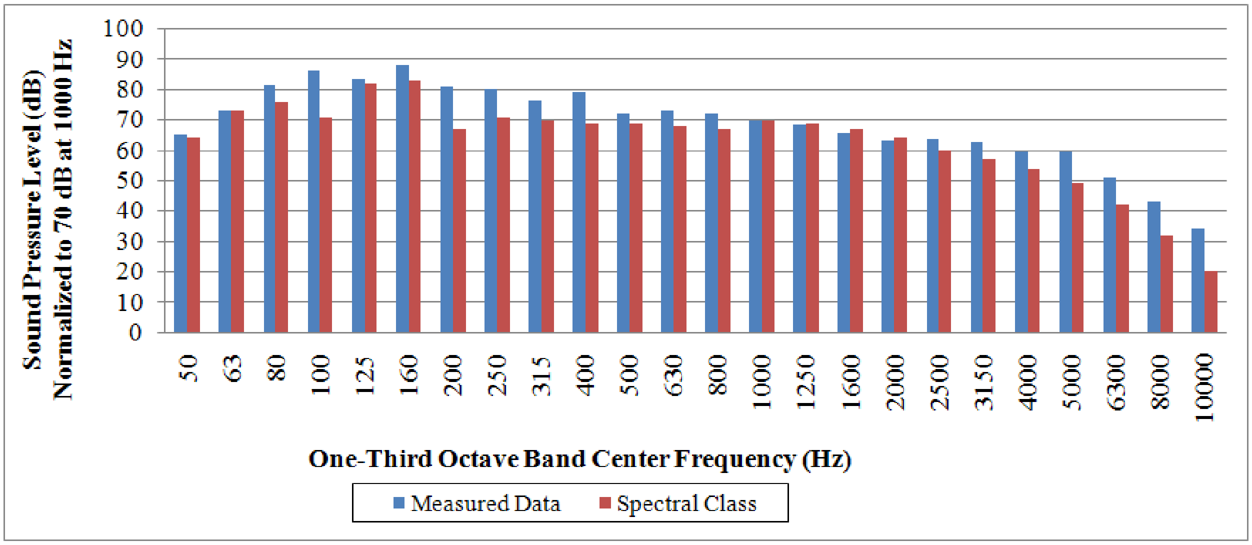

Figure 53. DHC-2 Average 1000-ft 600 Series APP Spectrum (normalized)

APPENDIX F: ACRONYMS AND ABBREVIATIONS

AC	Alternating Current
AC-93-2	Advisory Circular-93-2
AEDT	Aviation Environmental Design Tool
AEE	FAA Office of Environment and Energy
AGL	Above Ground level
Ah	Amp Hours
ANSI	American National Standards Institute
APP	Approach
AS_{seg}	Reference Speed at closest point of approach from flight and receiver
ATMPs	Air Tour Management Plans
B&K	Brüel and Kjær
BHP	Brake Horse Power
BNC	Bayonet Neill-Concelman
dB	Decibel
dBA	Decibel A-weighted
DC	Direct Current
DEP	Departure
DGPS	Differential Global Positioning System
DHC	De Havilland Canada
DUR_{adj}	Duration Adjustment
EPNL	Effective Perceived Noise Level
F	Fahrenheit
FAA	Federal Aviation Administration
FAR	Federal Aviation Regulations
FICAN	Federal Interagency Committee on Aircraft Noise
ft	Feet
GCNP	Grand Canyon National Park
GLB	GLB Electronics, Inc. (Buffalo, New York)
GPS	Global Positioning System
hr	Hour
Hz	Hertz
ICAO	International Civil Aviation Organization
INM	Integrated Noise Model
kHz	Kilohertz
KIAS	Knots Indicated Air Speed
kts	Knot(s)
L_{AE}	Sound Exposure Level
L_{ASmx}	Maximum, slow-scale, A-weighted sound level
lb	Pound(s) force or weight

LD824	Larson Davis model 824
L_{EPN}	Effective Perceived Noise Level
LFO	Level Fly Over
L_{PNTSmx}	Tone-adjusted, maximum, slow-scale, perceived noise level
mm	Millimeter
MTOW	Maximum Take-off Weight
MXSA	Maximum Time-weighted A-weighted Sound Level
MXSPNT	Tone-adjusted Maximum Slow Time-weighted Perceived Noise Level
NPATMA	National Parks Air Tour Management Act
NPD	Noise-Power-Distance
NPS	National Park Service
P&W	Pratt & Whitney
QA	Quality Assurance
QT	Quiet Aircraft Technology
ROC	Rate of Climb
RPM	Revolutions Per Minute
RMSE	Root Mean Square Error
s	Second
SAE-AIR-1845	Society of Automotive Engineers Aerospace Information Report No.1845
SEL	Sound Exposure Level
SD744T	Sound Device model 744T
SPL	Sound Pressure Level
TAMS	Transportable Automated Meteorological Station
TSPI	Time-Space-Position Information
Volpe	John A. Volpe National Transportation Systems Center
XLR	Ground Left Right

REFERENCES

1 National Parks Air Tour Management Act of 2000. Public Law 106-181, 114 Stat. 61, Title VIII, Section 801, April 2000.

2 FICAN Findings and Recommendations on Tools for Modeling Aircraft Noise in National Parks, Federal Interagency Committee on Aviation Noise: Washington, D.C., February 2005.

3 Fleming, Gregg G., Plotkin, Kenneth J., Roof, Christopher J., Ikelheimer, Bruce J., Senzig, David A., FICAN Assessment of Tools for Modeling Aircraft Noise in the National Parks, John A. Volpe National Transportation Systems Center: Cambridge, MA, Wyle Laboratories: Arlington, VA, Senzig Engineering: Winchester, MA, March 2005.

4 Fleming, et al., Integrated Noise Model (INM) Version 6.0 Technical Manual, Report No. FAA-AEE-02-01, John A. Volpe National Transportation System Center: Cambridge, MA, January 2002.

5 Environmental Impacts: Policies and Procedures, FAA Order 1050.1E, June 2004.

6 Airport Noise Compatibility Planning, Federal Aviation Regulations (FAR) Part 150, January 1985.

7 Federal Aviation Regulations, Part 36, Noise Standards: Aircraft Type and Airworthiness Certification, Federal Aviation Administration: Washington, D.C., September 1992.

8 Reherman, Clay, Samiljan, Robert, Scarpone, Christopher, Boeker, Eric, Roof, Christopher, Ruggiero, Joseph, Lau, Michael, Fleming, Gregg, Volpe Center Acoustics Facility Time-Space-Position-Information System User's Guide, Version 5.0, Volpe Center Report No. RVT-41-FA94TC1-LR1, John A. Volpe National Transportation System Center: Cambridge, MA, July 2008.

9 Annex 16, Environmental Protection, Volume I, Aircraft Noise, Third Edition, International Civil Aviation Organization (ICAO), July 1993.

10 Society of Automotive Engineers, Committee A-21, Aircraft Noise, Procedure for the Calculation of Airplane Noise in the Vicinity of Airports, Aerospace Information Report No. 1845, Society of Automotive Engineers, Inc.: Warrendale, PA, March 1986.

11 Report on Standard Method of Computing Noise Contours around Civil Airports Volume 1: Applications Guide; Volume 2: Technical Guide, European Civil Aviation Conference (ECAC) Doc 29 (3rd Edition), July 2005.

12 Recommended Method for Computing Noise Contours Around Airports (Doc 9911), First Edition, International Civil Aviation Organization (ICAO), January 2009.

[13] Acoustical Terminology, American National Standard, ANSI S1.1-1994 (R2004), American National Standards Institute: New York, New York, 2004.

[14] Cessna Model 182S Pilot's Operating Handbook and Airplane Flight Manual. 182SPHUS S15-03, 1997.

[15] Lycoming Aircraft Engine Series O-540, IO-540 Operator's Manual, 1999.

[16] DHC-2 Beaver Flight Manual, March 31, 1956.

[17] P&W R-985-39A Engine Technical Manual, Oct. 29, 1970.

[18] Spectral Classes for FAA's Integrated Noise Model Version 6.0, John A. Volpe National Transportation Systems Center Acoustics Facility: Cambridge, MA, December 1999.